ผลของการปรับสภาพด้วยออกซิเจนและสารประกอบของออกซิเจนต่อพฤติกรรมของตัวเร่งปฏิกิริยาแพลเลเดียม-ซิลเวอร์สำหรับปฏิกิริยาไฮโดรจิเนชันแบบเลือกเกิดของอะเซทิลีน

นางสาวบงกช งามสม

วิทยานิพนธ์นี้เป็นส่วนหนึ่งของการศึกษาตามหลักสูตรปริญญาวิศวกรรมศาสตรดุษฎีบัณฑิต

สาขาวิชาวิศวกรรมเคมี ภาควิชาวิศวกรรมเคมี

คณะวิศวกรรมศาสตร์ จุฬาลงกรณ์มหาวิทยาลัย

ปีการศึกษา 2545

ISBN 974-17-2059-9

EFFECTS OF PRETREATMENT WITH OXYGEN AND OXYGEN-CONTAINING COMPOUNDS ON THE CATALYTIC BEHAVIOUR OF Pd-Ag CATALYST FOR THE SELECTIVE HYDROGENATION OF ACETYLENE

Miss Bongkot Ngamsom

A Dissertation Submitted in Partial Fulfillment of the Requirements
for the Degree of Doctor of Engineering in Chemical Engineering

Faculty of Engineering

Chulalongkorn University

Academic Year 2002

ISBN 974-17-2059-9

Thesis Title	EFFECTS OF PRETREATMENT WITH OXYGEN AND OXYGEN-CONTAINING COMPOUNDS ON THE CATALYTIC BEHAVIOUR OF PD-AG CATALYST FOR THE SELECTIVE HYDROGENATION OF ACETYLENE
By	Miss Bongkot Ngamsom
Field of Study	Chemical Engineering
Thesis Advisor	Professor Piyasan Praserthdam, Dr.Ing.
Thesis Co-advisor	Professor David Trimm, Ph.D.
	Nina Bogdanchikova, Ph.D.

Accepted by the Faculty of Engineering, Chulalongkorn University in Partial Fulfillment of Requirements for the Doctor's Degree

...…...…….Dean of Faculty of Engineering
(Professor Somsak Panyakeow, D.Eng)

THESIS COMMITTEE

...…….Chairman
(Professor Wiwut Tanthapanichakoon, Ph.D.)

…….. Thesis Advisor
(Professor Piyasan Praserthdam, Dr.Ing.)

…….. Thesis Co-advisor
(Professor David Trimm, Ph.D.)

…….. Thesis Co-advisor
(Nina Bogdanchikova, Ph.D.)

…….. Member
(Associate Professor Tharathon Mongkhonsi, Ph.D.)

…….. Member
(Suphot Phatanasri, D.Eng.)

…….. Member
(Nakarin Mongkolsiri, D.Eng.)

บงกช งามสม: ผลของการปรับสภาพด้วยออกซิเจนและสารประกอบของออกซิเจนต่อพฤติกรรมของตัวเร่งปฏิกิริยาแพลเลเดียม-ซิลเวอร์สำหรับปฏิกิริยาไฮโดรจิเนชันแบบเลือกเกิดของอะเซทิลีน (EFFECTS OF PRETREATMENT WITH OXYGEN AND OXYGEN-CONTAINING COMPOUNDS ON THE CATALYTIC BEHAVIOUR OF Pd-Ag CATALYST FOR THE SELECTIVE HYDROGENATION OF ACETYLENE) อ. ที่ปรึกษา: ศ.ดร. ปิยะสาร ประเสริฐธรรม, อ. ที่ปรึกษาร่วม: Professor David Trimm, Ph.D. และ Nina Bogdanchikova, Ph.D. 125 หน้า ISBN 974-17-2059-9.

ทำการศึกษาผลของการปรับสภาพด้วยออกซิเจนและสารประกอบของออกซิเจน (ไนตริก-ออกไซด์ ไนตรัสออกไซด์ คาร์บอนมอนอกไซด์ และ คาร์บอนไดออกไซด์) ต่อตัวเร่งปฏิกิริยาแพลเลเดียม-ซิลเวอร์สำหรับปฏิกิริยาไฮโดรจิเนชันแบบเลือกเกิดของอะเซทิลีน พบว่า ความว่องไวของตัวเร่งปฏิกิริยาในการกำจัดอะเซทิลีนเพิ่มขึ้นหลังจากการปรับสภาพ อย่างไรก็ตาม มีเพียงการปรับสภาพด้วยไนตรัสออกไซด์และไนตริกออกไซด์เท่านั้นที่ทำให้เอทิลีนเพิ่มขึ้น ทำการพิสูจน์เอกลักษณ์ของตัวเร่งปฏิกิริยาในแง่มุมของทั้งกลุ่มและบนพื้นผิวโดยเทคนิคต่าง ๆ นั่นคือ การกระเจิงรังสีเอ็กซ์ การส่องผ่านด้วยกล้องจุลทรรศน์อิเล็กตรอน การดูดซับด้วยคาร์บอนมอนอกไซด์ การรีดักชันแบบโปรแกรมอุณหภูมิ การหลุดออกแบบโปรแกรมอุณหภูมิ การออกซิเดชันแบบโปรแกรมอุณหภูมิ เอ็กซ์-เรย์ โฟโตอิเล็กตรอน สเปกโทรสโกปี และ ฟูริเออร์ทรานสฟอร์ม อินฟราเรดสเปกโทรสโกปี การกระเจิงรังสีเอ็กซ์และการส่องผ่านด้วยกล้องจุลทรรศน์อิเล็กตรอนแสดงให้เห็นว่า เฟสทั้งกลุ่มของโลหะผสมแพลเลเดียม-ซิลเวอร์มีเส้นผ่านศูนย์กลางประมาณ 6.7 นาโนเมตร หลังจากการรีดักชัน ซิลเวอร์ทำให้เกิดการเปลี่ยนแปลงคุณสมบัติในเชิงความสามารถในการรีดักชันและการดูดซับไฮโดรเจนของแพลเลเดียม การวิเคราะห์พื้นผิวด้วยเอ็กซ์-เรย์โฟโตอิเล็กตรอนสเปกโทรสโกปียืนยันถึงการมีอยู่ของโลหะผสมแพลเลเดียม-ซิลเวอร์ในสัดส่วนที่มีซิลเวอร์มากหลังจากการรีดักชัน การปรับสภาพทำให้สัดส่วนของซิลเวอร์บนพื้นผิวน้อยลง เห็นได้จากสัดส่วนของแพลเลเดียมต่อซิลเวอร์ที่น้อยลง (ส่วนของแพลเลเดียมเพิ่มขึ้นเล็กน้อย ประมาณ 3-3.6 เปอร์เซ็นต์) มีการเลื่อนของพลังงานยึดเหนี่ยวของซิลเวอร์หลังการปรับสภาพด้วยไนตริกออกไซด์และไนตรัสออกไซด์ พื้นผิวหลังปฏิกิริยาไม่มีการเปลี่ยนแปลงสภาวะทั้งของแพลเลเดียมและซิลเวอร์เมื่อเทียบกับสภาวะที่ทำการวัดก่อนการทำปฏิกิริยา ดังนั้นการเปลี่ยนแปลงพื้นผิวจึงเกิดขึ้นหลังการปรับสภาพและคงอยู่หลังจากการทำปฏิกิริยาเป็นเวลา 8 ชั่วโมง ไม่เกิดการเกาะของคาร์บอนหลังจาก 8 ชั่วโมงของการทำปฏิกิริยาจากการวัดด้วยการออกซิเดชันแบบโปรแกรมอุณหภูมิและเอ็กซ์-เรย์ โฟโตอิเล็กตรอน สเปกโทรสโกปี อินฟราเรดสเปกโทรสโกปีของตัวอย่างที่ผ่านการปรับสภาพด้วยไนตริกออกไซด์และไนตรัสออกไซด์แสดงให้เห็นสารประกอบเชิงซ้อนแบบเชิงเส้นของแพลเลเดียมไนโตรเจนออกซิเจน สปีชีส์ไนเตรทและไนไตรท์บนซิลเวอร์บนตัวรองรับอะลูมินา การดูดซับอะเซทิลีนแสดงสปีชีส์เอทิลิไดน์ซึ่งลดลงอย่างมากเมื่อทำการปรับสภาพด้วยไนตรัสออกไซด์ การปรับสภาพด้วยไนตริกออกไซด์และไนตรัสออกไซด์ทำให้เกิดการกีดกันไซท์แพลเลเดียมที่ทำให้เกิดอีเทนโดยตรงผ่านสปีชีส์เอทิลิไดน์ ดังนั้นเอทิลีนจึงเพิ่มขึ้นตามมา ในอีกแง่หนึ่ง การปรับสภาพด้วยออกซิเจน คาร์บอนมอนอกไซด์ หรือ คาร์บอนไดออกไซด์ ทำให้การกระจายตัวของแพลเลเดียมบนตัวรองรับเพิ่มขึ้น ซึ่งจะเพิ่มความว่องไวในปฏิกิริยาไฮโดรจิเนชันของอะเซทิลีนด้วย

ภาควิชา.....วิศวกรรมเคมี.....	ลายมือชื่อนิสิต.....
สาขาวิชา.....วิศวกรรมเคมี.....	ลายมือชื่ออาจารย์ที่ปรึกษา.....
ปีการศึกษา.....2545.....	ลายมือชื่ออาจารย์ที่ปรึกษาร่วม.....
	ลายมือชื่ออาจารย์ที่ปรึกษาร่วม.....

##4271808821: MAJOR CHEMICAL ENGINEERING
KEY WORD: Pd-Ag catalyst/ pretreatment/ oxygen-containing compound/ selective hydrogenation of acetylene

BONGKOT NGAMSOM: EFFECTS OF PRETREATMENT WITH OXYGEN AND OXYGEN-CONTAINING COMPOUNDS ON THE CATALYTIC BEHAVIOUR OF Pd-Ag CATALYST FOR THE SELECTIVE HYDROGENATION OF ACETYLENE. THESIS ADVISOR: PROF. PIYASAN PRASERTHDAM, Dr. Ing., THESIS CO-ADVISOR: PROF. DAVID TRIMM, Ph.D., and NINA BOGDANCHIKOVA, Ph.D., 125 pp. ISBN 974-17-2059-9.

Effects of pretreatment with oxygen and oxygen-containing compounds (NO, N_2O, CO and CO_2) on Pd-Ag catalysts for the selective hydrogenation of acetylene have been studied. Enhancement of the catalyst activity for C_2H_2 removal has been found after pretreatment. However, only pretreatment with N_2O and NO have revealed the improved ethylene gain. Catalysts have been characterised either on the bulk or surface aspects by various techniques, i.e., XRD, TEM, CO-adsorption, TPR, TPD, TPO, XPS and FT-IR. XRD and TEM suggest bulk phase of Pd-Ag alloy with diameter ca. 6.7 nm after reduction. Modification in the reducibility and hydrogen sorption properties of palladium was influenced by the presence of Ag. Surface analysis by XPS has confirmed the existence of surface Pd-Ag alloy with Ag enrichment after reduction. Pretreatment results in dilution of surface Ag enrichment, indicating from the smaller Pd:Ag ratio (Palladium fraction becomes slightly increased 3-13.6%). Significant shift of the Ag 3d binding energy is revealed after NO and N_2O pretreatment. The surface after reaction shows no state change of either Pd or Ag compared to those measured prior to reaction, therefore surface modification occurs after pretreatment and is retained after reaction for 8 h. No carbonaceous deposits is formed after 8 h on stream from TPO measurement and XPS. Infrared spectroscopy of NO and N_2O treated samples shows the linear complex Pd-NO, nitrate and nitrite species on Ag-Al_2O_3. C_2H_2 adsorption displays ethylidyne species which is sufficiently decreased by N_2O pretreatment. Pretreatment with NO and N_2O results in blockage of Pd sites responsible for direct ethane formation via ethylidyne species, ethylene gain is thus increased as a consequence. On the other hand, pretreatment with O_2, CO or CO_2 increases dispersion of Pd on the support, which increases C_2H_2 hydrogenation activity.

Department……Chemical Engineering…Student's signature……

Field of Study…Chemical Engineering…Advisor's signature……

Academic year……..2002…….Co-advisor's signature……..

Co-advisor's signature……...

ACKNOWLEDGEMENTS

The author would like to gratefully acknowledge her advisor, Professor Piyasan Praserthdam, for his invaluable suggestions and for being a great driving force for her study. Without the constructive guidance and comments from her co-advisor, Professor David Trimm from the University of New South Wales, Australia, this work would never have been achieved. She would also like to acknowledge Dr. Nina Bogdanchikova, her another co-advisor, from CCMC, UNAM, Mexico, for providing her with the opportunity to work in Mexico and for the many fruitful discussions during her stay. The effort of producing surface analysis data in this project was predominantly carried out by Professor Robert Lamb, the University of New South Wales. Without the continual support from Professor Peter Silveston from the University of Waterloo and Dr. Miguel Avalos from CCMC, UNAM, Mexico, she would never have passed the tough time during thesis writing. She would also like to register her thanks to Professor Wiwut Tanthapanichakoon who has been the chairman of the adjudicating committee for this Thesis, as well as Dr. Suphot Phatanasri, Dr. Nakarin Mongkolsiri and Associate Professor Tharathon Mongkhonsi, who have been members of the aforesaid committee.

She is indebted for financial support to the Thailand Research Fund (TRF) and TJTTP-JBIC.

The practical assistance and expertise of Dr. Bin Gong, and Mr. Wilhelm Holzschuh, of the Surface Science and Technology, and Mr. Eric Flores, of CCMC, UNAM, was invaluable. She would also like to thank Dr. Mario Farias and Dr. Jesus Antonio Diaz for the help with *ex situ* XPS measurement. Gratitude is highly expressed to Dr. Choowong Chaisuk, Dr. Sunee Srihiranpullop, Mr. Mongkolchanok Pramottana, Miss Araya Kittivanichawat, Mr. Okorn Mekasuwandamrong, Mrs. Eloisa Aparicio, Mr. Eduardo Guerra, Miss Antonella Pretalli, Mr. Douglas Lawes and Mr. Everett Lee, her dear friends, for their pastoral care and patience during her study. To the many others, not specifically named, who have provided her with information, support and encouragement, please be assured that she thinks of you.

Finally she would like to dedicate the achievement of this work to her dearest family and her fiancé, Mr. Stephen Moore. Their unyielding support and generous love not only made this work possible but worth doing in the first place.

CONTENTS

PAGE

CONTENTS (Cont.)

PAGE

LIST OF TABLES

LIST OF FIGURES

LIST OF FIGURES (Cont.)

LIST OF FIGURES (Cont.)

LIST OF FIGURES (Cont.)

CHAPTER I

INTRODUCTION

Ethylene is the lightest olefinic hydrocarbon and is the basic chemical raw material for a large variety of industrial processes. The importance of ethylene for chemical industries results from the reactivity due to the double bond in its molecular structure. Although ethylene is less reactive than acetylene, it is simpler, safer, and less costly to produce and further convert. As a result, ethylene has largely replaced acetylene as the basic building block for an entire branch of industrial organic chemistry. Ethylene does not freely occur in nature, but is generally produced by the pyrolysis or catalytic cracking of refinery gas, ethane, propane, butane and the like [1]. Ethane and natural gas liquids (often a mixture of ethane and propane) are preferably used in ethylene production. Produced ethylene contains small proportions of acetylenic compounds, depending on feedstock used. An ethane feedstock produces the smallest amount of acetylene by-product, which averages about 0.26 wt% of the product stream. However, for other feeds, this quantity can become as large as 0.95 wt% [2-4].

The removal of acetylene contaminant in ethylene stream is vital, as acetylene acts as a poison to the catalyst used for polymerisation of ethylene. Additionally, acetylene can form metal acetylides, which are explosive contaminants [5]. Thus, less than 10 ppm acetylene and most preferably less than 5 ppm are allowed in polymer-grade ethylene [1-7].

One typical technique used for removing trace amount of acetylene in an ethylene stream has involved selective hydrogenation. Acetylene is catalytically hydrogenated. However, it is desirable that ethylene should remain intact during hydrogenation, since over-hydrogenation to ethane reduces yields.

Supported palladium catalysts have proved to be the best catalysts so far for the reaction with good activity for the hydrogenation of acetylene in excess ethylene. Numerous factors have been found to affect the selectivity of such palladium catalysts [1,5-7]. Typically, as the temperature is increased above that which gives substantial

elimination of acetylene, there is a progressive increase in the amount of ethylene and acetylene that is converted to ethane. As the amount of olefin that is hydrogenated increases, the temperature of the catalyst also increases, resulting in runaway ethylene hydrogenation. It is thus desirable to be able to operate with the catalyst and conditions that will allow a relatively wide spread between the temperature which produces either effective elimination of acetylene or the smallest amount of ethane formation. Regrettably, oligomer or green oil formation during acetylene hydrogenation (which shortens the catalyst lifetime) and high ethylene loss due to ethane formation at high levels of acetylene conversion are still inevitable over palladium based catalysts [1-8].

Carbon monoxide acts as an inhibitor to the palladium catalyst system by occupying the active sites. The role of CO on the selectivity improvement results from the blockage of adsorption sites for adsorbed hydrogen, resulting in a decrease in activity and in a suppression of acetylene dissociation. Commercially, trace amounts of carbon monoxide are added into the ethylene feedstream in order to improve the selectivity of the Pd catalysts [9-14]. However, catalyst poisoned by this substance can occur especially at higher percentages. CO also leaves with the hydrocarbon stream, and may be harmful to product quality in the pursuing reactions as well as in ethylene processing.

Promotion with a second metal such as Ag [1,15-18], Au [19,20], Cu [9], Si [21], K [22], and Co [23], has been reported as an alternative way for selectivity enhancement for palladium catalysts. Among those bimetallic catalysts, Pd-Ag has been reported as a promising catalyst that can reduce green-oil formation as well as enhance selectivity. This catalyst does not require CO for selectivity enhancement.

Recently, the activation of catalysts comprising elements of group IB and transition metals with oxygen and/or oxygen-containing compounds has been claimed [24] and the effect of the pretreatment with N_2O on acetylene selective hydrogenation catalysts was reported [25,26]. However, no mechanistic studies based on this information have been reported yet.

In this study, catalytic evaluation and characterisation have been performed in order to clarify effects of such pretreatment on catalytic behaviour for the selective hydrogenation of acetylene. The study has been scoped as follows:

1. Preparation of 0.03wt%Pd-0.235wt%Ag/Al_2O_3 and 3wt%Pd-4wt%Ag/Al_2O_3 catalysts by incipient wetness impregnation method.

2. Pretreatment of catalyst with five oxygen-containing compounds, i.e., O_2, N_2O, NO, CO_2 and CO, by injecting certain proportions of these gases into the catalyst prior to the reaction test.

3. Characterisation of catalysts:

- chemical analysis by atomic absorption spectroscopy (AAS)
- study of catalyst structure and morphology by X-ray diffraction (XRD) and transmission electron microscope (TEM)
- study of metal dispersion by CO-adsorption
- surface analysis by X-ray photoelectron spectroscopy (XPS) and Fourier Tranform-infrared spectroscopy (FT-IR)
- measurement of carbonaceous deposits by temperature-programmed oxidation (TPO)

4. Catalyst evaluation as a function of reaction temperature and time on stream.

5. Study of the reaction mechanism for the selective hydrogenation of acetylene over the untreated and pretreated catalysts.

This thesis is intended to give an understanding of effects of pretreatment with oxygen and oxygen-containing compounds on the reactivity of alumina supported Pd-Ag catalyst for the selective hydrogenation of acetylene. It is divided into two parts: the first three chapters describe general information about the study, while the following three chapters emphasise the results and discussion observed from the present study. The background and scope of the study are described in chapter I. Chapter II reviews research works on the selective hydrogenation in the past and comments on previous works. Fundamental aspects of the selective hydrogenation of acetylene on the basis of industrial applications are compiled in chapter III. The experimental in chapter IV consists of the catalyst preparation, pretreatment, evaluation and characterisation. The experimental results, including an expanded

discussion, are described in chapter IV. In the last chapter, the overall conclusion emerging from this work and some recommendations for future work are presented.

CHAPTER II

LITERATURE REVIEW

The present review is intended to collect and analyse the results of palladium-catalysed selective hydrogenation of acetylene as reported in recent years. An attempt will also be made to summarise the present knowledge and understanding of various factors influencing the performance of Pd catalysts for the selective hydrogenation of acetylene. In the last section of this review, comments on previous studies that have directly influenced the aims of this study are given.

Selective hydrogenation of hydrocarbons with multiple unsaturation, i.e., dienes and acetylenes (alkynes) to achieve partial hydrogenation and to synthesise monoenes is of fundamental importance. Specifically, the selective hydrogenation of acetylene in ethylene rich stream is a crucial process in polyethylene production with the aim of the complete elimination of acetylene, which poisons the polymerisation catalysts [1-35].

Studies of the acetylene hydrogenation in the presence of excess ethylene show that there are different sites involved in the reaction: one fraction of sites acetylene is selectively hydrogenated to ethylene whereas the other, non-selective sites promote ethylene hydrogenation even in the presence of acetylene [27-31]. ^{14}C labelling experiments have shown the existence of a direct route from acetylene to ethane [9,27-32]. Simultaneously, oligomer formation from acetylene can also take place. Therefore, the mechanism of acetylene hydrogenation to produce either ethylene or ethane was proposed to proceed via three pathways [27-29,33,34]:

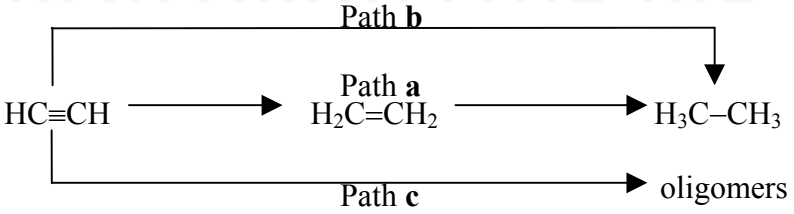

Figure 2.1 Acetylene hydrogenation pathways [27-29,33,34].

Path **a** is the acetylene hydrogenation to ethylene followed by desorption and possible readsorption of ethylene which further hydrogenates to ethane. Path **b** is the reactive adsorption of acetylene to produce multiple bound intermediates, which are directly hydrogenated to ethane. The relative significance of the two paths and, therefore, the selectivity can be controlled by the catalysts and the reaction parameters. Oligomerisation/polymerisation of acetylene (path **c**) leads to the formation of hydrocarbons of even carbon numbers ranging from C4 to C32. This path results in green oil which can affect catalyst activity by masking active sites [35].

There have been seven intermediate species, shown in Figure 2.2, participating in the above processes. These have been suggested from surface science observations (FT-IR, EELS, SFG, HREELS, etc.) combined with kinetic studies.

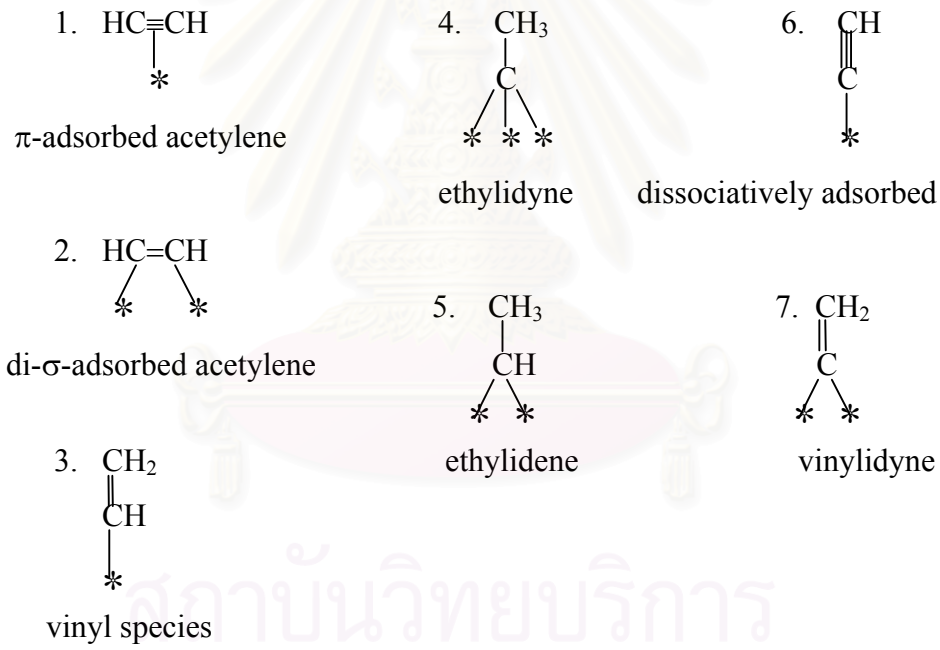

Figure 2.2 Proposed surface intermediates in hydrogenation of acetylene [9,32,35-39].

π-adsorbed acetylene (1) is transformed to associatively adsorbed (di-σ-adsorbed acetylene) flat-lying acetylene (2), then to vinyl species (3) which are the precursors for the formation of ethylene (Figure 2.2). Multiply bound surface intermediates such as ethylidyne (4) and ethylidene (5) are hydrogenated to ethane.

Dissociatively adsorbed acetylene (6) and vinylidene (7) were suggested to participate in forming oligomers and benzene [40]. Recently, species (7) was also assumed to be the reactive intermediate in ethylene formation [41-45]. However, some of those proposed species were identified under UHV conditions, which might not be formed under atmospheric conditions. FT-IR and deuterium labelling (location of the D position) are of crucial importance in interpreting the formation of reactive and spectator species. These techniques verified the presence of species 2, 4 and 6.

Formation of C4 from vinylidene or flat lying acetylene has been investigated. Benzene is also observed as a side product in the formation of oligomers during atmospheric hydrogenation since, after C6 ring closure, further insertion of the C2 unit is terminated [40,46-49]. Reaction paths leading to all possible products and the corresponding surface intermediates are summarised in Figure 2.3. It is noted that only π- and di-σ-adsorbed acetylene species are involved in ethylene formation.

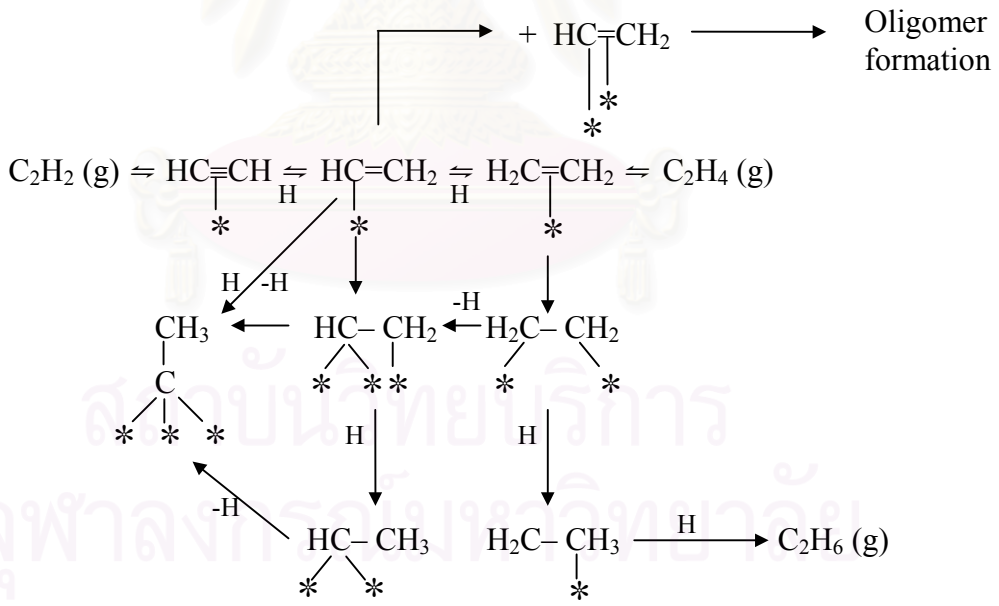

Figure 2.3 Reaction paths for acetylene hydrogenation proceeding over surface intermediates [35].

A great deal of work has been focused on the effect of Pd particle size, basically by using different supports, for example, alumina [2,9,10,13,14,16,17,50-65], silica [15,18,21,53,66,67], pumice [53,57], mesoporous and microporous materials [68]. Most studies suggested a structure sensitive reaction when dispersion is high. However, some controversial behaviour was also observed, e.g., increasing metal dispersion was found to bring about a decrease in specific activity especially over catalysts of small particle size [59-62], while small particles of a medium dispersed Pd/Al_2O_3 catalyst exhibited slightly higher activity [65]. Structure insensitivity was reported recently [66], activity drop with increasing dispersion was also found [53]. Direct comparisons of the results, however, are difficult since different substrates were studied under different reaction conditions. Nevertheless, strong complexion of the highly unsaturated alkyne to atoms of low co-ordination number on small metallic particles is usually invoked to explain the diminishing activity of small metal particles [59,60,62,69].

With respect to selectivity changes, catalysts of low dispersion have been suggested to give better selectivity towards ethylene [59,60]. In other cases, no effect was observed [53,59,60]. However, it is necessary to take into account that the problem of selectivity cannot be discussed independently from influence of other important parameters, i.e., carbonaceous deposits and oligomer formation.

Carbonaceous deposits have been found to have a profound effect on the selectivity to ethylene during acetylene hydrogenation. [C^{14}] acetylene and [^{14}C] ethylene adsorption studies suggest two stage adsorption, i.e., in the first stage irreversible dissociative adsorption occurs, while in the second stage acetylene and ethylene adsorb and react upon the catalyst covered by the primary layer [27-29]. A work reported later suggests that highly dehydrogenated C_xH_y species formed in the early stages of hydrogenation can be regarded as hydrogen sources which play a crucial role in the hydrogenation process [70].

Carbonaceous deposits may result in both decreasing and increasing activity and selectivity depending on the catalyst (metal loading, properties of the support) and operating conditions (hydrogen pressure, C_2H_2:H_2 ratio). The mechanism of carbonaceous deposits is still not entirely clarified. It is likely, however, that the very

unreactive deposits are formed from multiple adsorbed species or reactive oligomers upon losing hydrogen [35].

Many different explanations have been put forward to interpret the involvement of carbonaceous deposits on the reaction pathways. Acetylene hydrogenation was suggested to take place on top of the irreversibly adsorbed carbon-rich first layers, which served as a hydrogen transfer agent to supply hydrogen from the underlying palladium to the acetylene adsorbed in the second layer [70]. Detailed studies with ethylidyne have convincingly shown that this species due to its low reactivity, behaves as a spectator in ethylene hydrogenation and cannot serve as hydrogen donor. However, the results from deuterium exchange occurring in parallel with hydrogen addition were found to be different on each metal, indicating the adsorption of the reactive species directly on the metal [71].

A different explanation to disprove the direct involvement of the carbonaceous deposits in the hydrogenation was also proposed [51,72]. Decreasing activity during the initial stage of the reaction testifies to the inactivity of the carbonaceous layer. Modification of selectivity by this layer is explained by the ensemble site effect [73]. Large ensembles are able to form multiple metal-carbon bonds and, therefore, are probably sites for ethane formation via strongly bound intermediates, i.e., responsible for low selectivity. Carbonaceous deposits, in turn, diminish the average ensemble sites of the active metal available for the reaction. Such smaller ensembles bind acetylene less strongly resulting in the suppression of dissociatively adsorbed, possibly multiple bound species. The formation of ethane, therefore, is suppressed, resulting in a higher selectivity to ethylene.

Surface electronic metal-support interaction studied over the Pd/pumice catalyst has been suggested to govern the activity by changing the oxidation properties of the metal and surface-reagent interaction as well as by affecting the formation of carbonaceous deposits. The existence of low hindered sites accessible to all reagents and of poisoned sites covered by carbonaceous deposits, not accessible to any reagents, are suggested on the surface. Poisoned sites interacting with neighbouring sites generate high-hindered sites, which become accessible only to acetylene and hydrogen and, consequently, favour selective hydrogenation to

ethylene. The carbonaceous layer was also supposed to affect selectivity through a ligand effect, which causes a diminution of the adsorption strength of unsaturated molecules and favours the selectivity towards ethylene [53,57].

The effect of carbonaceous deposits on the catalytic performance has also been investigated as a function of time on stream. Experimental results for the mixture of acetylene and ethylene have clearly revealed that ageing increased the selectivity of over-hydrogenation and the appearance of sites which hydrogenate ethylene to ethane even if there is sufficient amount of acetylene in the gas phase [65].

Carbonaceous deposits on the support were confirmed to exert the undesirable effect on the selectivity of acetylene hydrogenation. The effect of oligomers/deposits acting as hydrogen reservoir was suggested for over-hydrogenation. Migration of polymeric material from the metal to the support may facilitate hydrogen surface transport (or hydrogen spillover) to certain fraction of sites that are not covered by acetylene, providing hydrogenation of intermediate ethylene [12,55,65]. This was assumed to be the reason for the increased ethane formation over a $Pd/\gamma\text{-}Al_2O_3$ catalyst compared with $Pd/\alpha\text{-}Al_2O_3$ [65]. However, the effect of carbonaceous deposits serving as hydrogen spillover agent is still obscure and requires a thorough study.

It was suggested that, over Pd/Al_2O_3 catalysts, carbonaceous deposits substantially decrease effective diffusivity by blocking the catalyst pores [55,58]. Mass transfer limitations severely hinder intraparticle diffusion of acetylene and, thereby increase the rate of ethylene hydrogenation in the interior of catalyst grains.

The amount of carbonaceous deposits was not directly related to formation of undesired ethane in the hydrogenation of acetylene over the supported catalysts [56]. Instead, the surface coverage of hydrogen during the deactivation was found to be a crucial parameter by influencing the proportion of “harmful coke” and “harmless coke”. The former type, generated at low hydrogen coverage, was proposed to be responsible for increased ethane selectivity by, for example, a spillover mechanism.

Separation between the two types of carbonaceous deposits could not be achieved by temperature-programmed oxidation studies.

A comprehensive mechanistic scheme assuming the existence of three types of active sites created on palladium surface by carbonaceous deposits has been proposed, and is illustrated in Figure 2.4 [74]. Certain sites representing small spaces of the palladium surface between carbonaceous deposits (A sites) are sterically inaccessible to ethylene. The hydrogenation of ethylene was believed to take place on large palladium spaces, where ethylene and acetylene competitively adsorb (E sites). However, as ethylene was not supposed to adsorb on A sites, the two substrates that competitively adsorb on A sites should be acetylene and hydrogen. Two types of active sites were then suggested; A_1 and A_2 sites. A_1 sites on palladium are where hydrogenation proceeds according to a mechanism involving the competitive adsorption of acetylene and hydrogen. A_2 sites exist on the carbonaceous deposits where only hydrogenation of acetylene to ethylene proceeds involving to the non-competitive adsorption of acetylene. In this latter case, acetylene is hydrogenated by hydrogen transferred to acetylene from the carbonaceous deposits. Accordingly, it was suggested that the hydrogenation of acetylene on A sites primarily proceeds to ethylene. A key intermediate in hydrogenation of acetylene on A sites is believed to be vinylidene species, whereas π-bonded ethylene adsorbed on E sites is a key intermediate in ethylene hydrogenation. The larger steric hindrance to the adsorbed ethylene compared to that for adsorbed acetylene is a result of the difference in position of the molecules in the adsorbed state: π-adsorbed ethylene is flat lying, whereas acetylene adsorbed as vinylidene is either perpendicular or tilted with respect to the surface. This proposed model, does not consider the effect of transport hindrance on consecutive reactions and the effect of the accumulation of deposits on the local effective diffusivity [75]. Additionally, the above mentioned model cannot explain the reactivity of freshly reduced supported palladium catalysts.

Despite formation of carbonaceous deposits, it is well known that acetylene readily undergoes polymerisation. In the hydrogenation of acetylene, both gas phase oligomers (C4-C8) and heavier hydrocarbons (C8+) are formed. The liquid part of the oligomers (C8+) (often referred to as “green oil”) appears downstream.

Oligomers formed in acetylene hydrogenation consist of different alkene, dienes and, to a lesser extent, alkanes of even carbon atoms with little branching and an H:C ratio of about 1.9 [3,4]. There are diverging results concerning the effect of the H_2:C_2H_2 ratio on the selectivity of the oligomers. Some researchers suggested the suppression of oligomerisation in the ratio range 1.5-4 [76], whereas some observed no effects at the ratios between 3-7 [77]. However, it was observed that hydrogen was requisite for oligomer formation as, in the absence of hydrogen, there was no oligomer formed [78].

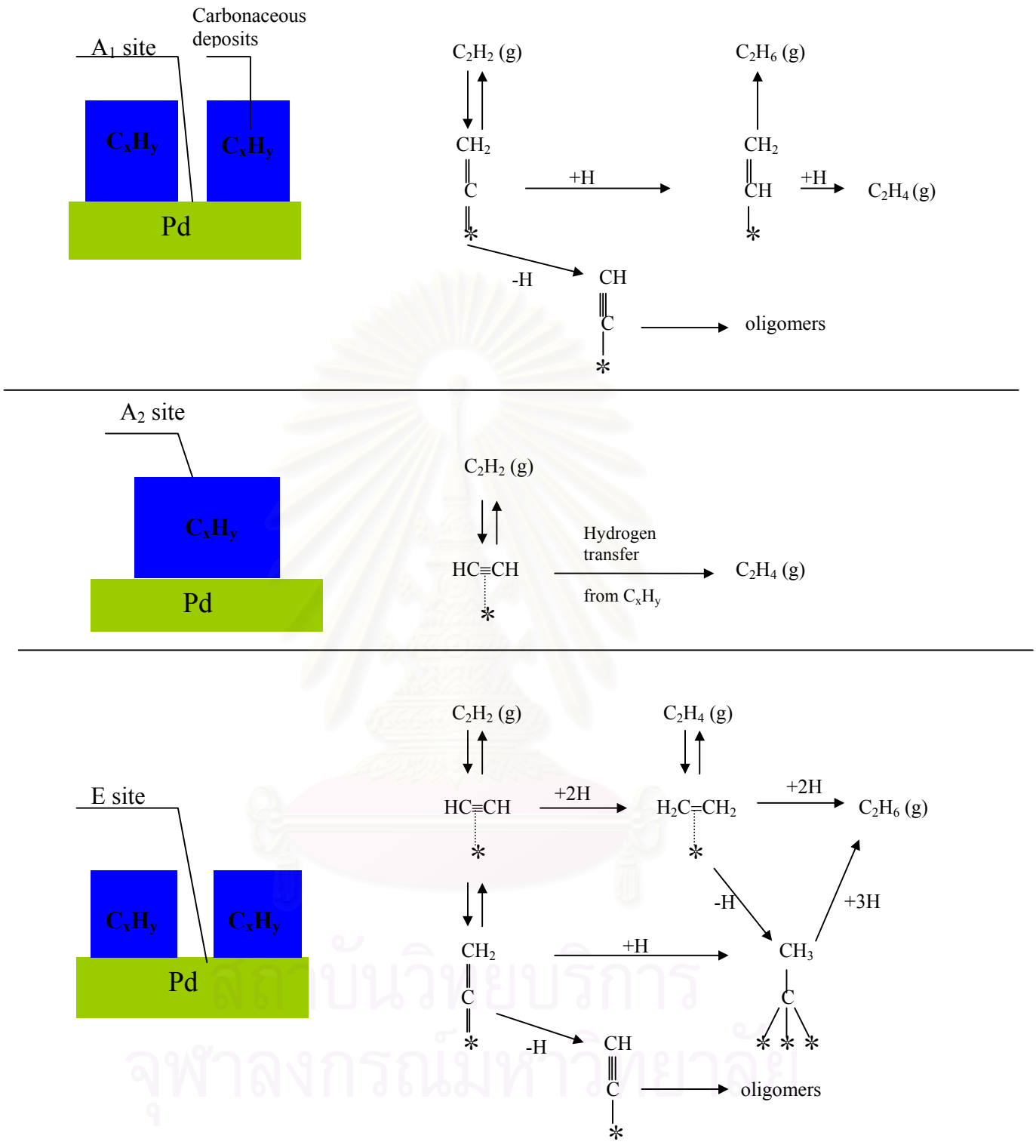

Figure 2.4 Three types of active sites created on the palladium surface by carbonaceous deposits (C_xH_y) and schemes of the reactions occurring on the sites [74].

As far as the mechanism of oligomer formation is concerned, C-C bonds might be formed by recombination of neighbouring intermediates or by insertion of a C2 unit into an existing Pd-C bond. Free-radical type vinyl intermediates were proposed to participate in the oligomer formation [79,80]. Recently, work using spin-trapping technique confirmed the presence of radicals, although the origin of these species was not clearly understood [81,82]. Studies with the mixture of acetylene and propylene showed that oligomers arise entirely from acetylene. Recombination of neighbouring vinylidene was proposed to be a source for C4 formation [41-45].

Attempts to improve the ethylene selectivity of the palladium catalyst have been made by many workers. Using additives to interfere with the adsorption of reactants or to influence the formation of surface residues is one possibility. The most common additive that has been applied for selectivity enhancement in industry is carbon monoxide. It is well known that a small amount of carbon monoxide can hinder hydrogenation of alkenes. Carbon monoxide is thus used as a feed additive in the selective hydrogenation of acetylene to avoid over-hydrogenation [83]. CO in those systems behaves as reversible poison. Approximately 1000 ppm (0.1%) of CO is commonly added to acetylene streams containing a large excess of hydrogen. Under industrial conditions a 1% increase in CO level reduces the ethylene loss by 4-6%, however, ca. 25% decrease in acetylene conversion occurs simultaneously [84]. The role of CO in selectivity improvement has been investigated by many researchers [3,9-14,29,30,83-87]. Competitive adsorption of ethylene and CO was originally suggested [85]. Blockage of the Pd surface for hydrogen and ethylene adsorption by CO was another explanation for increased selectivity for acetylene hydrogenation [86,87]. It was found that CO played a more important role in inhibiting ethylene hydrogenation than that of acetylene over Pd/Al_2O_3 surface [30]. Most of the studies reported recently explain the effect of CO in terms of competitive adsorption of CO with hydrogen, resulting in a decrease in the surface concentration of hydrogen [3,12,29]. Acetylene deuteration experiments suggested that the probability of hydrogenation of adsorbed vinyl decreased when CO was added, which could be explained by the decreased concentration of hydrogen atoms. The experiment with ethylene has shown, however, that desorption of ethylene increased in the presence of CO, allowing the conclusion that displacement of ethylene by CO causes a decrease in its surface concentration [10].

Additionally, the presence of CO in the acetylene feed affects the formation and composition of oligomers. A fast decrease in acetylene reaction rate as a function of CO partial pressure was reported, but, insignificant effect was found on the selectivity of C4+ [12]. However, in the pilot plant studies, CO crucially increased the carbon content of the catalyst [78].

Despite commercial application of carbon monoxide as a selectivity promoter, ammonia [88], quinoline [89], other organic bases such as piperidine [90,91], have also been reported to increase alkene selectivity. The general interpretation is that nucleophilic compounds are able to increase the electron density of palladium through electron donation. Increased electron density of palladium, in turn, leads to decreased strength of interaction with electron-rich compounds such as hydrocarbons with multiple unsaturation. The decreased strength of adsorption of the intermediate alkene favours desorption of the alkene and increases the overall selectivity [35]. On the other hand, electron acceptors (such as sulfur compounds) exhibit an opposite effect with the effect of sulfur decreasing the content of carbonaceous deposits on the metal [89,90]. The effects of various nitrogen bases as well as of sulfur compounds on the selectivity to alkene are relatively complex and cannot be explained by competition, site poisoning or electronic/ligand effects. Additionally, the fact that the modifiers can alter the surface morphology of palladium by semi-extractive adsorption should not be disregarded due to the lowest lattice energy of palladium with respect to other noble metals [91].

Modification of palladium surfaces by promoting with a second metal, or use of bimetallic catalyst, has also been reported to improve selectivity as well as catalyst lifetime. Addition of a second metal, e.g., K [22], Cu [9,94], Au [19,20], Ag [8,15-18,69,92], Si [21], and Co [23], to the palladium catalysts may improve selectivity by altering electronic or geometric properties of palladium [69,92]. Changing the electron density of palladium influences the relative adsorption strength of the reactant, intermediates and hydrogen. Additionally, active site may be partly blocked by a second metal, thereby affecting the geometry of the active site. In either way, the performance of the catalyst to yield ethylene may be improved.

Alloying palladium with Group IB elements usually brings about an enhanced selectivity and increased reaction rate. Promotion effects are thought to originate from the donation of electrons from these metals to palladium [8] or to the variation of the ensemble sites [73,93]. The beneficial addition of Cu was suggested to be attributed to the decrease in the ensemble sites needed for multiple adsorbed (alkylidene) species [94], whereas, for Pd-Ag/Al_2O_3, selectivity enhancement by Ag was claimed to originate from the suppression of the formation of absorbed hydrogen, which results in direct ethane formation from acetylene [17]. Ag has also suggested to act as a desorption site for spillover hydrogen migrating from the metal to the support by means of carbonaceous deposit bridges [55].

Recently, activation of the catalyst comprising Group IB and transition metals by pretreatment with oxygen and/or oxygen-containing compounds was discovered [24]. The application of such effect was performed over Pd-Ag/Al_2O_3 for the selective hydrogenation of acetylene by pretreatment with N_2O. Addition of N_2O was proposed to move two silver atoms closely to an oxygen atom and to form Ag_2O on the surface that might expose the Pd sites responsible for acetylene hydrogenation to ethylene [25,26]. Surface characterisation to prove the existence of Ag_2O was not performed.

Comments on previous works

According to the above review, selective hydrogenation of acetylene over supported Pd catalysts developed for industrial applications is capable of removing acetylene impurities to ppm level without loss of ethylene. The selective catalyst, which provides highest selectivity towards ethylene, has yet to be found. The basic factors influencing selectivity over palladium catalysts have been investigated. Studies of reaction mechanism for the explanation of the selective process have been made on either dynamic or kinetic aspects. Active catalytic sites generated upon exposure with reactant are suggested to change from the initially cleaned surface as a consequence of carbonaceous deposit/oligomer formation and restructuring. Operating conditions (reaction temperature, C_2H_2:H_2 ratio) as well as the characteristics of the catalyst themselves (metal dispersion, interaction between metal and support) bring about different catalytic behaviour, especially in terms of

carbonaceous deposits over the active sites. Selectivity enhancement by additives, e.g., CO and nitrogen-containing compounds, was a result of the interference of adsorption properties of reactant and formation of carbonaceous deposits. Promoters modify geometric as well as electronic properties of the palladium surface.

The selective hydrogenation of acetylene over silver promoted palladium catalyst has been chosen as a model for the selective hydrogenation due to selectivity enhancement as well as catalyst lifetime. This catalyst, additionally, does not require CO as a selective promoter. A reasonable mechanism on this bimetallic system has also been proposed. Activation of the silver-promoted catalysts has been achieved by the addition of some small proportions of N_2O prior to the reaction. Nevertheless, definitive insight into the microscopical involvement of the surface reaction between N_2O and Pd-Ag alloy atoms has not been provided up to now. It was also interesting to study effects of other oxygen-containing compounds, which were claimed for activation of catalysts comprising group IB and transition metals. A study of mechanism of pretreatment by such compounds on acetylene hydrogenation over Pd-Ag catalysts is of interest. As a result, the objective of this study is to study the effects of pretreatment with oxygen and oxygen-containing compounds (i.e., O_2, NO, N_2O, CO and CO_2) on the catalytic behaviour of Pd-Ag catalyst for the selective hydrogenation of acetylene.

CHAPTER III

INDUSTRIAL ACETYLENE HYDROGENATION

In the previous chapter, a review of recent researches on palladium-catalysed selective acetylene hydrogenation has been demonstrated. There, the present knowledge and understanding of parameters influencing on the performance of Pd catalysts for the selective hydrogenation of acetylene was summarised. Apparently, Pd has high activity in activation of molecular hydrogen and, in the presence of stream additives or catalyst modifiers, provides extremely high selectivity in competitive hydrogenation of acetylene.

This chapter focuses on the fundamental theory of the selective hydrogenation of acetylene over supported palladium catalysts based on the real industrial conditions. Studies on the reaction mechanism of acetylene hydrogenation proceeding on alumina-supported palladium catalysts are also described. The chapter consists of four main sections. Reactions proceeding during acetylene hydrogenation as well as influencing parameters on such reactions are discussed in section 3.1. Details of the acetylene converter in which the selective hydrogenation of acetylene is commercially undertaken in are described in section 3.2. The catalysts for the acetylene converter as well as their operating conditions are detailed in section 3.3. Finally, the reaction rate and the selectivity for acetylene hydrogenation over supported palladium catalyst is discussed in section 3.4.

3.1 Reactions [1,6,7,9,83,95-100]

Generally, there are two primary reactions proceeding during acetylene hydrogenation:

$$C_2H_2 + H_2 \xrightarrow{k_1} C_2H_4 \qquad \Delta H = -42.3 \text{ kcal/mol} \qquad (3.1)$$

$$C_2H_4 + H_2 \xrightarrow{k_2} C_2H_6 \qquad \Delta H = -32.6 \text{ kcal/mol} \qquad (3.2)$$

The first reaction (3.1) is the desired reaction whereas the second reaction (3.2) is an undesired side reaction due to the consumption of ethylene product. There is also a third reaction occurring during normal operation, which adversely affects the catalyst performance, i.e., the polymerisation reaction of C_2H_2 with itself to form a longer chain molecule, commonly called "green oil".

$$C_2H_2 + (n)\ C_2H_2 \xrightarrow{k_3} C_xH_x \text{ (polymer/green oil)} \qquad (3.3)$$

According to the above three reactions involving acetylene hydrogenation, two parameters influencing on the desired reaction can be assigned. The first parameter is reaction temperature, which has a direct relationship with the kinetics of the system. However, it affects not only the reaction rate of the desired reaction (k_1), but also the rate of ethylene hydrogenation (k_2). The rate of polymerisation (k_3) also increases with temperature and the resulting green oil can affect catalyst activity by occupying active sites. When the catalyst is new or has just been regenerated, it has high activity. With time on stream, activity declines as the catalyst becomes fouled with green oil and other contaminants. By the end-of-run (EOR), the inlet temperature must be increased (25-40^{o}C) over start-of-run (SOR) inlet temperature in order to maintain enough activity for complete acetylene removal. In order to selectively hydrogenate acetylene to ethylene, it is critical to maintain the differential between the activation energies of reaction (3.1) and (3.2). However, it is desirable that the ethylene remains intact during hydrogenation. Once energy is supplied to the system over a given catalyst by increasing the temperature, the differential between the activation energies disappears and complete removal of acetylene, which generally has the lower partial pressure, becomes virtually impossible. In other words, higher temperature reduces selectivity; more hydrogen is used to convert ethylene to ethane, thereby increasing ethylene loss. The inlet temperature should therefore be kept as low as possible while still removing acetylene to specification requirements. Low temperature minimises the two undesirable side reactions and helps optimise the converter operation.

Another crucial parameter affecting the selectivity of the system is the ratio between hydrogen and acetylene (H_2:C_2H_2). Theoretically, the H_2:C_2H_2 ratio would be 1:1, which would mean that no hydrogen would remain for the side reaction (3.2)

after acetylene hydrogenation (3.1). However, in practice, the catalyst is not 100% selective and the H_2:C_2H_2 ratio is usually higher than 1:1 to get complete conversion of the acetylene. As hydrogen is one of the reactants, the overall acetylene conversion will increase with increasing hydrogen concentration. Increasing the H_2:C_2H_2 ratio from SOR to EOR can help offset the decline in catalyst activity with time on stream. However, this increased acetylene conversion with a higher H_2:C_2H_2 ratio can have a cost in selectivity which leads to ethylene loss. Typically, the H_2:C_2H_2 ratio is between 1.1 and 2.5 [1,35,83].

3.2 Reactor [1,35,83]

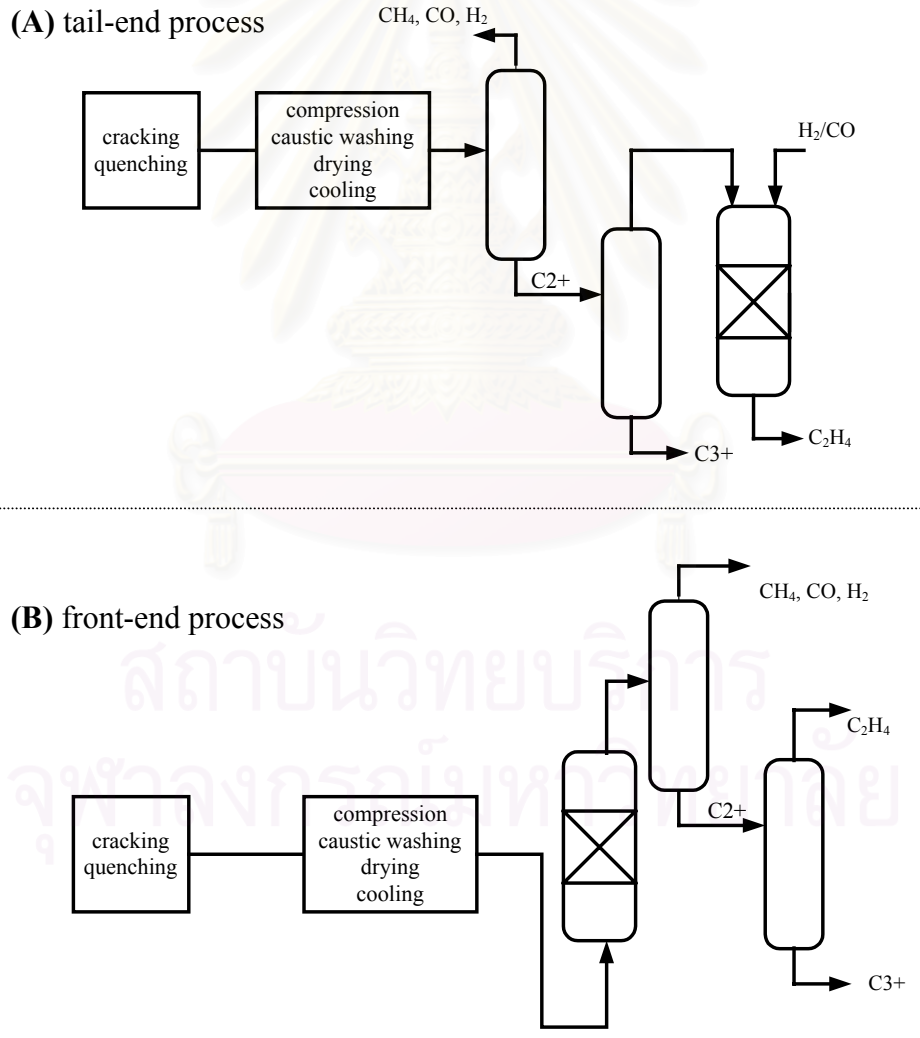

Figure 3.1 Simplified process flow of tail-end **(A)** and front-end **(B)** hydrogenation of acetylene [35].

The hydrogenation converter, or acetylene-removing unit (ARU), follows the rectification line and is integrated in the low temperature section of the ethylene plant, illustrated in Figure 3.1. The C2 fraction can be taken from the de-ethaniser overhead (tail-end hydrogenation) or from the compression train of the cracked gas at one of the compressor interstage levels before H_2, CH_4, CO and C3+ were removed (front-end hydrogenation). In the front-end mix, the C2 stream contains a high percentage of methane and hydrogen. It is a convenient way of acetylene removal to treat the overhead in an ethylene-ethane fractionator.

In the tail-end cuts taken from de-ethaniser top, the C_2H_4:C_2H_2 ratio is typically 50-200 and the acetylene is present in 0.5-2% v/v (5000-20000 ppm). The H_2:C_2H_2 ratio ranges from 1.1 to 2.5. The operation is performed in the gas phase at 15-30 bar with a space velocity between 1000 and 10000 h^{-1}. Reactors for the selective hydrogenation of acetylene have been designed to operate adiabatically or isothermally. In most ethylene plants, adiabatic reactors are preferred on the basis of lower capital investment. Depending on the acetylene concentration, hydrogenation is performed in a cooled tubular reactor or one or two adiabatic reactors. For normal gas streams containing up to 0.3% acetylene, a two-bed reactor is needed with an intercooler to remove the heat of reaction. With higher acetylene proportions in the feed gas, the number of beds and intercoolers is increased to handle the higher heat of reaction and to maintain the temperature rise per bed at less than 15^{o}C. The normal operating temperature lies in the range 65-85^{o}C. During start-up, the reaction can proceed at as low as 45^{o}C. After a short period when the catalyst has stabilized, the reactor temperature will reach the normal operating range and will remain constant throughout its life. The activity of the fresh regenerated catalyst is regulated by CO. The CO concentration is gradually decreased as oligomer/polymers build up on the catalyst bed and the catalytic sites become poisoned. As a consequence of self-poisoning, the catalyst bed temperature should then be increased to maintain conversion of acetylene. The overall selectivity of ethylene depends primarily on the catalyst applied. The trend of these converters is to use a small amount of CO (1-3 ppm) or to operate without CO.

Front-end hydrogenation of acetylene requires early separation of C4's to preserve butadiene. The operating conditions are similar to those used in the tail-end system. Hydrogenation is performed in tubular or bed reactors with two or three separate beds to allow heat removal and careful control of the temperature along the bed. The Pd catalysts (0.01-0.05 wt% Pd) are designed to meet strict requirements: high selectivity for ethylene yield, excellent stability and high flexibility in feedstock qualities. In front-end hydrogenation, CO is a necessary feed additive due to the high percentage of hydrogen. Bimetallic promoted catalysts have been proved to provide better ethylene selectivity with respect to monometallic Pd catalysts. The second component, such as Ag, increases the temperature gap between the clean up temperature (the temperature required for a given level of acetylene) and the run away temperature (the temperature at which the ethylene selectivity is still positive).

3.3 Catalysts [1,5-7,9,96-98,100]

There are several options for catalysts that are feasible for industrial hydrogenation of acetylene. Commonly, macroporous alumina-supported palladium (Pd/Al_2O_3) catalyst is used. This catalyst has a relatively small surface area of approximately 0.1 to 3 m^2/g and also requires carbon monoxide to enhance its selectivity towards ethylene. Due to these limitations, silica-supported Pd catalyst is preferable. The catalyst normally contains 0.001-1 wt% Pd and 0.005-5wt% of a promoter metal, preferably potassium. The catalyst is prepared by impregnating the silica support with a solution containing the promoter metal, then drying the impregnated support. The product will be impregnated again with a solution containing Pd, then dried and calcined. The BET surface area of this catalyst is about 100 to 300 m^2/g, and is usually processed as an extrudate. This catalyst can be activated by reduction with hydrogen or hydrogen-containing gas, which produces a thin layer of Pd over the promoter metal oxide. The operating conditions for this catalyst involve a slight excess of hydrogen, pressure of 10-30 bar, and a relatively low temperature, usually less than 150^oC. The reactor is adiabatically operated and can reduce some acetylene content to approximately 1 ppm.

Another catalyst that is available is Pd-Ag/Al_2O_3. The addition of silver improves the catalyst performance so that only an insignificant amount of ethylene is lost due to over-hydrogenation, thus it is not necessary for CO addition for this catalyst. This catalyst can be prepared by both incipient wetness impregnation or wet reduction with an alkali metal borohydride/alkali metal hydroxide solution, followed by drying and calcination. It can also be oxidatively regenerated. The amount of Pd and Ag varies between 0.01 to 0.2 wt% and 0.02 to 2 wt%, respectively. BET surface areas of this catalyst are ca. 1 to 100 m^2/g. The feed should be premixed before entering the reactor with a ratio of hydrogen to acetylene more than 1. The operating temperature of this catalyst is between 0-150^oC. Regeneration is performed by heating up to 700^oC in the presence of air.

Other possible catalyst options are metal oxides and sulfides, usually ZnO, as well as other supported group VIII metals. Also, if the plant is configured differently, it would be possible to operate as a liquid process. In this case, the proper catalyst would be Pd/Al_2O_3 with the addition of 0.1 to 1 wt% of an amine compound, and the reactor should be operated at 10-50 bar and 20-150^oC with excess hydrocarbon.

As mentioned above, some catalysts require an addition of small amounts of carbon monoxide in order to enhance the catalyst selectivity. However, catalyst poisoning by this substance can occur especially at higher percentages, and it also leaves with the hydrocarbon stream. Additionally, carbon monoxide can be harmful to product quality in the subsequent reactions as well as ethylene processing.

Another option for regeneration of palladium-based catalyst from green oil accumulation on the surface is to burn off, or oxygenate. The process must be done periodically, ca. every 1-3 months. As the process needs to be operated at very high temperature, the catalyst lifetime could be lessened due to its heat sensitivity. Additionally, it also produces CO and CO_2, which are undesirable by-products. Regeneration can alternatively be made by hydrogen stripping. The process involves feeding a mixture of 5-10% hydrogen in an inert gas to the spent catalyst at 350^oC and 50 psi. This process is much less time-consuming than oxygenation. However, the catalyst deactivates more quickly, so that the process has to be performed more often.

3.4 Reaction rate and selectivity mechanism [2,9,25,26,32,39,54,74,102-104]

The rate of ethylene hydrogenation (3.1) is 10-100 times faster than the rate of acetylene hydrogenation (3.2) [2]. Accordingly, the selectivity mechanism cannot be explained if hydrogenation of acetylene and ethylene competitively proceeds. If reaction rate were the controlling mechanism, then a considerable amount of ethylene would be hydrogenated before complete hydrogenation of acetylene could take place. Consequently, a different mechanism is required to explain the preferential hydrogenation of acetylene in spite of its low reaction rate.

Acetylene can only be selectively hydrogenated with no ethylene hydrogenation by total exclusion of ethylene from all active sites on the catalyst, which is possible only if active sites are always saturated with components other than ethylene. As a consequence, adsorption and desorption rates are considered as the controlling kinetic mechanism.

Due to the higher adsorption enthalpy of alkynes, the ratio of surface coverage by an alkyne compared to that of an alkene remains very high until virtually all traces of alkyne disappears. This means that the alkyne either displaces the alkene from the surface or blocks its readsorption. Consequently, an alkene is not hydrogenated in the presence of an alkyne, although it readily undergoes hydrogenation in the absence of the alkyne. However, evidence regarding the adsorption of acetylene and ethylene on supported palladium catalyst shows that adsorption of acetylene and ethylene on palladium surface could take place both separately and competitively and ethylene hydrogenation could proceed even at high acetylene partial pressures. Involvement of different reaction sites has been suggested: on a fraction of sites acetylene was selectively hydrogenated to ethylene whereas on others, no-selective sites ethylene was hydrogenated even in the presence of acetylene.

Mechanistic study of the selective hydrogenation of acetylene on the Pd/Al_2O_3 catalyst by a double-labelling method (DLM) [9,32,39,103] suggested that three routes are operative during the reaction:

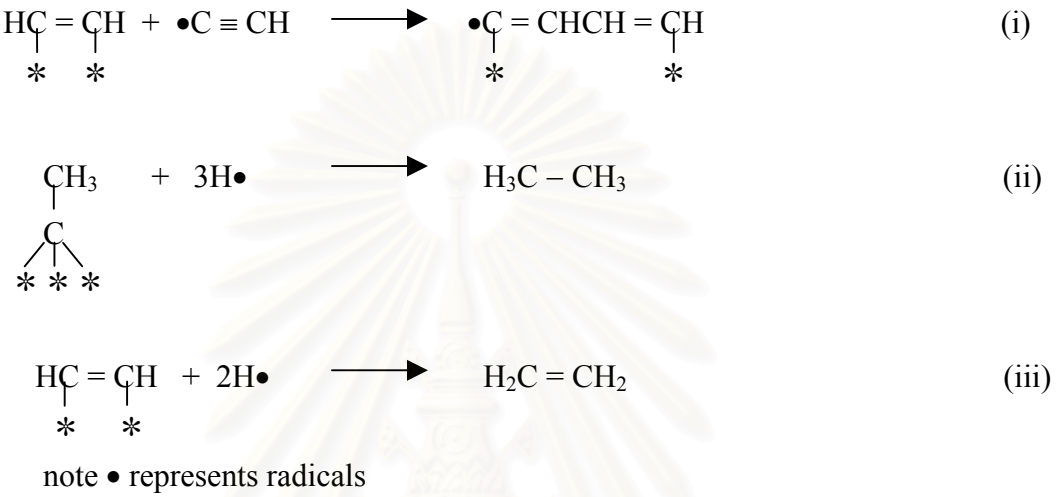

Figure 3.2 Surface intermediates in acetylene hydrogenation over Pd/Al_2O_3 catalyst [9,103].

Dissociative adsorption of acetylene to form polymer species has been suggested from C4+ formation, as equation (i) in Figure 3.2. [27-29,102,103]. Reactive adsorption of acetylene with adsorbed hydrogen atoms to form ethylidyne species leads directly to ethane formation, (equation (ii), Figure 3.2) [32,102,103]. Equation (iii) proceeds via associatively adsorbed acetylene (di-σ-adsorbed acetylene) that hydrogenates to the desired ethylene product. The ratio of the different routes is controlled by the reaction parameters.

On aged catalysts, strongly held residues or so-called carbon deposits, also referred to as carbonaceous overlayer, are formed. The accumulation of such residues is often manifested in a non-steady-state initial period and a decline in catalytic activity. A feasible explanation has been put forward to interpret the effect of carbonaceous deposits located on the alumina supported palladium catalysts. It is believed that hydrogenation of acetylene takes place on top of the irreversibly

adsorbed carbon-rich first layer, which serves as a hydrogen transfer agent to supply hydrogen from the underlying palladium to the acetylene adsorbed in the second layer. Additionally, when located on the support, carbon deposits are confirmed to exert an undesirable product. Migration of oligomers/deposits from the metal to the support may facilitate hydrogen surface transport to a certain fraction of sites that are not covered by acetylene. Hydrogen spillover might provide a way to interpret hydrogenation of the intermediate ethylene. This explanation can be simply understood by the conceptual model in Figure 3.3.

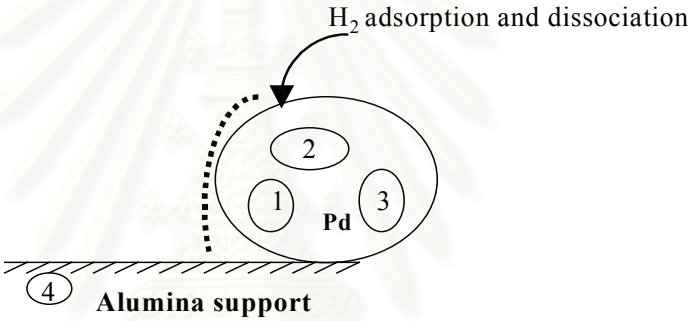

1: Site for oligomer formation
2: Site for direct ethane formation from acetylene
3: Site for ethylene production from acetylene
4: Site for ethane production from ethylene
..... carbonaceous deposit bridge to support

Figure 3.3 Conceptual model demonstrating four main types of surface sites on alumina-supported palladium catalyst [25,26].

Three sites located on palladium surface (sites 1, 2, and 3) accessible for the three different reactions. Site 1 is responsible for oligomer formation from dissociatively adsorbed acetylene according to reaction (i) in Figure 3.2. Reactive adsorption of acetylene via ethylidyne species, leading directly to ethane formation,

occurs on site 2. The desired acetylene hydrogenation to ethylene, proceeding via associative adsorption of acetylene, takes place on site 3. The existence of a small number of C_2H_4 hydrogenation sites on the palladium surface is recognised. However, the majority was on the carbonaceous covered support (site 4). It was proposed that ethylene adsorbed on the support and was hydrogenated there. Spillover hydrogen was tentatively identified as the source of hydrogen. The parallelism between polymer formation and ethylene hydrogenation suggested that the surface polymer served as a hydrogen pool and facilitated diffusion of hydrogen from palladium surface to the support.

However, a disparity in the selectivity mechanism has also been reported. Kinetic study on the hydrogenation of acetylene-ethylene mixtures over a $Pd/\alpha\text{-}Al_2O_3$ catalyst over a wide range of acetylene and ethylene partial pressures has suggested that the hydrogen spillover mechanism from palladium to support was inactive for the ethylene hydrogenation [54,74,104]. The conclusion was confirmed by the observations that the rate of ethane formation was negligible at high acetylene pressures (above 0.2 kPa) and that the rate of acetylene and ethylene attained a steady state after the same period of time, i.e., about 9 h. Surface heterogeneity of the catalyst was suggested. Two types of active sites were proposed to involve in the hydrogenation of acetylene-ethylene mixtures, denoted as A and E sites as illustrated in Figure 3.4.

“A” sites are small spaces on the palladium surface between carbonaceous deposits where only hydrogen and acetylene are competitively adsorbed. Hydrogenation of acetylene to ethylene and ethane and hydro-oligomerisation of acetylene to butadiene proceed on these sites. “E” sites locating on large palladium ensembles which are not covered by carbonaceous deposits occur competitive adsorption of all reactants. On these sites occur hydrogenation of ethylene to ethane and hydrogenation of butadiene to butenes and butane (butadiene is readsorbed from “A” sites where it is formed).

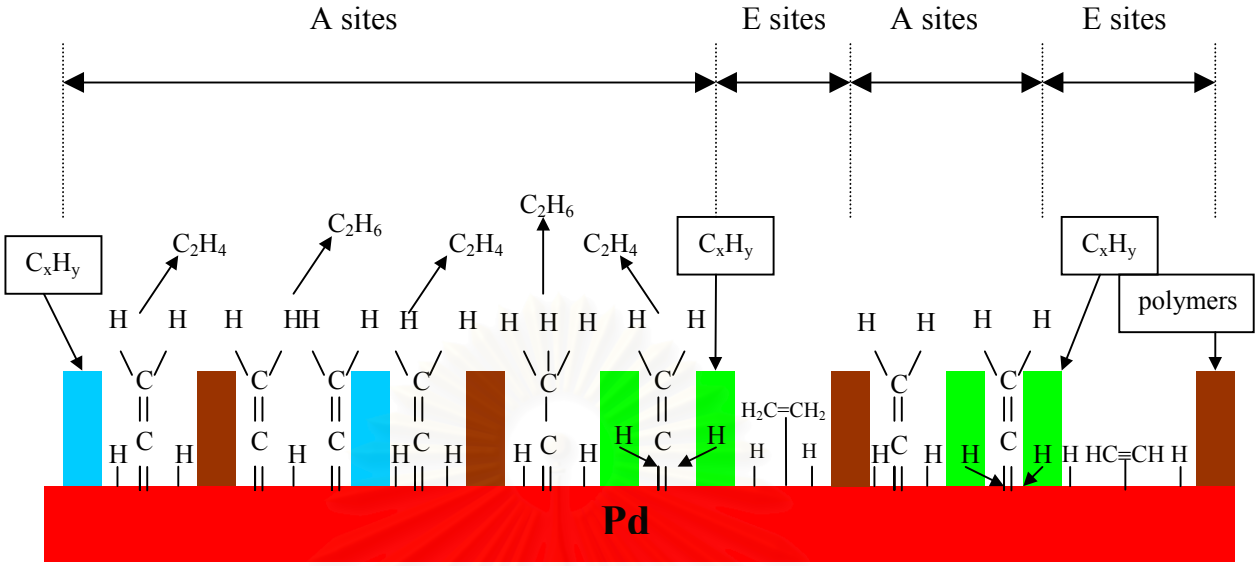

Figure 3.4 A simplified representation of active sites created on a palladium surface by carbonaceous deposits (C_xH_y) [104].

The selectivity mechanism of hydrogenation reactions proceeding on adsorption sites shown in Figure 3.4 can be summarized as the reaction scheme in Figure 3.5. Acetylene molecules are adsorbed as vinylidene on "A" sites perpendicularly to the palladium surface [41]. Acetylene is selectively hydrogenated to ethylene by hydrogen atoms that adsorbed either on "A" sites or transfers from the deposits. Evidence of a larger steric hindrance of the adsorbed ethylene molecule than that of the adsorbed acetylene molecule and relative sizes calculated from the bond lengths and angles in the ethylene molecule in the gas phase suggests that "A" sites are composed of a series of narrow adsorption sites (φ sites in Figure 3.5) able to adsorb vinylidene molecules or hydrogen molecules but too narrow to adsorb ethylene molecules, which need wider sites. The large space available on "E" sites allows adsorption of at least three species (e.g. flatly lying ethylene molecule and two hydrogen atoms or e.g. flatly lying ethylene molecule, flatly lying acetylene molecule and hydrogen) to adsorb on ε adsorption sites.

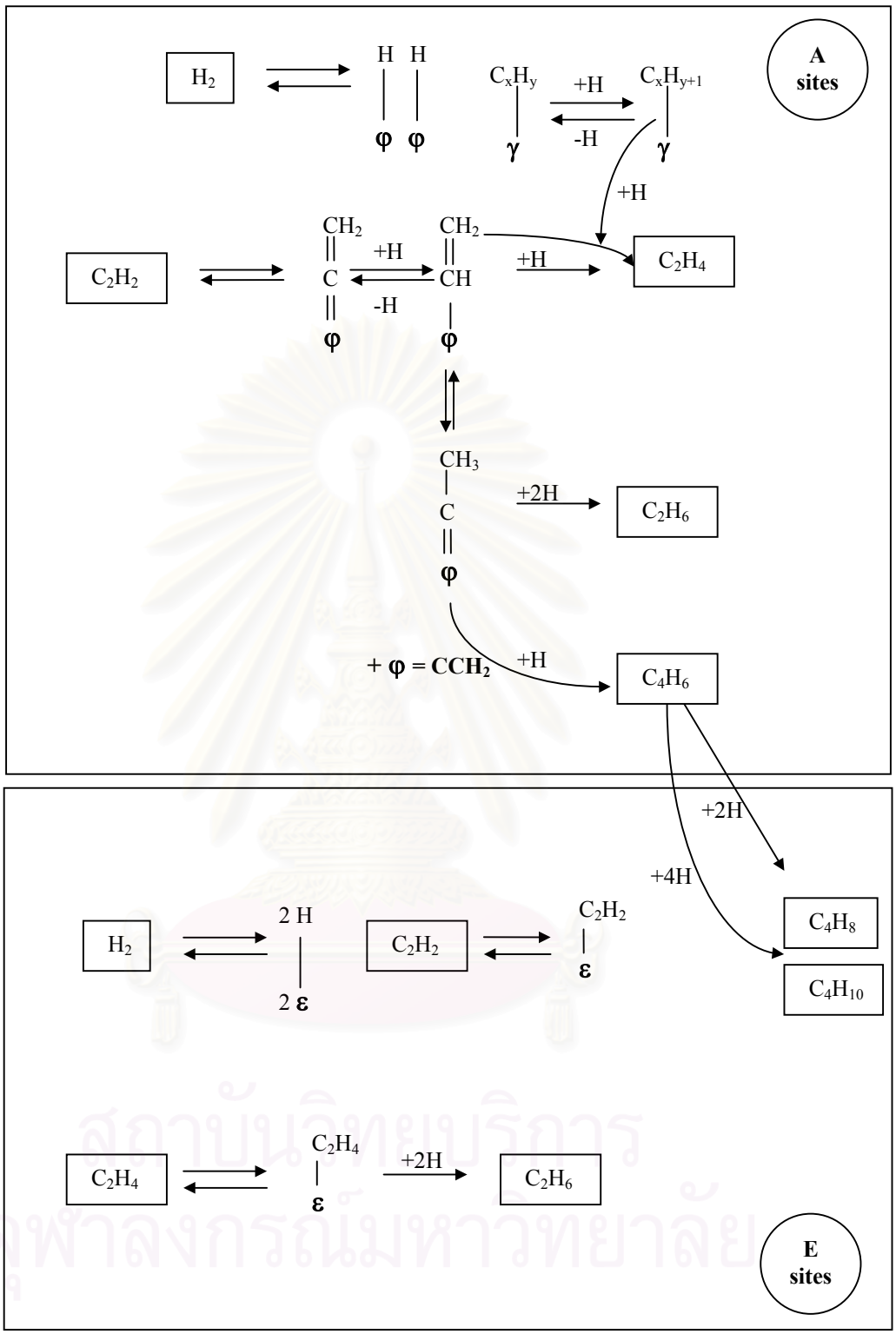

Figure 3.5 Proposed mechanism for acetylene hydrogenation of acetylene-ethylene mixtures over Pd/α-Al_2O_3 catalyst: φ and ε denote the surface palladium adsorption sites in "A" sites and "E" sites; γ denotes the surface palladium adsorption sites covered by irreversibly adsorbed carbonaceous deposits [104].

CHAPTER IV

EXPERIMENTAL

This chapter describes the experimental systems and the experimental procedures used in this study. The chapter is divided into three sections, i.e., catalyst preparation and pretreatment, catalyst evaluation and catalyst characterisation. The chemicals, apparatus and procedures for catalyst preparation and pretreatment with oxygen-containing compounds are explained in section 4.1. Details of catalyst evaluation to study catalytic activity are given in section 4.2. Finally, the composition, structure and surface properties of the catalyst characterised by various techniques are discussed in section 4.3.

4.1 Catalyst Preparation

Typically, catalysts containing low-surface area alumina and low palladium (Pd) content are used as commercial alkynes hydrogenation catalysts. These catalysts are chosen in order to minimise the formation of surface oligomers, resulting from the conjugation of adsorbed acetylene molecules, and to avoid the undesirable hydrogenation of alkenes due to re-adsorption of ethylene [1,9]. By alloying Pd with Ag, the parallel undesirable hydrogenation of alkenes and the direct hydrogenation of alkynes to alkanes are remarkably suppressed [17,64]. As a result, Ag promoted low Pd/α-alumina was prepared and used as a model catalyst for the selective hydrogenation of acetylene.

4.1.1 Materials

The support and metal precursors used for the catalyst preparation are listed in Table 4.1.

Table 4.1 Details of chemical reagents used for the catalyst preparation.

Chemical	Formula	Manufacturer
1. Alumina pellet (type CS-303)	α-Al_2O_3	United Catalyst Incorporation (UCI), U.S.A.
2. Palladium nitrate	$Pd(NO_3)_2$	Wako Pure Chemical Industries Co., Ltd., Japan
3. Silver nitrate	$AgNO_3$	Sigma-Aldrich Chemical Co., U.S.A.
4. Hydrochloric acid	HCl	Merck, Germany

4.1.2 Preparation Procedures [105]

4.1.2.1 Preparation of Alumina Support

Spherical alumina granules were ground to the required mesh size (40/60), then washed in distilled water to remove very fine particles and other impurities. The washed particles were subsequently dried in the oven at 110^{o}C overnight and calcined in air at 300^{o}C for 2 h.

4.1.2.2 Preparation of Palladium and Silver Stock Solutions

The palladium or silver stock solutions were obtained by dissolving 0.1 g palladium nitrate or 0.5 g silver nitrate in de-ionised water then making the total volume of the solution to 25 ml.

4.1.2.3 Preparation of Bimetallic Palladium-Silver Catalyst

A 0.03wt%Pd-0.235wt%Ag/α-Al_2O_3 catalyst was prepared by the sequential impregnation technique detailed as follows:

1.) The impregnating solution for 2 grams of support was prepared by calculating the amount of the stock solution to obtain the required metal loading (see Appendix A). The de-ionised water was then added to obtain 1 ml-solution.

2.) 2 grams of alumina support was placed in an Erlenmeyer flask then the impregnating solution from the palladium stock solution was gradually dripped into the support. Shaking the flask continuously during impregnation was required to ensure the homogeneous distribution of metal component on the support.

3.) The impregnated support was left to stand for 6 h to assure adequate distribution of metal complex. The support was subsequently dried at 110^{o}C in air overnight.

4.) The dried impregnated support was calcined under 60 ml/min nitrogen with the heating rate of 10^{o}C/min until the temperature reached 500^{o}C. 100 ml/min of flowing air was then switched into the reactor to replace nitrogen and the temperature was held at 500^{o}C for 2 h.

5.) The palladium impregnated sample was re-impregnated with silver complex using a similar procedures with the exception that the calcination were performed at 370^{o}C and held at that temperature for 1 h.

6.) The calcined sample was finally cooled down and stored in a glass bottle in a dessicator for later use.

4.1.3 Pretreatment Procedures

The prepared catalyst was pretreated with oxygen or other oxygen-containing compounds, i.e., N_2O, NO, CO_2 and CO, prior to the reaction test. After reduction in H_2 flow at 150^{o}C for 2 h at a heating rate of 10^{o}C/min, the catalyst was cooled in inert gas (Ar) to the predetermined pretreatment temperature. This varied between 80-110^{o}C. Effective amounts of each pretreatment gas (0.02-0.12 ml) were injected into the system afterwards. Effective conditions for pretreatment with oxygen and oxygen-containing compounds are given in Appendix C.

4.2 Catalyst Evaluation

The catalytic performance for the selective hydrogenation of acetylene was measured at a GHSV of 2000 h^{-1}. A temperature programmed reaction was conducted from 40 to 90^{o}C in order to cover the industrial window operation (65-85^{o}C [7,8]). Materials, apparatus and operating procedures are detailed as below:

4.2.1 Materials

The reactant gas used for the catalyst evaluation was the ethylene feedstream to the acetylene converter as supplied by the National Petrochemical Co. Ltd., Thailand. The gas mixture contained 0.716vol% C_2H_2, 0.823vol% H_2, 33.707vol% C_2H_6 and balance C_2H_4. Ultra high purity hydrogen and high purity argon manufactured by Thai Industrial Gas Limited (TIG) were used for reduction and cooling processes.

4.2.2 Apparatus

The catalytic test was performed in a flow system as shown diagrammatically in Figure 4.1. The apparatus consisted of a quartz tubular reactor, an electrical furnace and an automation temperature controller. The instruments used in this system are listed and explained as follows:

4.2.2.1 Reactor

The reaction was performed in a conventional quartz tubular reactor (inside diameter = 0.9 cm), at atmospheric pressure.

4.2.2.2 Automation Temperature Controller

This unit consisted of a magnetic switch connected to a variable transformer and a RKC temperature controller series connected to a thermocouple attached to the catalyst bed in a reactor. A dial setting established a set point at any temperature within the range between 0 to 999^{o}C. The accuracy was ± 2^{o}C.

4.2.2.3 Electrical Furnace

The furnace supplied the required temperature to the reactor which could be operated from room temperature up to 800^{o}C at maximum voltage of 220 volts.

4.2.2.4 Gas Controlling System

Reactant, hydrogen and carrier gas for the system was each equipped with a pressure regulator and an on-off valve and the gas flow rates were adjusted by using metering valves.

4.2.2.5 Gas Chromatograph

The products and feeds were analyzed by a gas chromatograph equipped with a FID detector (SHIMADZU FID GC 9A, carbosieve column S-2) for separating C_2H_2, C_2H_4 and C_2H_6. H_2 was analyzed by a gas chromatograph equipped with a TCD detector (SHIMADZU TCD GC 8A, molecular sieve 5A). The operating conditions for each instrument are summarised in Table 4.2.

Table 4.2 Operating conditions of gas chromatographs.

Gas Chromatograph	SHIMADZU GC-9A	SHIMADZU GC-8A
Detector	FID	TCD
Packed column	carbosieve column S-II	Molecular sieve 5A
Carrier gas	Ultrahigh purity He	Ultrahigh purity Ar
Carrier gas flow rate (ml/min)	30	30
Injector temperature (^{o}C)	185	80
Initial Column temperature (^{o}C)	100	50
Initial holding time (min)	50	-
Programme rate (^{o}C/min)	10	-
Final column temperature (^{o}C)	180	50
Initial final holding time (min)	160	-
Current (mA)	-	70
Analysed gas	CH_4, C_2H_2, C_2H_4, C_2H_6	H_2

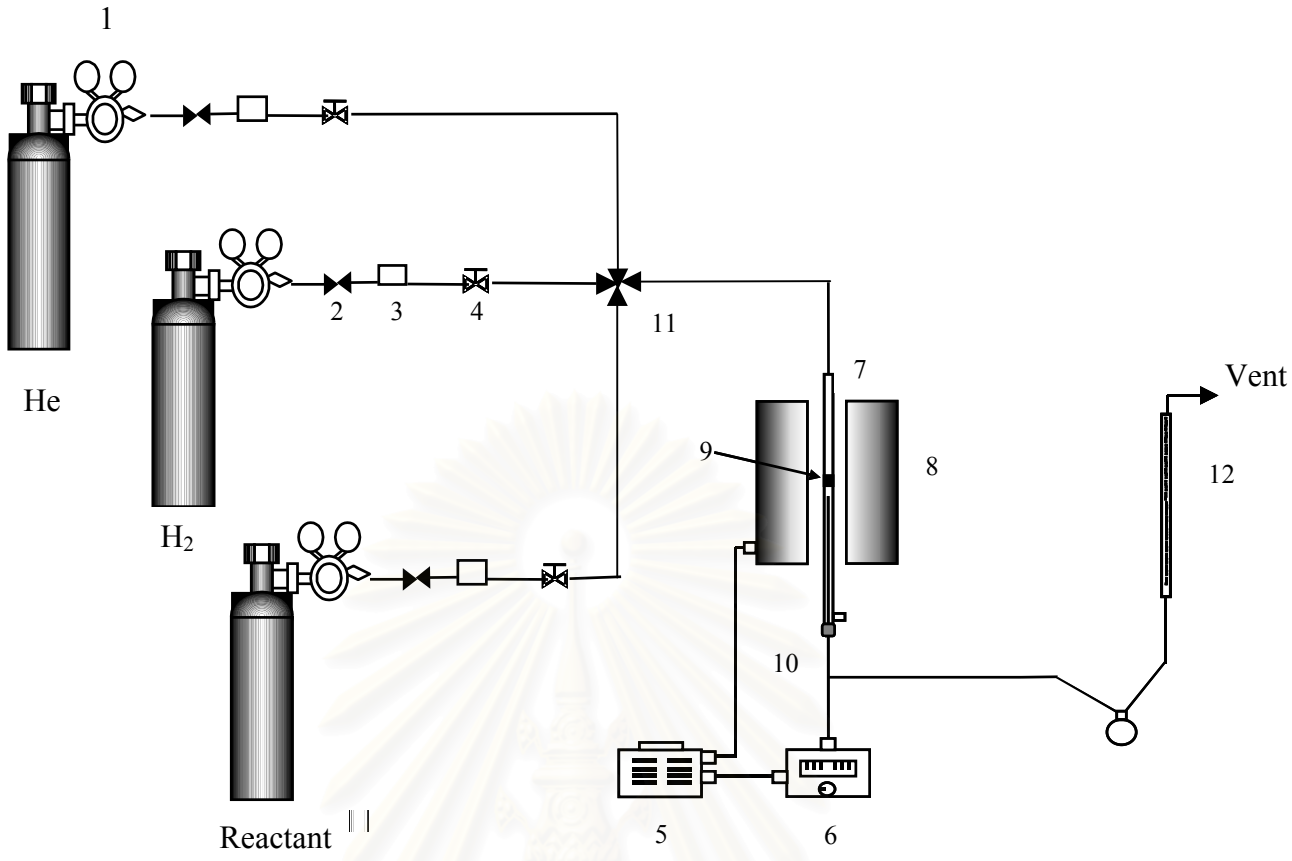

1. pressure regulator
2. on-off Valve
3. gas filter
4. needle valve
5. variable voltage transformer
6. temperature controller
7. reactor
8. furnace
9. catalyst bed
10. thermocouple
11. 4-way joint
12. bubble flow meter

Figure 4.1 Flow diagram of the selective hydrogenation of acetylene.

4.2.3 Procedures

0.5 g of catalyst was packed in a quartz tubular downflow reactor. The catalyst bed length was about 0.6 cm. The reactor was placed into the furnace and argon was introduced into the reactor in order to remove remaining air. Prior to reaction, the catalyst was reduced with 100 ml/min hydrogen at a temperature of 150^{o}C and held at that temperature for 2 h. Afterwards, argon was switched in to replace hydrogen and held at that temperature for 10 min in order to remove the remaining hydrogen. Subsequently, the system was cooled to pretreatment temperature where effective amount of pretreatment gas, i.e., CO, CO_2, O_2, NO or N_2O, were injected with the carrier flow. The system was held at that temperature for 10 min before cooling down to reaction temperature.

A reactant gas which contained 0.716vol% C_2H_2, 0.823vol% H_2, 33.707vol% C_2H_6 and balance C_2H_4 at a total flow rate of 15 ml/min (GSHV = 2000 h^{-1}) was used as a model gas to test the catalytic performance through temperature programmed reaction. The reactant was introduced at elevated temperature from 40 to 90^{o}C. At each temperature, sampling was undertaken when the steady state of the system was reached, which was approximately within 20 min. Effluent gases were sampled to analyse the concentration of CH_4, C_2H_2, C_2H_4 and C_2H_6 using GC-9A equipped with a carbosieve S-II column, whereas H_2 concentration was analysed by GC-8A equipped with a molecular sieve 5A column. Details of the calculation of the catalyst activity to convert acetylene and the selectivity towards ethylene in term of ethylene gain are given in Appendix B.

4.3 Catalyst Characterisation

Various characterisation techniques were used in this studied in order to clarify the catalyst structure and morphology, surface composition and adsorption properties of catalysts as a result of pretreatment with oxygen or oxygen-containing compounds on the behaviour of Pd-Ag/Al_2O_3 catalyst for acetylene hydrogenation. The structure and morphology of the prepared catalyst before and after pretreatment were studied using surface area measurements, x-ray diffractometer (XRD) and transmission electron microscopy (TEM) and the details of each technique will be

described in section 4.3.1. In the second part, the surface analysis of the catalyst was investigated employing CO chemisorption, X-ray photoelectron spectroscopy (XPS), Temperature programmed reduction (TPR) and hydrogen temperature programmed desorption (H_2-TPD). Details of the study of species formation upon pretreatment and reactant adsorption employing infrared spectroscopy (FT-IR) will be described.

4.3.1 Bulk Structure and Morphology of the Catalyst

4.3.1.1 Specific Surface Area Measurement

Surface area measurements were carried out by low temperature nitrogen adsorption in a volumetric equipment Gemini 2600 from Micromeritics at Catalysis Laboratory, CCMC, UNAM, Mexico. Calculations were performed on the basis of the BET isotherm.

4.3.1.2 Determination of Bulk Chemical Composition

The actual percentage of metal content of the prepared catalyst was measured by atomic absorption spectroscopy (AAS) method at Thailand Institute of Science and Technology Research, Bangkok, Thailand.

4.3.1.3 X-ray Diffraction (XRD) Analysis

The crystallinity, structure and composition of catalysts were analysed by XRD analysis. The refraction or diffraction of the X-ray was monitored at various angles with respect to the primary beam. XRD measurements were carried out on Phillips X'pert XRD diffractometer using Cu K_α radiation. The preparation of pretreated samples was performed in an atmospheric bag using inert gas and covered with the paraffin film in order to prevent air exposure at Catalysis Laboratory, CCMC, UNAM, Ensenada, Mexico.

4.3.1.4 Particle Size by TEM

The morphology of the catalyst sample as well as particle size measurements were performed by transmission electron microscopy (TEM), using a JEOL instrument (JEM-200CX) at the Scientific and Technological Research Equipment Centre, Chulalongkorn University (STREC), Bangkok, Thailand.

4.3.2 Surface Analysis

4.3.2.1 Metal Active Site Measurement

Metal active sites were measured using CO chemisorption technique where a known amount of CO was pulsed into the catalyst bed at room temperature. The number of metal active sites was measured on the basic assumption that only one CO molecule adsorbed on one metal active site [110]. Carbon monoxide that was not adsorbed was measured using thermal conductivity detector. Pulsing was continued until no further carbon monoxide adsorption was observed. The quantity of carbon monoxide adsorbed by the catalyst sample could then be calculated and hence a metal surface area and a metal dispersion obtained [107]. Calculation details of %metal dispersion are given in Appendix D.

a) Materials

Ultrahigh purity helium and ultrahigh purity hydrogen were used as a carrier gas and reducing agent, respectively. Pure carbon monoxide was used as an adsorbent gas. All gases used in this experiment were supplied by Thai Industrial Gas Limited.

b) Apparatus

The amount of carbon monoxide adsorbed on the metal surface was measured by a thermal conductivity detector within a gas chromatograph (GOW-MAC). The operating conditions of gas chromatograph is

illustrated in Table 4.3. The extensive diagram of instruments in the measurement of the metal active sites is illustrated in Figure 4.2.

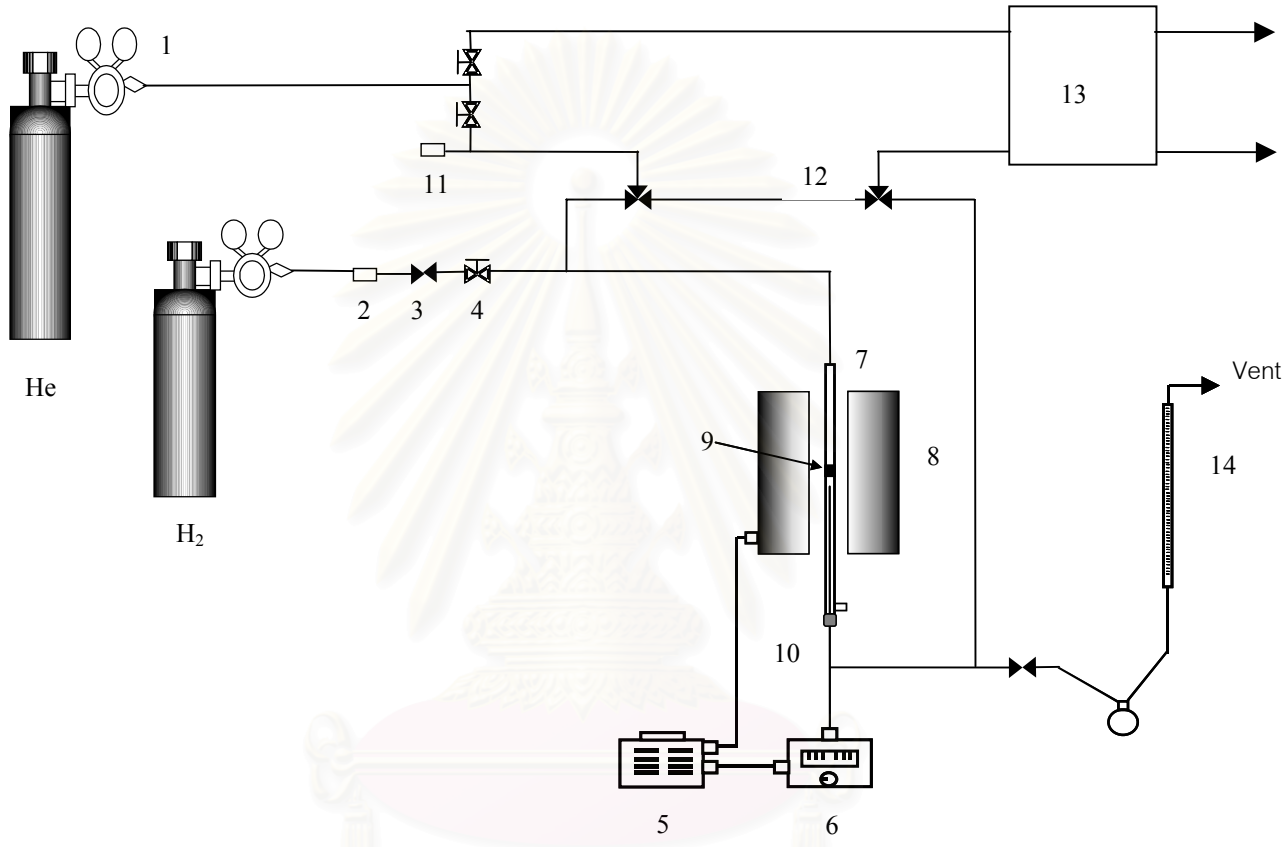

1. pressure regulator
2. gas filter
3. on-off valve
4. needle valve
5. variable voltage transformer
6. temperature controller
7. reactor
8. furnace
9. catalyst bed
10. thermocouple
11. injection port for CO
12. three-way valve
13. thermal conductivity detector
14. Bubble flow meter

Figure 4.2 Flow diagram of measurement of CO chemisorption.

Table 4.3 Operating conditions of the thermal conductivity detector within the gas chromatograph (GOW-MAC) for CO-adsorption measurement.

Model	GOW-MAC
Detector type	TCD
Carrier gas	Ultrahigh purity helium
Carrier gas flow rate (ml/min)	30
Detector temperature (^{o}C)	80
Detector current (mA)	80

c) Procedures

0.5 g of the catalyst sample was packed in a stainless steel tubular reactor. Helium gas was introduced into the reactor at the flow rate of 30 ml/min for 10 min in order to remove remaining air. The system was switched to 100 ml/min of hydrogen and heated at an increasing rate of 10^{o}C/min until the temperature reached 150^{o}C and held at that temperature for 2 h. After finishing reduction, the catalyst was cooled to ambient temperature under flowing helium.

50 μl of purity carbon monoxide gas was injected into the injection port to adsorb on the metal surface of the catalyst sample. The pulse was repeated until adsorption no longer occurred.

4.3.2.2 Surface Analysis by X-ray Photoelectron Spectroscopy (XPS)

a) Apparatus

The *ex situ* XPS analysis was performed originally using an analysis chamber equipped with a Riber-CAMECA MAC-3 system, CCMC-UNAM, Mexico. An improved XPS analysis was performed on a Kratos XSAM 800 spectrometer (Surface Science Technology, School of Chemistry, The University of New South Wales, Australia), equipped with a Mg K_{α} X-ray as a primary excitation, hemispherical energy analyser and triple channeltron detectors. A schematic

diagram of this instrument is shown in Figure 4.3. For a typical analysis, the source was operated at voltage of 15 kV and current of 12 mA. The pressure in the analysis chamber was less than 10^{-9} Torr and the area analysed was approximately 4 mm^2. A dynamic ion gun was available for argon etching. The Kratos XSAM 800 system is computer controlled using the Kratos "Vision" software.

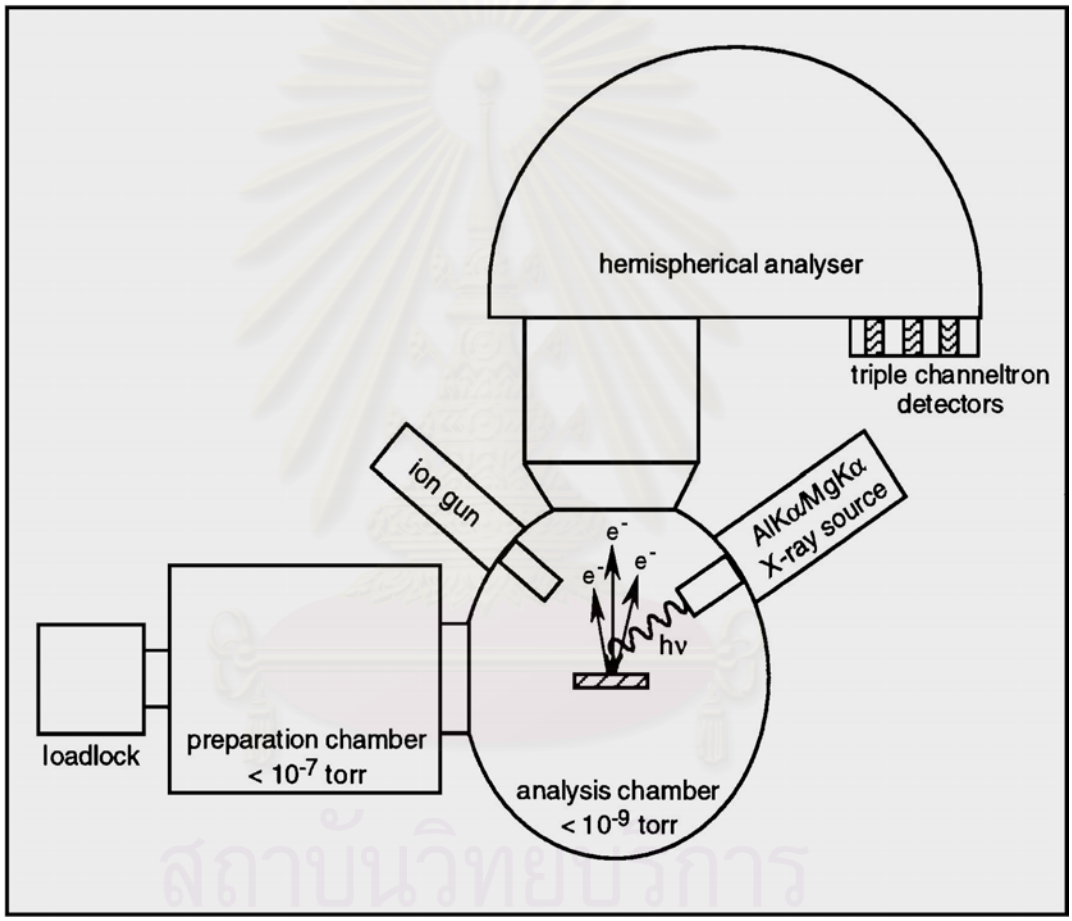

Figure 4.3 Schematic diagram of the XPS machine (Kratos XSAM 800).

b) Procedures

An improved XPS method was obtained by transferring the catalyst sample from the reaction system described in section 4.2 (Figure 4.1) to an atmospheric bag where the samples were prepared for analysis by manual grinding using a mortar and pestle in an inert (N_2) atmosphere. Evenly spread powders were mounted on sample stubs using a double-side adhesive tape, and transferred into the loadlock of the Kratos XSAM, XPS Spectrometer. The sample was further transferred into the preparation chamber where the pressure of the system was kept below 10^{-7} Torr by a transferring device. In order to analyse all elements containing in the sample, wide scan with a pass energy of 160 eV and a collection time of 300 seconds per 1 eV step was first performed. The high resolution scans were obtained using an analyser pass energy of 20 eV and a collection time of 298 milliseconds per 0.1 eV

Assigning the major component of the Aluminium (Al) 2p photoelectron peak envelope to 74.6 eV made corrections to binding energy values to compensate for sample charging. The spectra were resolved into Gaussian-Lorentzian components after background subtraction, using Shirley fitting routine.

4.3.2.3 Temperature Programmed Experiments

a) Materials

The reducing gas for TPR experiment was a mixture of 10% H_2 in Ar. Carrier gas for the TPR system and the thermal conductivity detector was ultrahigh purity Ar.

b) Apparatus

TPR and H_2-TPD were conducted using a thermo-desorption apparatus AMI-M, Altamira, CCMC-UNAM, Mexico.

c) Procedures

Approximately 1 g catalyst was packed in the TPR pyrex cell and a 20 ml/min Ar flow was switched into the system. The sample was heated in Ar at 200°C for 1 h in order to remove adsorbed H_2O. TPR of the oxidised sample was then performed using 10%H_2/Ar as the reducing agent. The temperature was ramped up to 500°C at a rate of 20°C/min and maintained at 500°C for 10 min. TPD was performed after reduction at 150°C for two hours. The system was switched to Ar atmosphere and cooled down to room temperature in order to expose to H_2. Hydrogen was then adsorbed on the sample before flushing with argon. Desorption spectra were registered during temperature increase (20°C/min).

4.3.3 Study of Surface Species Formation

Characterisation of the surface species on the Pd-Ag/Al_2O_3 catalysts was made by Fourier transform infrared (FT-IR) spectroscopy.

a.) Materials

Ultrahigh purity helium and ultrahigh purity hydrogen were used as carrier and reducing gases, respectively. High purity C_2H_2 and C_2H_4 were used as probe molecules to study species formed on the Pd-Ag/Al_2O_3 catalyst for the selective hydrogenation of acetylene.

b.) Apparatus

The FTIR spectrometer was used as a detector in the experiments. A Nicolet model Impact 400 FT-IR equipped with a deuterated triglycine sulfate (DTGS) detector and connected to a personal computer with Omnic version 1.2a on Windows software (to fully control the functions of the IR analyser) were applied to this study. The IR gas cell used in this experiment, shown in Figure 4.4, was made of a quartz and covered with 32×3 mm NaCl windows at each end of the cell. Each

window was sealed with two O-rings and a stainless flange fastened by a set of screws.

The quartz sample holder for the sample disk (to keep it perpendicular to the IR beam) was arranged in the IR cell. A thermocouple was used to measure the sample temperature, which was controlled by a variable voltage transformer and a temperature controller.

The schematic diagram of the *in situ* FT-IR apparatus is depicted in Figure 4.5. All gas lines, valves and fittings in this apparatus were made of pyrex glass except the IR gas cell and the sample disk holder, which were made of quartz. A Labconco 195-500 HP vacuum pump, which theoretically had capacity at 10^{-4} Torr, was used for system evacuation.

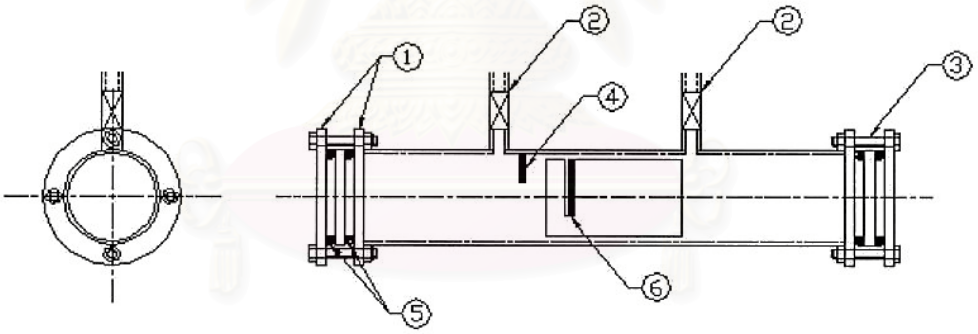

1. stainless steel flange
2. valve
3. bolt
4. thermocouple position
5. O-ring
6. self-supporting disk (sample)

Figure 4.4 IR gas cell used in in situ FT-IR experiments.

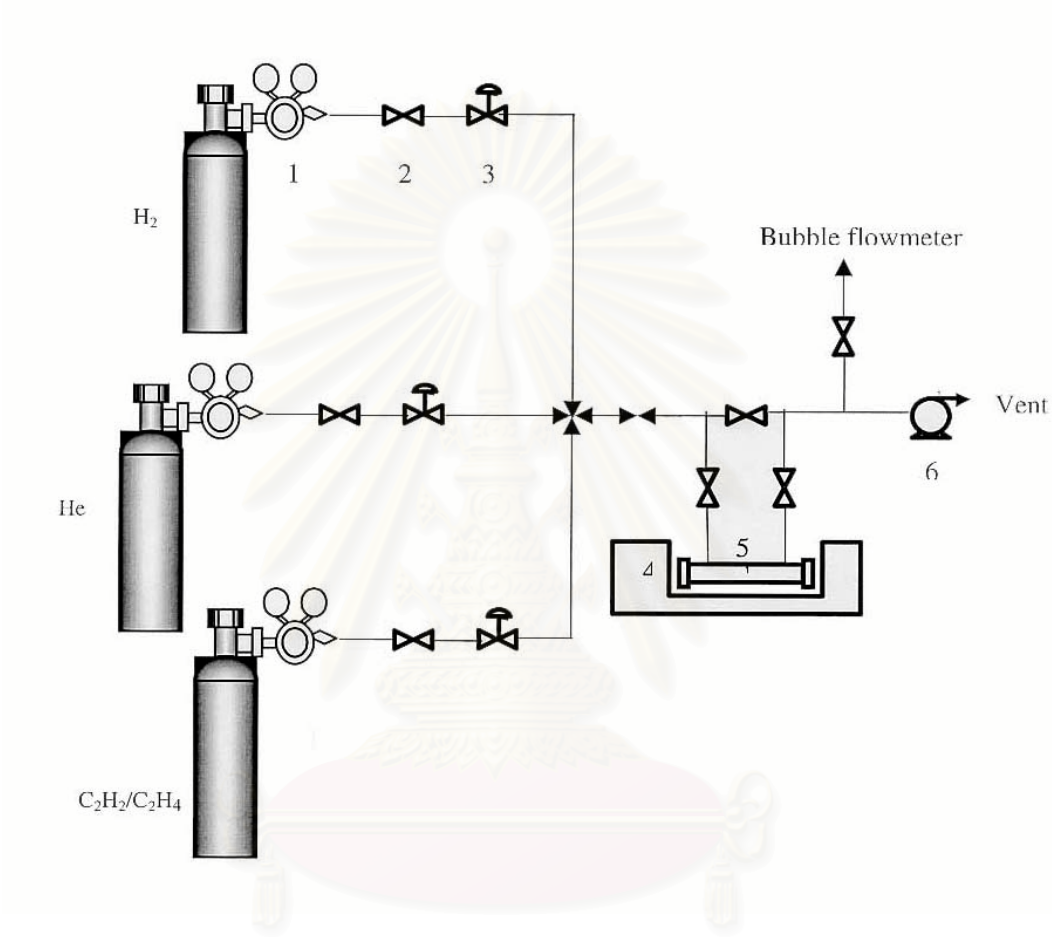

1. pressure regulator
2. on-off valve
3. Metering valve
4. FT-IR analyser
5. IR quartz gas cell
6. vacuum pump

Figure 4.5 Flow diagram of instrument used for *in situ* FTIR experiments.

c.) Procedures

Catalyst samples were pressed into self-supporting pellets (20 mm in diameter) and loaded into the IR cell. Infrared spectra were collected in the absorbance mode with a resolution of 4 cm^{-1}.

The catalysts were reduced in flowing hydrogen at 150^{o}C for 2 h, after which time H_2 was switched off and the sample was purged with argon. The sample after reduction will be called untreated sample hereafter. The spectrum of the untreated sample was collected after the system was cooled down to the ambient temperature.

For samples with pretreatment, the system was cooled after reduction by purging with argon until pretreatment temperature. A known amount of pretreatment gases, i.e., CO, CO_2, NO and N_2O, was then injected into the system and the temperature was held for ten minutes before cooling to room temperature. The spectra were then measured.

The surface species formation upon exposure with reactants was determined by individual exposure of the catalyst surface with acetylene or ethylene at the reaction temperature (40^{o}C) after reduction and pretreatment described above. The spectra were observed after surface saturation (details will be given later in section 5.2.4.2.).

CHAPTER V

RESULTS AND DISCUSSION

The main topic of this study involves an attempt to clarify effects of pretreatment with oxygen and oxygen-containing compounds on the reactivity behaviour of Pd-Ag catalysts for the selective hydrogenation of acetylene. In order to accommodate the detailed consideration, this chapter is categorised into three sections. The catalyst evaluation for the selective hydrogenation of acetylene is firstly discussed in section 5.1. Characterisation of the catalyst is described in section 5.2. Correlation between the reactivity in section 5.1 and catalyst characterisation in section 5.2 leads to the subsequent section 5.3 where a plausible explanation of the synergetic effect of pretreatment is postulated.

5.1 Catalyst Evaluation

The performance of a catalyst for the selective hydrogenation of acetylene is generally evaluated in terms of acetylene conversion and selectivity towards ethylene. Acetylene conversion, is defined as moles of acetylene converted with respect to acetylene in the feed. Selectivity is the ratio of the amount of acetylene converted to ethylene and total amount of acetylene converted. Ideally, there should be one acetylene molecule converted for every hydrogen molecule consumed, or 100% selectivity, since all of the acetylene is converted into ethylene. In actual practice, some hydrogen will always be consumed in the side reaction of ethylene conversion to ethane. With time on stream, the H_2 consumption increases until all of the acetylene is converted to ethane and none remains as ethylene. At that point, the selectivity is 0%. The selectivity can be measured by observing the change in ethane and ethylene from the inlet and the outlet. However, this is not practical since a change of 0.05% in the measurement would be a 10% change in selectivity for 0.5% of acetylene at the inlet. The selectivity in term of ethylene gain can also be measured by looking at the hydrogen consumed in the converter and the amount of acetylene converted. The performance of the catalyst in this study will therefore be reported in terms of acetylene conversion and ethylene gain observed from hydrogen and acetylene concentrations as detailed below:

Ethylene gain is considered from the following reaction schemes:

$$C_2H_2 + H_2 \longrightarrow C_2H_4 \qquad (5.1)$$

$$C_2H_4 + H_2 \longrightarrow C_2H_6 \qquad (5.2)$$

Ethylene gain is defined as the ratio of those parts of acetylene that are hydrogenated to ethylene to the amount of totally hydrogenated acetylene:

$$C_2H_4 \text{ gain } (\%) = 100 \times \frac{C_2H_2 \text{ hydrogenated to } C_2H_4}{\text{totally hydrogenated } C_2H_2} \qquad (i)$$

where totally hydrogenated acetylene is the difference between moles of acetylene in the product with respect to those in the feed (dC_2H_2).

Acetylene hydrogenated to ethylene is the difference between the total hydrogenated acetylene (dC_2H_2) and the ethylene being loss by hydrogenation to ethane (equation 5.2). Regarding the difficulty in precise measurement of the ethylene change in the feed and product, the indirect calculation using the difference in the hydrogen amount (hydrogen consumed: dH_2) is used.

The ethylene being hydrogenated to ethane is the difference between all the hydrogen consumed and all the acetylene having been totally hydrogenated.

C_2H_4 gain from equation (i) can be rewritten as:

$$C_2H_4 \text{ gain } (\%) = \frac{100 \times [dC_2H_2 - (dH_2 - dC_2H_2)]}{dC_2H_2} \qquad (ii)$$

Or in the other words, as equations (5.1) and (5.2) show, 2 moles of hydrogen are consumed for the acetylene lost to ethane, but only 1 mole of hydrogen for the acetylene gained as ethylene. The overall gain can also be written as:

$$C_2H_4 \text{ gain } (\%) = 100 \times \left[2 - \frac{dH_2}{dC_2H_2}\right] \qquad (iii)$$

Equations (ii) and (iii) are, of course the same, and ethylene gain discussed in this research is then calculated, based on equation (iii). This value is the percentage of the theoretically possible ethylene gain which has been achieved in the operation. A positive value represents net production of ethylene. When the negative value refers to ethylene loss. However, it should be noted that these calculations cannot provide a measure of the acetylene polymerisation reaction that forms green oil.

Typically, the normal operating temperature in an acetylene converter lies in the range 65-85^{o}C [1,83,35]. During start-up, the reaction can proceed at as low as 45^{o}C. After a short period during which the catalyst has stabilized, the reactor temperature will reach the normal operating range and will remain constant throughout its life-time. According to the literature, acetylene hydrogenation usually exhibits three distinct phases [3,28,31]. In a brief initial period (0-2 min-on stream), the reaction is rapid, forming both ethylene and ethane. In the second phase (ca. 2-60 min on stream), the rates of acetylene consumption, and ethylene and ethane production are all constant. During this period, hydrogenation of acetylene is the primary reaction. The selectivity is usually high, and is characteristic of changes occurring in the catalyst. The third phase begins when acetylene hydrogenation is nearly complete, and in this region approximates to the industrial situation. As previously described, the reaction during 2-60 min on stream is in the constant rate period, consequently, the performance of the catalyst as a function of reaction temperature is evaluated from the data taken in this period.

5.1.1 Temperature Dependence

Study of temperature dependence of 0.03wt%Pd-0.235wt%Ag/Al_2O_3 on acetylene conversion is evaluated in the range between 40-90^{o}C at a space velocity of 2000 h^{-1} as illustrated in Figure 5.1. The untreated catalyst presented refers to a catalyst reduced at 150^{o}C and studied immediately thereafter. A sample of the same catalyst was similarly reduced, but a small amount of oxygen or oxygen-containing compounds was introduced into the catalyst before being used for the reaction (previously described in section 4.1.3, Chapter 4). The catalyst with such pretreatment would be named as CO-, CO_2-, O_2-, NO- or N_2O-treated catalyst according to the pretreatment gas that was used.

As shown in Figure 5.1 **(A)**, activity of all catalysts directly increases with rising temperature as the kinetic energy of the system increases with increasing temperature. All the treated catalysts exhibit higher activity ca. 20-37 % than that of the untreated catalyst at low reaction temperature (40-50^{o}C). At higher temperature (60-90^{o}C) where almost all the acetylene is converted, the effect of pretreatment on activity enhancement is less pronounced. Ethylene gain, Figure 5.1 **(B)**, observed over all samples, declines when the temperature is increased. This can be explained by either the decrease in the extent to which acetylene is more strongly adsorbed than ethylene [3] or the increase in the rate of ethylene hydrogenation to ethane with increasing temperature. With respect to the untreated catalyst, the catalysts treated by NO and N_2O show higher ethylene gain at all reaction temperature while lower ethylene gain is observed from other pretreatment.

Regarding the very low concentration of metal loading in the catalyst samples (0.03wt%Pd-0.235wt%Ag/Al_2O_3), a higher amount of metal was impregnated into the alumina support in order to perform the characterisation more easily. Reactivity of the high metal loaded catalyst was conducted under the identical reaction conditions as performed at low metal loading. Figure 5.2 displays the catalytic performance of 3wt%Pd-4wt%Ag/Al_2O_3 for the acetylene hydrogenation as a function of temperature. Similar behaviour of the activity enhancement by pretreatment is seen in the high metal loading catalyst. Again, only pretreatment with NO and N_2O results in higher ethylene gain compared to the value observed from untreated catalyst. However, negative values of ethylene gain at high reaction temperature (80-90^{o}C) are revealed, indicating that all of the acetylene is converted to ethane and some of the ethylene feed is additionally converted to ethane.

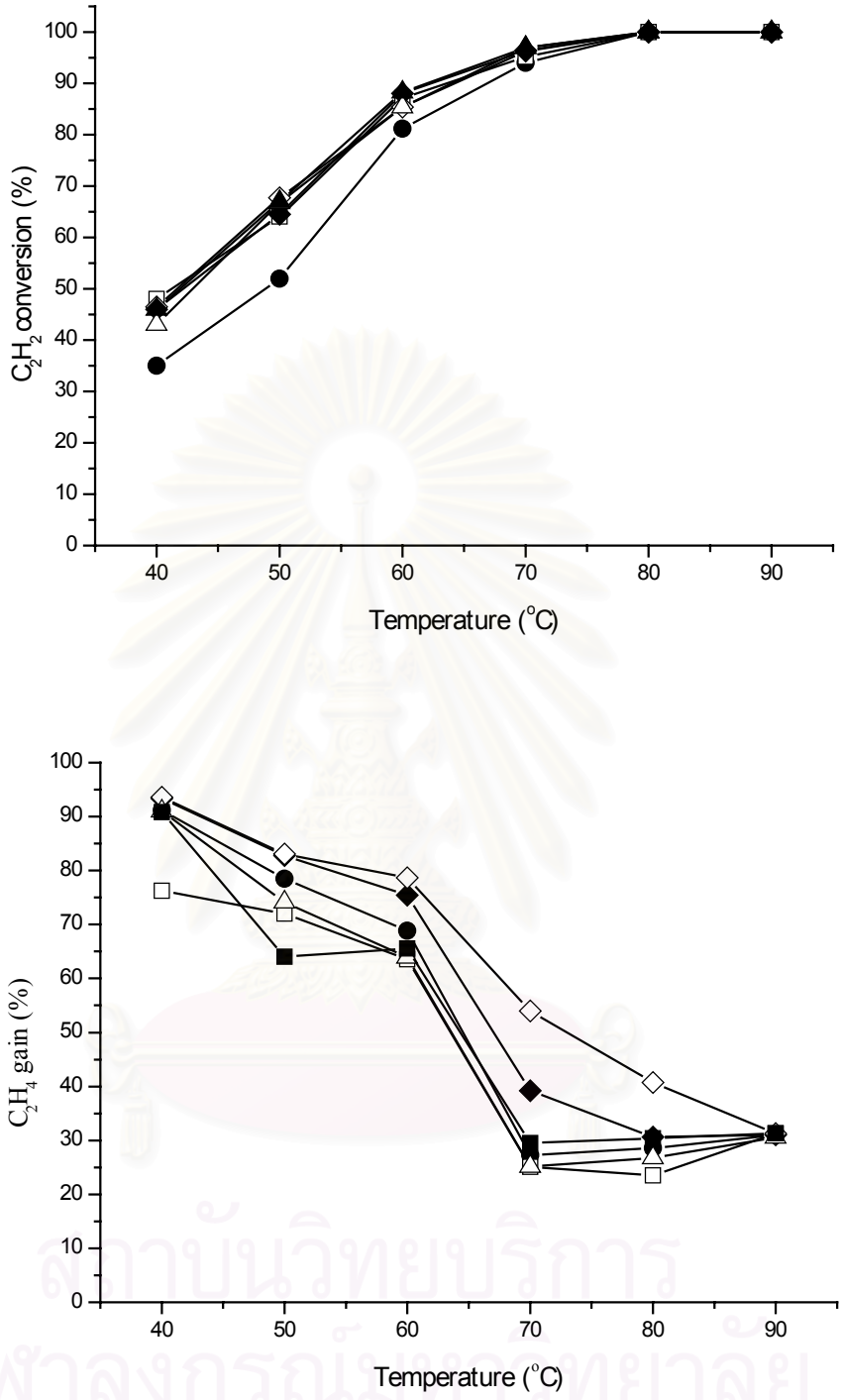

Figure 5.1 Dependence of the catalytic performance of 0.03%Pd-0.235%Ag/Al_2O_3 catalysts on the reaction temperature: (**A**) % C_2H_2 conversion and (**B**) % C_2H_4 gain; (●) untreated, (▲) CO_2-treated, (Δ) CO-treated, (□) O_2-treated, (◆) N_2O-treated, and (M) NO-treated. (Feed contains: 0.716%C_2H_2, 0.823%H_2, 33.707% C_2H_6, balance C_2H_4)

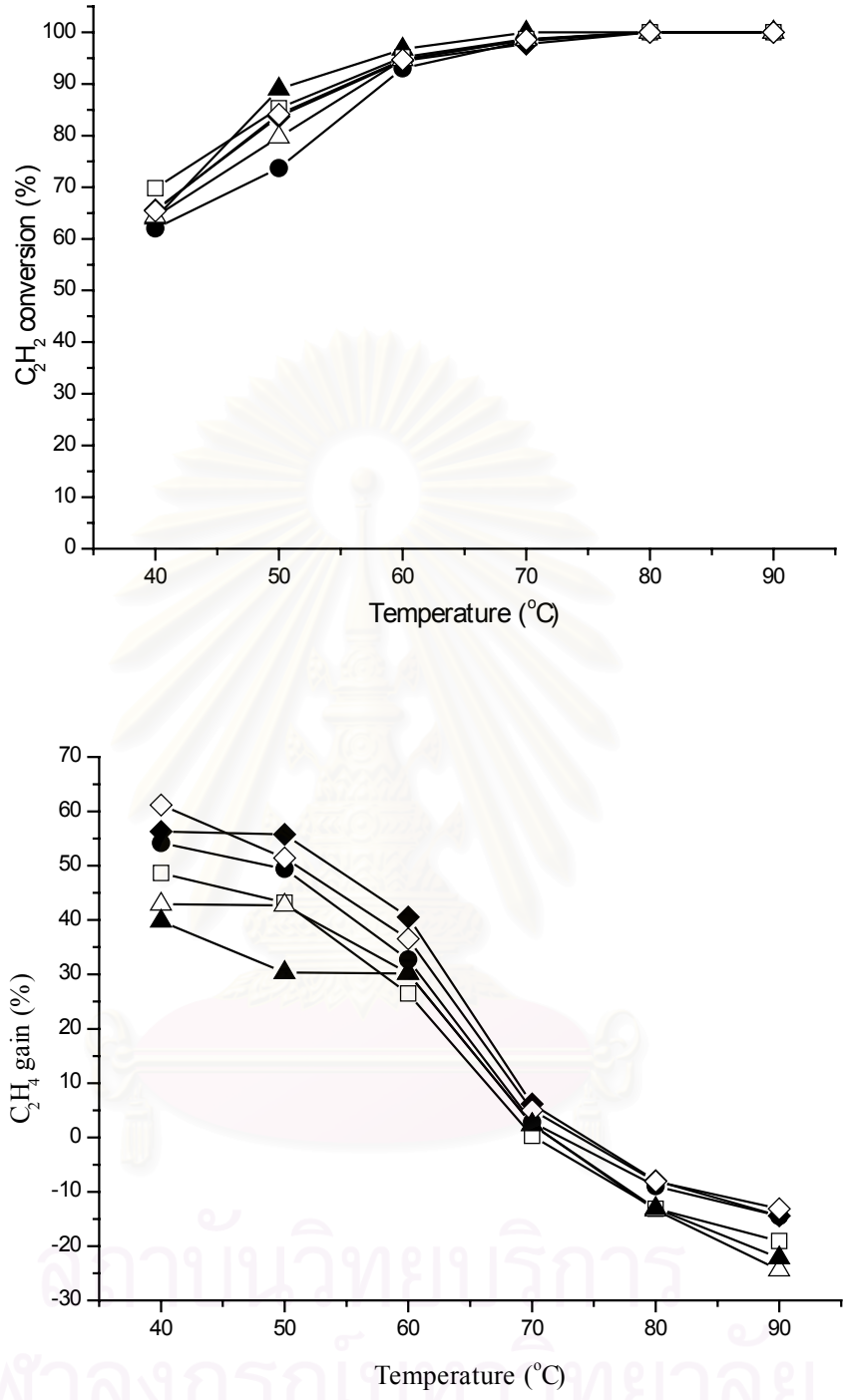

Figure 5.2 Dependence of the catalytic performance of 3%Pd-4%Ag/Al_2O_3 catalysts on the reaction temperature: (**A**) % C_2H_2 conversion and (**B**) % C_2H_4 gain; (●) untreated, (▲) CO_2-treated, (Δ) CO-treated, (□) O_2-treated, (◆) N_2O-treated, and (M) NO-treated. (Feed contains: 0.716%C_2H_2, 0.823%H_2, 33.707% C_2H_6, balance C_2H_4).

5.1.2 Time on Stream

According to the temperature dependence results shown in Figure 5.2, the promotion effect of pretreatment is dominant in the low temperature region (40-50^{o}C) when acetylene conversion was not close to 100%. However, the effect of pretreatment was determined only after 20 min on stream. It is interesting to see whether or not the promoting effect is retained after ageing. The performance of the catalyst for acetylene hydrogenation upon ageing, was therefore, measured at 50^{o}C for 8 h. Observation of the catalytic behaviour was performed for the first 20 min, then every 2 h as illustrated in Figure 5.3. For the untreated catalyst, C_2H_2 conversion increases over the first two hours and reaches a constant value afterwards, see Figure 5.3 **(A)**. N_2O pretreatment shows a similar behaviour, while CO pretreatment requires approximately 6 h to reach a stable conversion. On the other hand, NO and CO_2 pretreatment slightly changes over 8 h on stream. However, all pretreatment improves the activity for acetylene hydrogenation but different magnitudes. N_2O pretreatment increases steady state conversion from 73% to 88% whereas NO pretreatment has only a small shift to 76%. Pretreatment with O_2 and CO_2 have a similar effect on acetylene hydrogenation to that of NO, whereas CO pretreatment is similar to the N_2O pretreatment.

Figure 5.3 **(B)** illustrates a graph of ethylene gain versus time on stream. Generally, ethylene gain observed over 8 h on stream for all catalysts is similar to the conversion data in Figure 5.3 **(A)**, i.e., independent with time on stream. For the untreated catalyst, ethylene gain reaches steady value of ca. 75% after 2 h on stream. After 4 h on stream, ethylene gain for O_2, CO and CO_2 pretreatments reach constant values, which are lower than that for the untreated sample (63%, 68% and 70%, respectively). Preatreatment with NO and N_2O, on the other hand, increases ethylene gain to 83% and 88%, respectively.

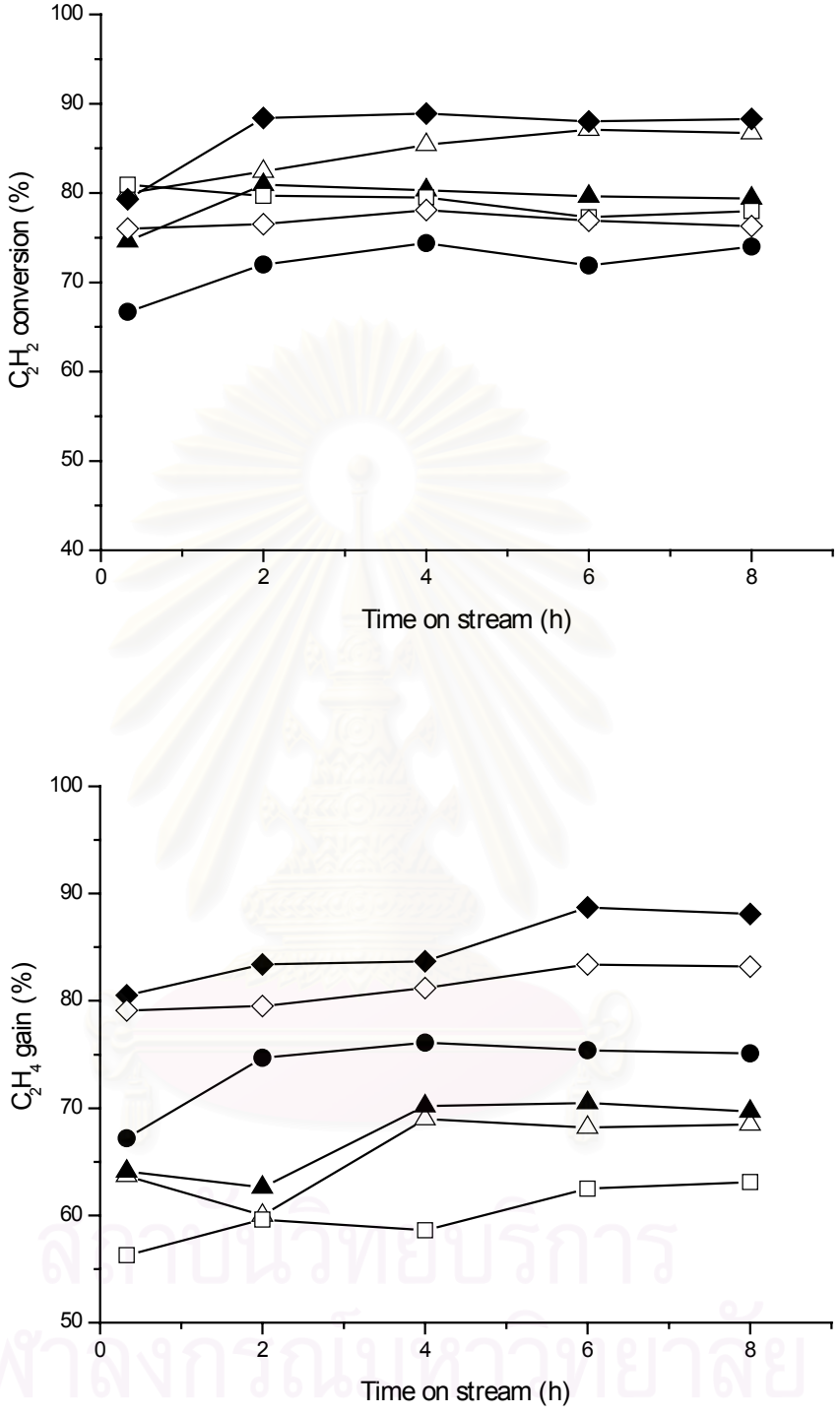

Figure 5.3 Dependence of the catalytic performance of 3%Pd-4%Ag/Al_2O_3 catalysts as a function of time on stream: (**A**) % C_2H_2 conversion and (**B**) % C_2H_4 gain; (●) untreated, (▲) CO_2-treated, (Δ) CO-treated, (□) O_2-treated untreated, (◆) N_2O-treated, and (M) NO-treated. (Feed contains: 0.31%C_2H_2, 31.15%H_2, 19.73%C_2H_6, balance C_2H_4.)

Consideration of acetylene conversion and ethylene gain data suggests that the catalysts behave independently with ageing time for 8 h. No evidence of carbonaceous deposits is expected in the studied system, since if carbonaceous deposits have formed over the catalyst surface during 8 h on stream, a decrease in activity as well as ethylene gain would have been found. However, carbonaceous deposits on the spent catalysts were measured by employing temperature programmed oxidation (TPO) experiments. As expected, no carbonaceous deposits on the catalysts after reaction for either 20 min or 8 h. The ethylene hydrogenation proceeding on the support via spillover mechanism proposed model suggested in Figure 3.3, therefore, fails to explain the results observed.

From the reactivity results, it can be concluded that the Pd-Ag/Al_2O_3 can be activated for the selective hydrogenation of acetylene by pretreatment with oxygen and other oxygen-containing compounds, i.e., CO, CO_2, NO and N_2O. Effect of pretreatment on the activity is more pronounced at low temperature region (40-50^oC) where acetylene is not completely removed (100% conversion). Ethylene gain is increased only by pretreatment with NO_x pretreatment, particularly by N_2O pretreatment. Observation of the time-independence of all catalyst behaviour studied in 8 h on stream as well as the TPO results suggest that there is no effect of carbonaceous deposits involved the mechanism of acetylene hydrogenation in this study. How pretreatment affects the reactivity of the Pd-Ag/Al_2O_3 for the selective hydrogenation of acetylene is described in the following sections.

5.2 Catalyst Characterisation

According to difficulties in characterisation of a very low metal loading 0.03wt%Pd-0.235wt%Ag/Al_2O_3 catalyst, the characterisation here was performed on the 3wt%Pd-4wt%Ag/Al_2O_3 catalyst, whose resemble reactivity behaviour for the selective hydrogenation of acetylene was revealed. In order to elucidate promoting effects of pretreatment on the selective hydrogenation of acetylene described in section 5.1, various characterisation techniques have been performed. The catalyst structure, morphology and metal dispersion are firstly discussed. Reducibility and the property of catalyst toward hydrogen sorption are mentioned, afterwards. Surface

composition and electronic state of metal surface are also investigated. Finally, study on surface species formation is focused.

5.2.1 Catalyst Structure and Morphology

It is well known that the catalyst structure and morphology have crucial effects on catalysts. Their performance is strictly related to the preparation procedure and to the nature of the support which both determine the critical parameter represented by the metal particle size [109]. Studies on the effect of particle size for Pd/Al_2O_3 catalysts suggested that increase in metal dispersion decreased the specific activity of small particle catalyst [59-62], while small particles of a medium dispersed catalyst exhibited slightly higher activity [65]. Bulk composition and phase transitions of the catalyst, especially for a bimetallic system, are of another importance to be considered. Investigation of the catalyst structure and morphology by specific surface area measurements (BET), XRD and TEM is performed and detailed as follows:

5.2.1.1 Specific Surface Area and Bulk Chemical Composition

Table 5.1 shows the BET surface area of supported alumina Pd, Ag and Pd-Ag samples with different pretreatments. The surface area of alumina support used in this study is 4.64 m^2/g. A low surface area alumina is commercially used for alkynes hydrogenation catalysts in order to minimize the formation of surface oligomers and to avoid the undesirable hydrogenation of alkenes [111]. Introduction of Pd onto the alumina support decreases the surface area of alumina. However, when the Pd/Al_2O_3 sample is re-impregnated with Ag, the surface area after reduction is not affected, suggesting that the reduced Pd-Ag particle size is not bigger than that of the monometallic Pd sample after reduction. Pretreatment with O_2, CO_2 and N_2O has an insignificant effect on the surface area of the alumina-supported Pd-Ag catalyst. The Ag and Pd contents observed from atomic absorption spectroscopy (AAS) were 2.3 and 2.8 wt%, respectively.

Table 5.1 Surface areas of alumina supported Pd, Ag, and Pd-Ag catalysts.

Sample	BET surface area (m^2/g)
Al_2O_3	4.64
Pd/Al_2O_3 (reduced)	3.51
Reduced $Pd\text{-}Ag/Al_2O_3$ (untreated)	3.50
N_2O-treated $Pd\text{-}Ag/Al_2O_3$	3.59
O_2-treated $Pd\text{-}Ag/Al_2O_3$	3.52
CO_2-treated $Pd\text{-}Ag/Al_2O_3$	3.69

5.2.1.2 Catalyst Structure and Particle Size Distribution

The phase identification is carried out on the basis of data from x-ray diffraction analysis. XRD diffractograms of the alumina supported 3wt%Pd-4wt%Ag catalysts before reaction as well as reference spectra of monometallic Pd and Ag are depicted in Figures 5.4. Apart from alumina peaks, the reduced Pd sample shows main peaks of Pd (111), Pd (200) at $2\theta = 40.2^o$ and 46.7^o, respectively. The reduced Ag sample registers the Ag (111), Ag (200) and Ag (220) planes at $2\theta = 38.1^o$, 44.3^o and 64.4^o, respectively. The calcined Pd-Ag sample exhibits oxide form of Pd; PdO (101) ($2\theta = 33.9^o$) and PdO (311) ($2\theta = 54.9^o$) without any peaks corresponding to Ag_2O ($Ag_2O(111) = 32.85$, $Ag_2O(220)=55.01$). After reduction, the broad peaks between the (111) and (200) Bragg lines of pure Pd and Ag are seen (magnified details are given in Figures 5.4 **(B)** and **(C)**. The position shift of the Pd features towards the lower degree by (-0.2) for (111) plane and (-0.5) for (200) plane indicates that solid solution between Pd and Ag was partly formed after reduction. However, Ag particles still exist in the bulk and possibly segregate on the Pd-Ag solid solution as the lower surface energy of Ag compared to that of Pd [111]. The results observed from XRD are in good agreement with the XPS results where alloy formation between Pd-Ag is suggested from the significantly negative shift of Ag $3d_{5/2}$ binding energy as will be discussed in the following section. Pretreatment with oxygen and other gases shows unaltered peak positions compared to the untreated (reduced) Pd-Ag sample. Accordingly, there is no change in the bulk composition of the catalyst upon pretreatment.

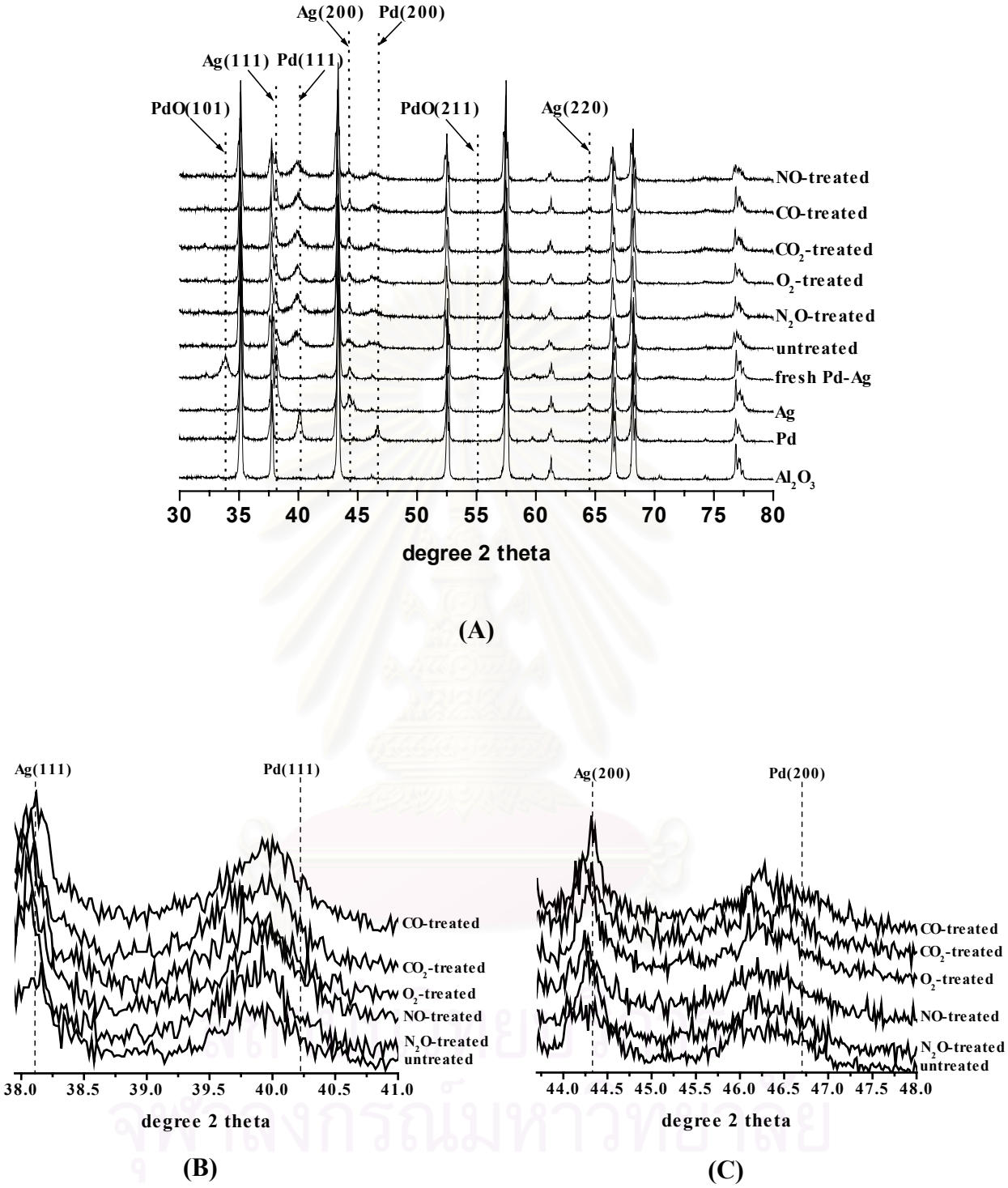

Figure 5.4 (A) XRD profiles of the alumina support and alumina-supported Pd, Ag and Pd-Ag catalysts, **(B)** and **(C)** are magnified details of the 111 and 200 Bragg's lines from **(A)**, respectively.

The study of catalyst morphology was carried out using transmission electron microscope (TEM). Figures 5.5 **(A)** and **(B)** depict TEM micrographs of alumina supported Pd and Pd-Ag samples, respectively. The palladium particles observed for monometallic Pd sample are quite round with the diameter of ca. 15 nm. The shape of Pd-Ag catalyst after reduction is unaltered, however, smaller particles with a diameter ca. 6.7 nm are observed. The shape and size of the pretreated samples (N_2O and CO_2) remain the same as for untreated sample, as shown in Figures 5.5 **(C)** and **(D)**, respectively. It is consequently concluded that pretreatment has no effect on the bulk structure of the Pd-Ag catalyst.

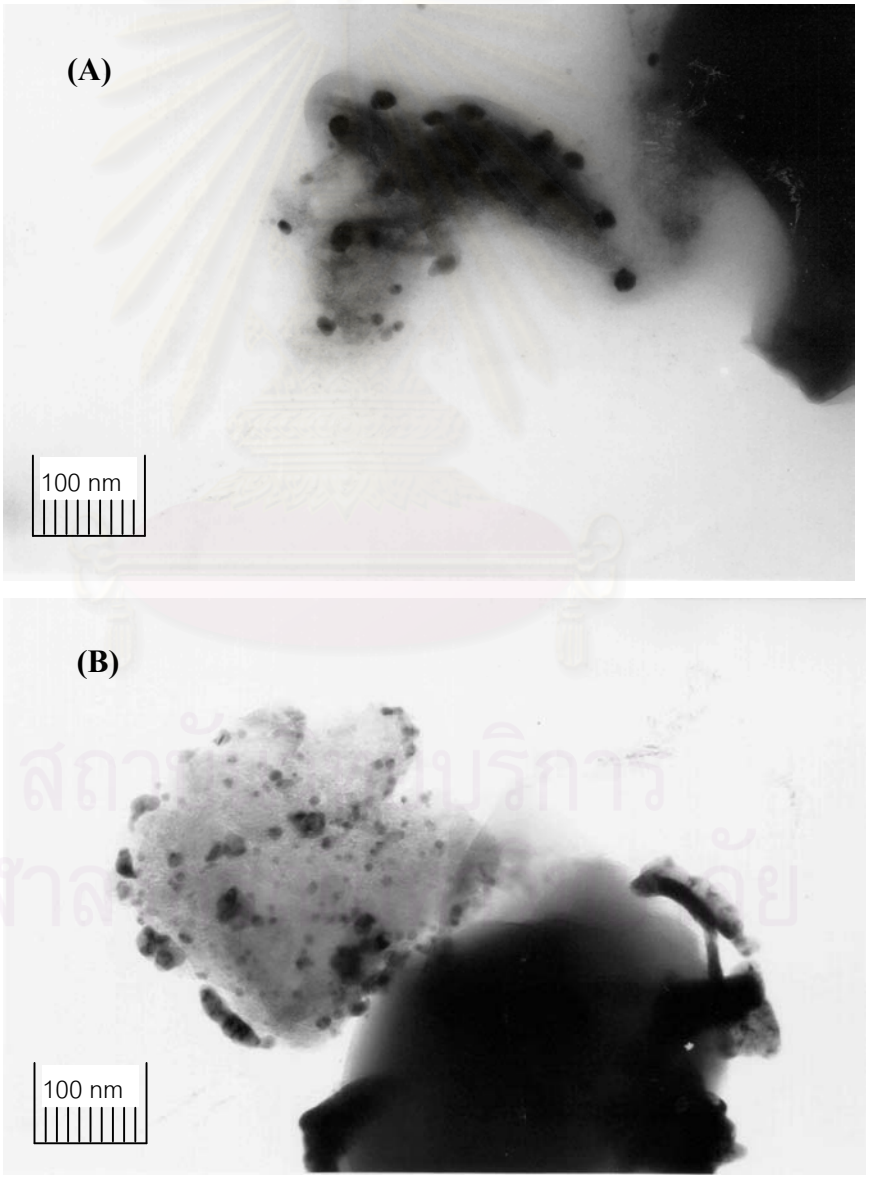

Figure 5.5 TEM micrographs of **(A)** Pd/Al_2O_3 and **(B)** $Pd\text{-}Ag/Al_2O_3$ catalysts.

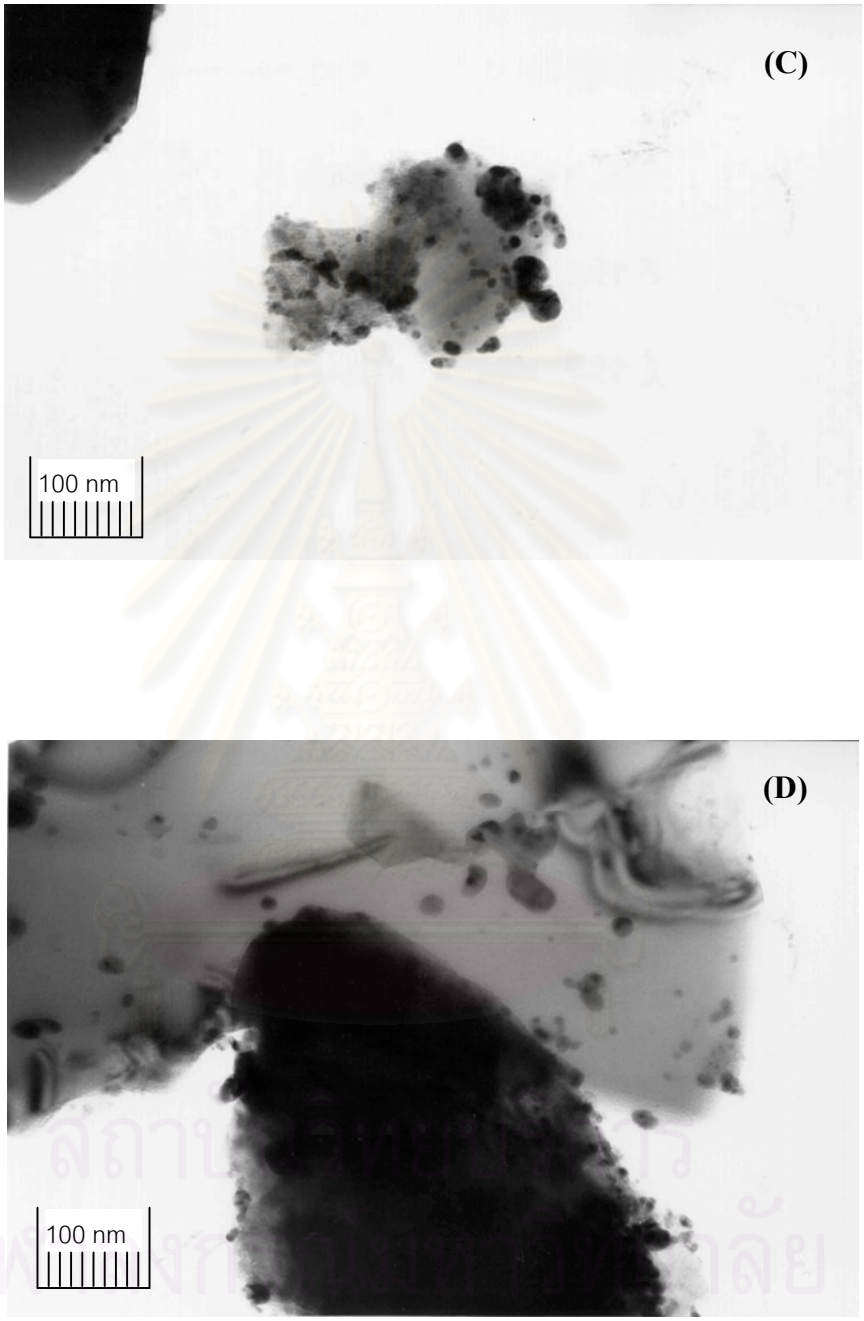

Figure 5.5 (continued) TEM micrographs of **(C)** N_2O-treated and **(D)** CO_2-treated Pd-Ag/Al_2O_3 catalysts.

5.2.1.3 Metal Active Sites

The metal active sites measurement is based on CO-chemisorption technique on the assumption that only one CO molecule adsorbed on one metal active site [106]. It has been reported in the literature that CO does not chemisorb either on the alumina support or on the Ag particles in alumina supported Pd-Ag bimetallic catalysts [112-118]. The metal active sites of the treated catalysts with an effective amount of oxygen or other oxygen-containing compounds are shown in Table 5.2. It is obvious that preatreatment increases number of palladium active sites, which should be the reason for activity enhancement, discussed previously.

Table 5.2 Number of metal active sites of the Pd-Ag/Al_2O_3 catalysts measured by CO-adsorption.

catalyst	Pd active sites ($\times 10^{-17}$ CO molecule/g of catalyst)	
	0.03%Pd-0.235%Ag/Al_2O_3	3%Pd-4%Ag/Al_2O_3
Untreated	1.16	22.6
O_2-treated	3.82	54.3
NO-treated	5.41	67.8
N_2O-treated	5.01	73.4
CO-treated	2.80	29.3
CO_2-treated	3.64	40.5

5.2.2 Reducibility and Hydrogen Sorption

It is of great importance to study the interaction of hydrogen with palladium particles for palladium based catalysts for hydrogenation. In this section, attempts have been made to use two temperature programmed techniques, i.e., TPR and TPD,

to probe the palladium surface for the understanding of its reducing capabilities and adsorption/desorption characteristics.

In order to understand the mechanism of the selective hydrogenation of acetylene over Pd-Ag catalyst, the role of Ag is elucidated first. Temperature programmed reduction of the fresh Pd-Ag/Al_2O_3 is illustrated in Figure 5.6, together with profiles of alumina support and monometallic Pd and Ag samples. The pure alumina support sample shows no reduction peak in the temperature range between 25°C to 500°C. The TPR profiles for Pd and Pd-Ag samples from Figure 5.6 **(A)** are shown in detail (with peak deconvolution) in Figures **(B)** and **(C)**, respectively. The monometallic Pd sample exhibits two positive peaks at 47°C and 79°C, followed by a reverse peak at 113°C. The two positive peaks are presumably attributed to the two-step reduction of PdO; the first peak can be due to the partial reduction of PdO to Pd_2O [117]:

$$2PdO + H_2 \rightleftharpoons Pd_2O + H_2O \qquad (5.3)$$

while the second corresponds to the reduction of Pd_2O to metallic Pd:

$$Pd_2O + H_2 \rightleftharpoons 2Pd + H_2O \qquad (5.4)$$

H_2 uptake for converting PdO to Pd_2O (equation (5.3)) is 13.4 μmol/g of catalyst while the H_2 consumption for converting Pd_2O to Pd (equation (5.4)) is 27.6 μmol/g of catalyst. However, the two TPR maxima observed could also be due to the reduction of PdO species that have different interaction with the support.

After reduction, the palladium crystallites may absorb hydrogen to form PdH in hydrogen environments, resulting in a hydrogen desorption peak at 113°C [110,111].

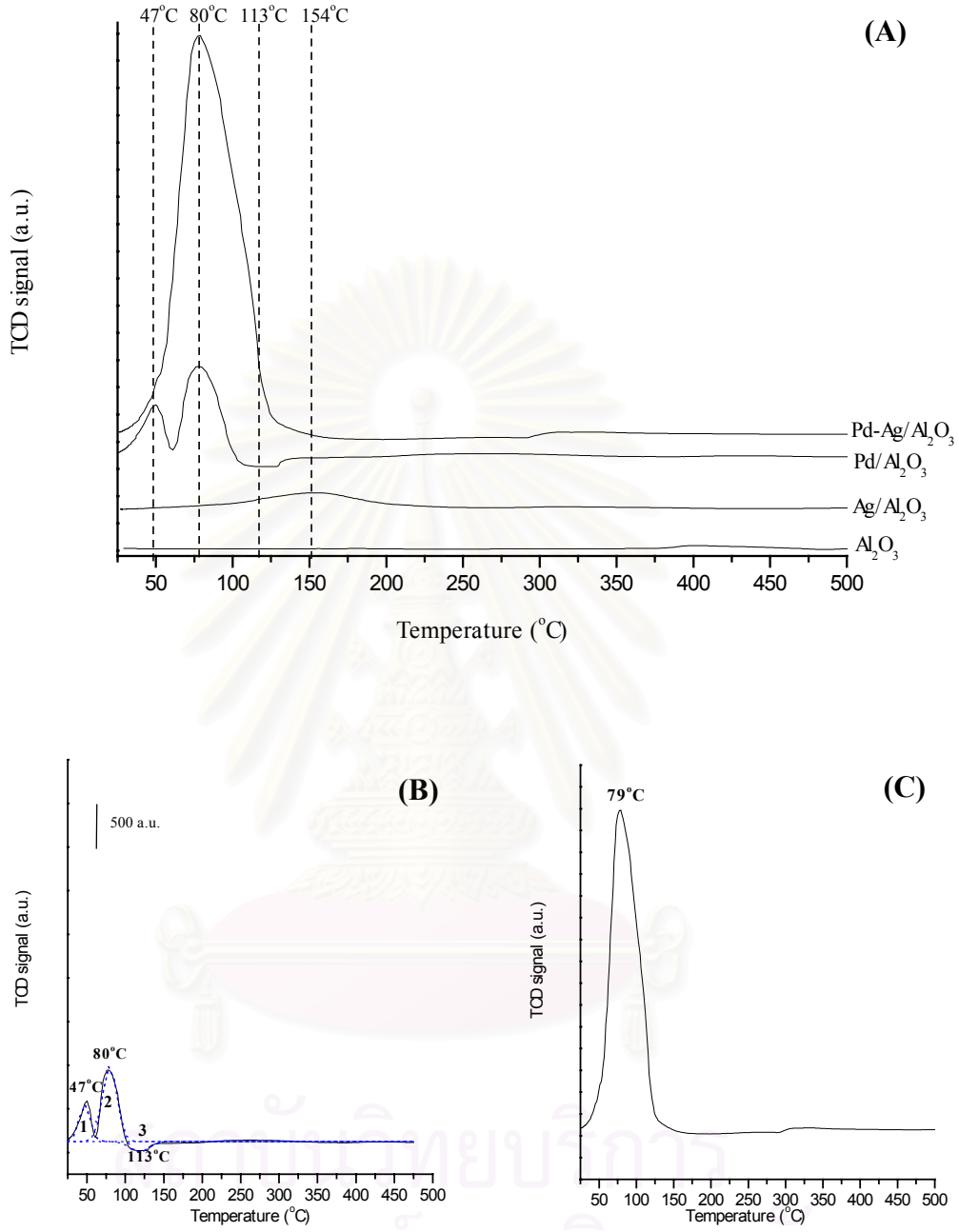

Figure 5.6 TPR profiles of **(A)** alumina supported Pd, Ag and Pd-Ag catalysts, **(B)** and **(C)** are magnified details of Pd and Pd-Ag catalysts from **(A)**, respectively.

For the bimetallic Pd-Ag sample, an intense positive peak is seen at 79°C. Absence of the peak attributed to reduction of Ag_2O (registered at 152°C for the monometallic Ag in Figure 5.7) in the Pd-Ag sample implies that hydrogen was spilt-over from reduced palladium to Ag_2O during the reduction of PdO [111]. The absence of a negative peak attributed to desorption of PdH is observed, indicating that the hydrogen absorption on bulk Pd is restricted by the presence of Ag. This is in a good agreement with the results observed on the Pd-Ag/Al_2O_3 [17] where the bulk of palladium of Pd-Ag catalyst adsorbed a smaller amount of hydrogen compared to that of the monometallic Pd catalyst.

The hydrogen desorption spectra of alumina-supported Ag, Pd and Pd-Ag samples are shown in Figure 5.7. No evidence of hydrogen adsorption peak on the monometallic Ag sample (dash line). For monometallic Pd sample (solid line), the shoulder registered at low temperature (67°C), may be ascribed to desorption of hydrogen in bulk Pd [110]. Initiating at ca. 80°C, the most intense peak at 120°C appears, followed by a peak at 289°C, which may be ascribed to adsorption of hydrogen on sites with different bonding energies.

According to the work on Pd/α-Al_2O_3 [110], three peaks located at 142°C, 216°C and 277°C were observed, and also on Pd/SiO_2 [119], which registered the three peaks at 125°C, 190°C and 300°C. The low temperature peaks were assigned to hydrogen desorption from a metal surface containing Pd(111) and Pd(100) planes whereas the high temperature desorption peak was assigned to hydrogen coming from subsurface Pd sites [119,120]. The latter case is presumed to take place when adsorbed hydrogen diffuses into subsurface sites during the TPD experiments and moves back when the desorption process is completed.

Another explanation for multiple desorption peaks is that hydrogen chemisorbs on different forms, i.e., top, bridge and multiple co-ordinated forms, on the Pd surface plane [111]. Theoretically, the interaction of atomic hydrogen with Pd (111) clusters has shown that the chemisorption bond for the three-fold hollow site is stronger than that of the bridge and atop sites [120]. Therefore the TPD maxima observed in the Pd catalyst may support the existence of monocrystalline particles.

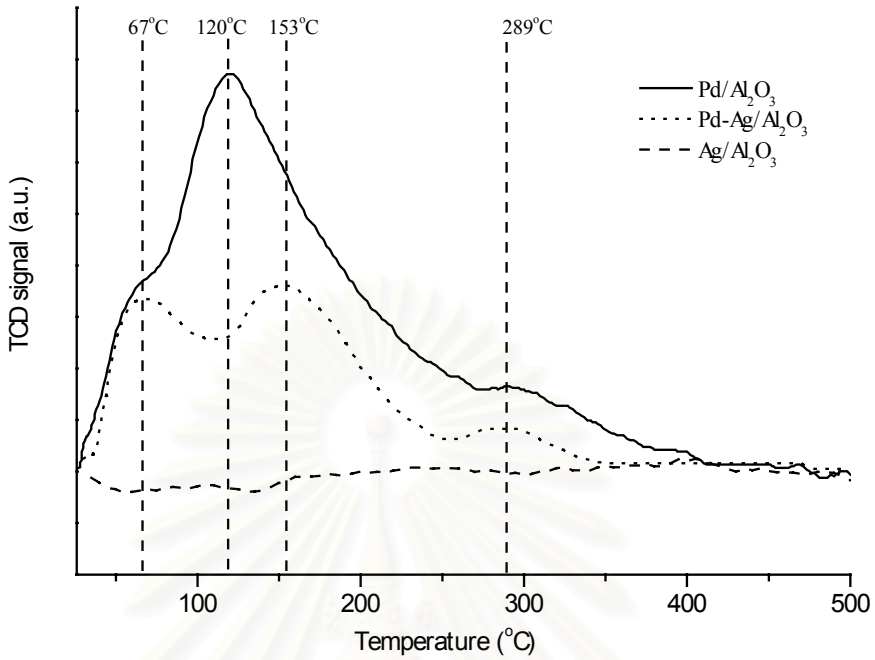

Figure 5.7 H_2-TPD profiles of alumina supported Pd and Pd-Ag catalysts.

For Pd-Ag/Al_2O_3 sample, the TPD profile is depicted as the dot line in Figure 5.7. The shoulder located for monometallic Pd at 67°C becomes better-defined on Pd-Ag sample. However, the intensity of such feature is not significantly changed. Starting at ca. 80°C, the most intense peak at 120°C was observed on the Pd sample, followed by a peak at 289°C, indicating that hydrogen may be bounded to two different Pd surface sites. Addition of Ag leads to the shift of the peak at 120°C to 153°C with lower amount of hydrogen desorption, while an unaltered peak position at 289°C but significant decreased intensity is observed. The shift of the peak at 120°C to 155°C indicates that the release of adsorbed hydrogen is restricted by the presence of Ag. However, a lower amount of desorption infers that Ag addition strongly affects the quantity of adsorbed H_2. With the presence of Ag, the smaller amount of the peaks located at either low temperature (155°C) or high temperature (283°C) may imply that hydrogen adsorption is effectively inhibited.

From TPR and H_2-TPD experiments, the role of Ag addition on reducibility and H_2-adsorption of the Pd/Al_2O_3 catalyst is elucidated. The presence of Ag modifies the reduction of PdO in calcined catalyst as seen from the altered TPR profile in Figure 5.7. The absence of the peak assigned to a reduction of Ag_2O suggests that hydrogen is effectively spiltover from reduced palladium to Ag_2O during the reduction of PdO. Additionally, the absence of the negative feature assigned to desorption of absorbed hydrogen when alloying with Ag suggests that Ag may inhibit the ability of hydrogen absorption of the bulk palladium. Observation of multiple desorption features in TPD measurements shows that hydrogen atoms are bounded with palladium surface in different co-ordinated forms; bulk absorption, atop sites and multiply bonded sites. Hydrogen adsorption is substantially lessened by Ag addition.

5.2.3 Surface Composition and Electronic State of Metals

Regarding the results obtained above, it is found that Ag modifies Pd surface and solid solution between Pd and Ag is revealed. However, surface concentration of each element as well as effect of pretreatment with oxygen-containing compounds has not been elucidated. This section is therefore aimed to study the surface composition as well as the electronic state of the metal catalyst with and without pretreatment using x-ray photoelectron spectroscopy (XPS). Surface analysis by XPS can provide useful information on surface composition drawing from electron binding energy values.

Ex situ XPS was firstly performed. However, an improved procedure to insure that the results were not falsified by exposure to air, either during storage or sample preparation, was conducted afterwards.

Results of *ex situ* XPS study are presented in Table 5.3. The Ag $3d_{5/2}$ binding energies of the $Pd\text{-}Ag/Al_2O_3$ catalysts line in the range 366.8-367.0 eV, indicating oxide form of Ag. The Pd $3d_{5/2}$ binding energies of Pd-Ag catalysts are found to be 334.0-334.2 eV, which are lower than that observed on the Pd/Al_2O_3 sample (binding energy of Pd $3d_{5/2}$ is 335.0 eV). Pd $3d_{5/2}$ binding energy recorded for Pd/Al_2O_3 catalyst is typical for metal Pd, while values of Pd $3d_{5/2}$ binding energy

observed for Pd-Ag/Al_2O_3 catalysts are unusually low. It is suggested that there is a change of electronic state of Pd in Pd-Ag/Al_2O_3 catalysts. Pd-Ag alloy or solid solution can be formed by electron density transfer from Ag to Pd resulting in the appearance of negative charge on Pd and positive charge on Ag.

Table 5.3 Elemental binding energies of studied samples.

sample	Binding energy	
	Pd $3d_{5/2}$	Ag $3d_{5/2}$
Pd/Al_2O_3	335.0	-
Pd-Ag/Al_2O_3 (untreated)	334.0	366.8
Pd-Ag/Al_2O_3 (N_2O-treated)	334.0	366.8
Pd-Ag/Al_2O_3 (CO_2-treated)	334.2	366.8

It is seen from Table 5.3 that the states of Pd and Ag do not change with the pretreatments. Thus, it is likely that the changes after pretreatment, which influenced the catalytic activity, occurred in the adsorbed layer of the catalyst without modification of the catalyst structure of the surface layers studied by XPS (ca. 15-25 Angstrom).

However, an improved method XPS which contamination from air exposure was prevented was redone. The catalyst surface was studied either before or after reaction. Reference spectra were checked using reference Pd and Ag samples, detailed in section 4.3.2.2, chapter 4. Figure 5.8 **(A)** illustrates XPS survey spectra for reference Pd and PdO samples. Only the core levels of metallic palladium (Pd 2p and Pd 3d) and its Auger electron signal (Pd (MNN)) are observed on the Pd sample. For the PdO sample, the palladium (Pd 2p and Pd 3d) and carbon (C 1s) core levels plus oxygen Auger electrons (O (KVV)) are revealed in the XPS survey spectrum. Figure 5.8 **(B)** shows x-ray photoelectron spectra of Pd 3d region taken from a clean palladium foil and commercial powder PdO sample. The clean Pd foil is characterised by the Pd $3d_{5/2}$ peak at 335.4 eV, whereas the Pd $3d_{5/2}$ binding peak for PdO registers at 337.5 eV, which are in good agreement with those in the literature

[121-124]. XPS survey spectra for Ag, Ag_2O and AgO are given in Figure 5.9 **(A)**. All samples show the features from core-level (Ag 2p and Ag 3d), Auger electron signal (Ag (MNN)), and the valence band of Ag. C 1s and O 1 s features are apparent in Ag_2O and AgO samples. As the studied catalysts were powder samples with relatively low metal concentration, noisy and low Auger electron signal were observed. Very low intensity of valence band spectra is also found. Accordingly, only the most intense core-level peaks (3d for Pd and Ag) are considered. High-resolution Ag 3d XPS spectra for Ag, Ag_2O and AgO samples are shown in Figure 5.9 **(B)**. Considering the Ag 3d binding energies of the peaks obtained from metallic Ag and oxide forms (Ag_2O and AgO) reveals that there is no distinctive change in peak position from Ag metal (BE = 368.0 eV) to Ag_2O (BE = 368.0 eV) with a slightly negative shift from metal Ag to AgO (367.9 eV). However, significant increase of full width of half maximum (FWHM) values (from 0.4 to 1.1 eV) from Ag to Ag_2O and AgO also indicates different oxidation states of silver in such samples [125-128]. Table 5.4 summarises the binding energies of the core-level Pd and Ag of reference samples. From the reference spectra, it can be seen that there is no shift of the Ag $3d_{5/2}$ signals due to chemical state change from Ag to Ag_2O, however, the bandwidth broadens by 0.4 eV.

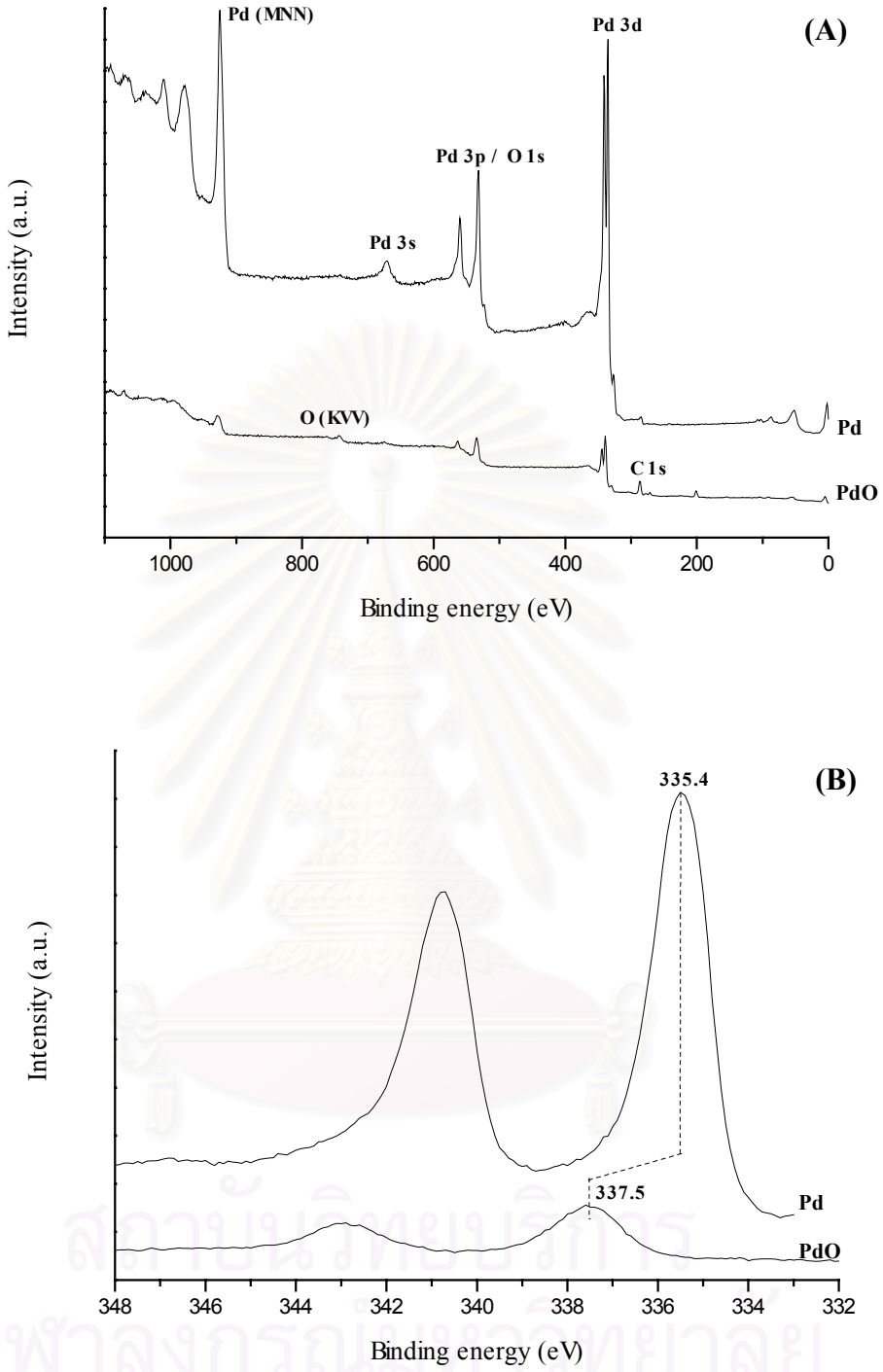

Figure 5.8 (**A**) XPS survey spectra for reference Pd and PdO, (**B**) XPS Pd 3d spectra for Pd and PdO from (**A**).

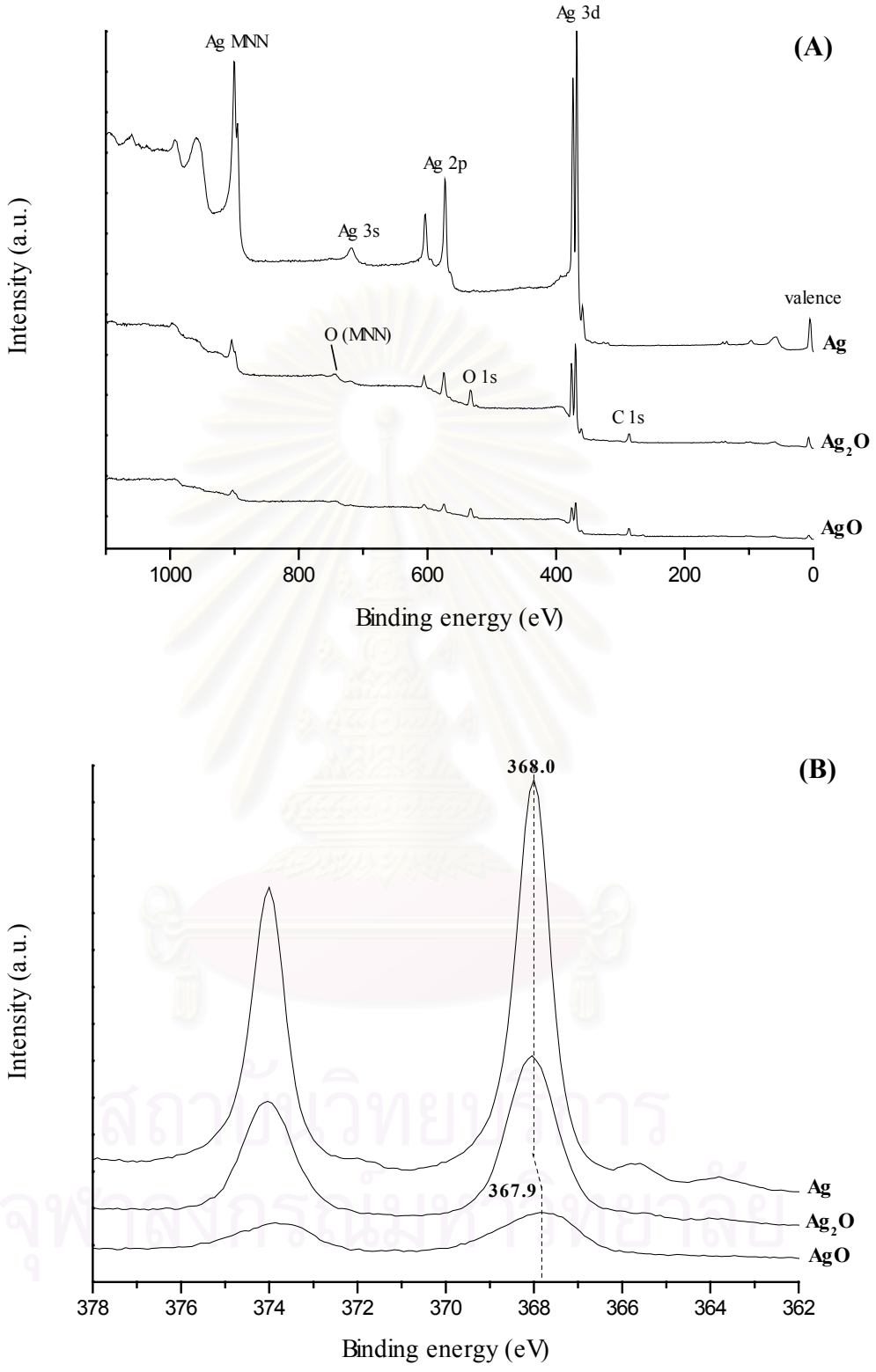

Figure 5.9 **(A)** XPS survey spectra for Ag, Ag_2O and AgO reference samples, **(B)** XPS Ag 3d spectra for Ag, Ag_2O and AgO from **(A)**.

Table 5.4 Binding energies (eV) of Pd $3d_{5/2}$ and Ag $3d_{5/2}$ for reference metallic and oxide forms of Pd and Ag species.

sample	Pd $3d_{5/2}$	Ag $3d_{5/2}$	FWHM (eV)
metallic Pd	335.4	-	-
PdO	337.5	-	-
metallic Ag	-	368.0	0.9
Ag_2O	-	368.0	1.3
AgO	-	367.9	2.0

As the Pd-Ag catalyst for the selective hydrogenation of acetylene was supported on Al_2O_3, the chemical states of Pd and Ag species deposited on alumina support are evaluated. Figure 5.10 displays the survey spectra obtained from the alumina support and alumina-supported catalysts. Alumina sample exhibits the features from oxygen Auger and core level signals, Al core level electrons and C 1s. Coverage of the alumina support by Ag results in appearance of Ag Auger and Ag 3d species, despite the features that belonged to alumina support. Similarly, deposition of Pd on alumina support leads to the appearance of Pd Auger and core level electron signals. For the bimetallic Pd-Ag catalyst, Auger electron and core-level features of Pd and Ag appear apart from the peaks corresponding to alumina support. High-resolution XPS Pd 3d and Ag 3d spectra obtained from fresh and reduced alumina supported monometallic (Pd or Ag) and bimetallic Pd-Ag catalysts are illustrated in Figures 5.11 **(A)** and **(B)**, respectively, and the binding energies of the Pd $3d_{5/2}$ and Ag $3d_{5/2}$ are listed in Table 5.5. It is seen that the Pd- and Ag-related binding energies of the alumina supported monometallic catalyst are slightly lower than the reference pure metal bulk values (-0.2 eV for Pd and -0.1 eV for Ag). In the case of Ag monometallic sample, line broadening (+0.8 eV) occurs compared to that observed from bulk Ag, corresponding to charging from alumina (powder sample).

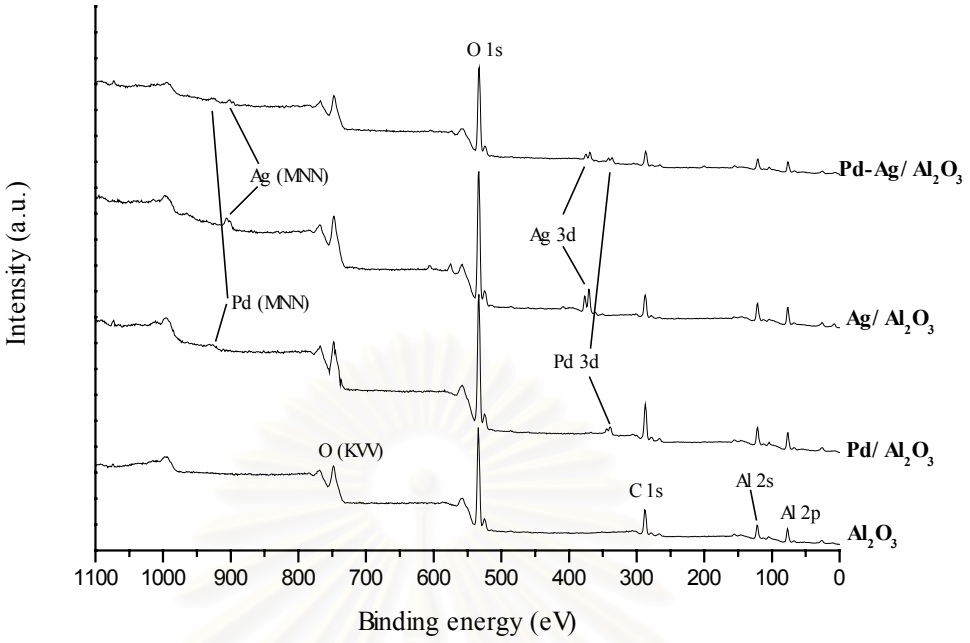

Figure 5.10 XPS survey spectra for alumina and alumina supported Pd, Ag and Pd-Ag catalysts.

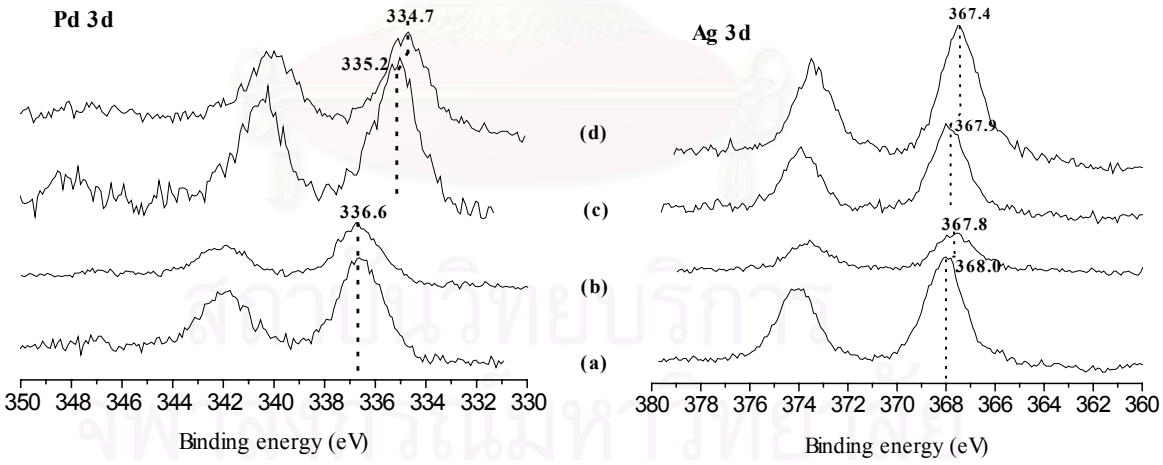

(A) **(B)**

Figure 5.11 XPS Pd 3d spectra **(A)** and Ag 3d spectra **(B)** for alumina-supported samples: (a) and (b) were obtained from fresh monometallic (Pd or Ag) and bimetallic samples, respectively, (c) and (d) were obtained from reduced monometallic and bimetallic samples, respectively.

Table 5.5 XPS data for alumina-supported Pd, Ag and Pd-Ag catalysts.

sample	Binding energy (eV)		FWHM (Ag $3d_{5/2}$) (eV)
	Pd $3d_{5/2}$	Ag $3d_{5/2}$	
Fresh Ag	-	368.0	1.9
Reduced Ag	-	367.9	1.7
Fresh Pd	336.6	-	-
Reduced Pd	335.2	-	-
Fresh Pd-Ag	336.6	367.6	2.1
Reduced Pd-Ag	334.7	367.4	1.8

High-resolution XPS spectra of the Pd 3d and Ag 3d doublets obtained from fresh and reduced Pd-Ag/Al_2O_3 samples are illustrated in Figures 5.11 **(A)** and **(B)**, respectively, along with those observed from the monometallic samples. The values of binding energy as well as FWHM of Ag$3d_{5/2}$ and Pd $3d_{5/2}$ lines are given in Table 5.5. The Pd $3d_{5/2}$ binding energy obtained from the fresh Pd-Ag sample is unaltered with respect to that of the fresh monometallic Pd sample (BE=336.6 eV), indicating PdO on the surface. Consideration of the Ag $3d_{5/2}$ binding energy, it is seen a -0.4 eV shift respective to the monometallic value with a line broadening (+0.3 eV). It is obvious that interaction with Pd results in the shift of the Ag 3d core level. Taking the line broadening observed in the reference bulk samples (Ag and Ag_2O) into account, it seems that Ag_2O is formed on that Pd-Ag surface after calcination (fresh Pd-Ag/Al_2O_3 sample).

After reduction, the core level Pd $3d_{5/2}$ electron shifts to 334.7 eV (-0.6 eV from the monometallic Pd (BE=335.3 eV)). It is also observed a -0.5 eV shift of the Ag $3d_{5/2}$ binding energy for the reduced Pd-Ag sample (BE =367.4 eV), with respect to the reduced monometallic Ag sample (BE=367.9 eV). This has obviously not resulted from the state change from oxide to metallic (Table 5.4 suggests a -0.1 eV shift and -0.3 eV line broadening from oxide to metallic state of monometallic Ag sample). The binding energy shift of core electron depends on changes in the bulk charge around an atomic site. Generally, the core level binding energy of the central

atom increases as the electronegativity of the attached atoms or groups increases [129,130]. According to the Pauling's electronegativity table, Pd is more electronegative than Ag [131,132]. Pd core levels should shift toward the lower binding energy. On the other hand, Ag core levels should shift toward higher binding energy. Obviously, the general rule based on the electronegativity values can explain only the Pd $3d_{5/2}$ shift, but fails to explain the observed shift of Ag $3d_{5/2}$. However, the Ag $3d_{5/2}$ core-level shifts to lower binding energy have also been reported. Partial charge transfer from Ag to Pd leading to a negative shift of both Ag and Pd signals from their monometallic values (-1.0 eV for Ag $3d_{5/2}$ and -0.5 eV for Pd $3d_{5/2}$) was reported on the 4.5Pd-4.5Ag/γ-Al_2O_3 [133]. Similar behaviour was found on 0.25Pd-0.05Ag/pumice catalyst (-0.2 eV for Ag $3d_{5/2}$ and -0.8 eV for Pd $3d_{5/2}$) [134]. The shifts on the Ag 3d binding energy of silver atoms embedded in a palladium matrix can be as high as 1 eV [130]. Consequently, it is plausible to conclude that a solid solution or alloy between Pd and Ag is formed on the studied Pd-Ag surface after reduction (untreated sample).

Surface analysis on the pretreated Pd-Ag/Al_2O_3 catalyst after reduction was performed either before or after reaction. According to the reactivity test mentioned above, pretreatment with oxygen or oxygen-containing compounds must have significant effects on the surface of the Pd-Ag/Al_2O_3. Surface modification is expected upon pretreatment, although no evidence was found by the *ex situ* XPS measurement firstly performed. It is also interesting to study whether or not the effect is retained after reaction.

XPS Pd and Ag 3d spectra of the pretreated Pd-Ag/Al_2O_3 catalysts before reaction are shown in Figures 5.12 **(A)** and **(B)**, respectively, compared with that of the untreated sample (after reduction). The binding energy as well as FWHM values of the Pd-Ag/Al_2O_3 catalysts are listed in Table 5.6. The Pd $3d_{5/2}$ binding energies obtained from pretreated samples lie in the range 334.8-335.2 eV, which indicate that a metallic state of Pd alloying with Ag. There is no evidence of a PdO signal, which would be expected between 335.4 and 337.5 eV (Table 5.4 shows a +2.1 eV between Pd and PdO.). However, it is speculated that oxygen atoms from pretreatment compounds are adsorbed on Pd.

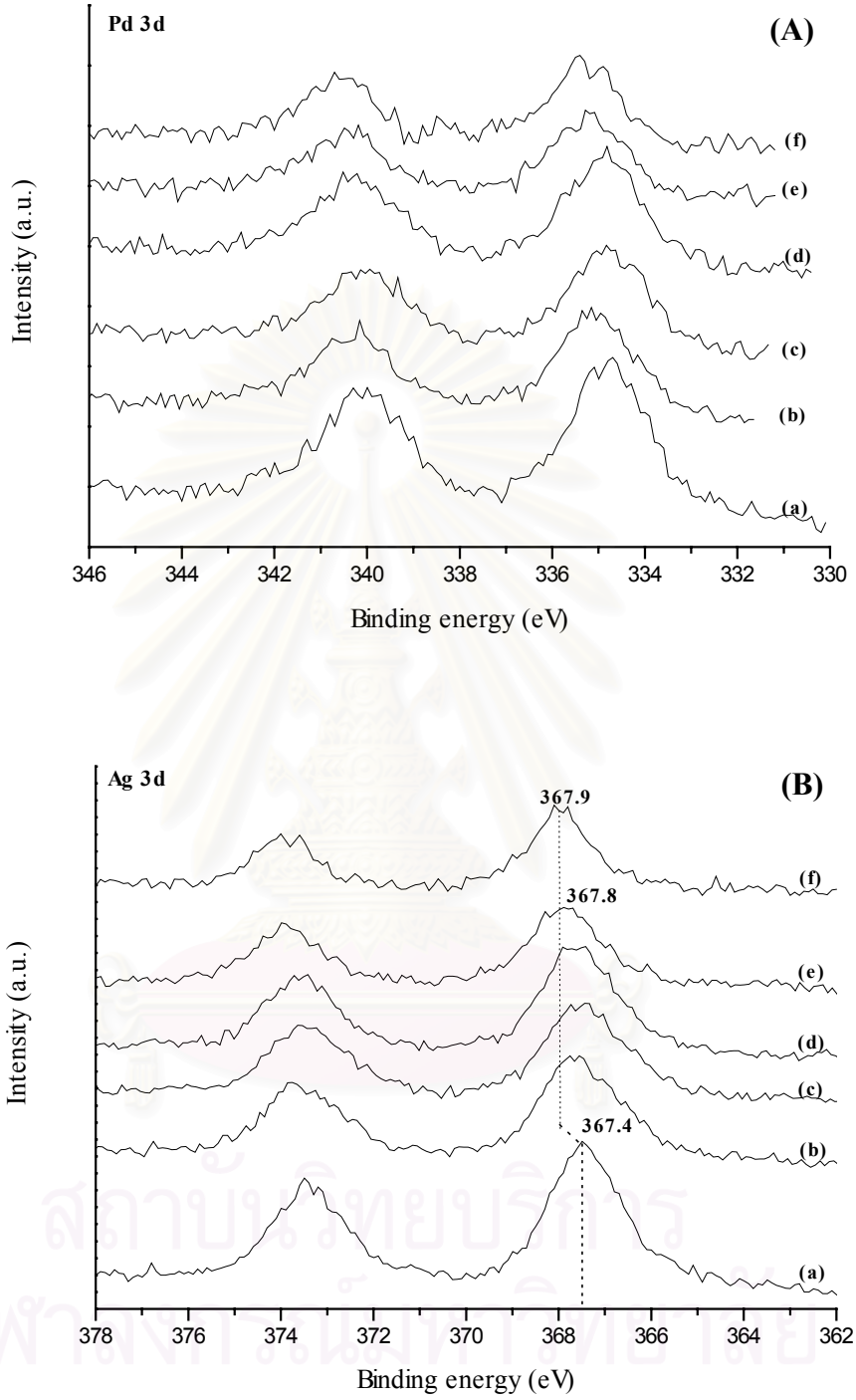

Figure 5.12 XPS Pd 3d **(A)** and Ag 3d **(B)** spectra for Pd-Ag/Al_2O_3 catalysts before reaction: (a) untreated, (b) O_2-treated, (c) CO_2-treated, (d) CO-treated, (e) NO-treated and (f) N_2O-treated.

After being pretreated with oxygen-containing compounds, the binding energies measured for Ag $3d_{5/2}$ from most samples show a positive shift in the range of 0.2 to 0.5 eV (from 367.4 to 367.6-367.9 eV). From the reference spectra of metallic and oxide forms of Ag (see Table 5.4), it can be seen that there is no shift of Ag $3d_{5/2}$ signals between Ag and Ag_2O, however the bandwidth broadens by 0.4 eV. Therefore, it is likely that there is no oxidation state change from metallic to oxide on the Ag particles. For O_2, CO_2 and CO pretreatment, no significant change of peak positions or bandwidth of the Ag 3d lines is seen. For NO and N_2O pretreatment, on the contrary, significant positive shifts of Ag $3d_{5/2}$ signals (BE = 367.8 eV and 367.9 eV, respectively) from the untreated sample are found together with narrower peak widths (-0.1 eV and -0.4 eV, respectively). Modification of Ag in Pd-Ag alloy surface by NO_x-treatment, therefore, must occur. This result is inconsistent with that observed from the *ex situ* measurement previously performed (Table 5.3). A study of charge redistribution in a series of ion-beam-mixed Pd_{1-x}-Ag_x (x=0.5-0.9) alloys showed that when the Ag concentration in a Pd-Ag alloy increased, the Pd $3d_{5/2}$ core level shifts toward lower binding energies, whereas increasing Pd resulted in a higher positive shift of Ag $3d_{5/2}$ [129,130]. On the contrary, work on Pd-Ag/γ-Al_2O_3 showed that increasing Pd surface concentration in Pd-Ag alloy (from Pd:Ag = 1.1 to Pd:Ag = 5.1) resulted in a +0.6 eV shift of Pd $3d_{5/2}$ whereas only -0.1eV shift was found on $Ag3d_{5/2}$ [133]. Thus, the significant shift resulted from NO_x pretreatment in this study should not originate from the change in composition of the Pd-Ag alloy. However, the values of surface composition of the catalyst are also considered and the results are listed in Table 5.6.

The lower palladium fraction at the surface (Pd:Ag = 0.66) than the bulk composition (Pd:Ag = 1.22) indicates surface enrichment with silver after reduction (untreated sample). This can be explained by the lower surface energy of Ag (930 erg/cm^2) respective to that of Pd (1500 erg/cm^2) [137]. The palladium fraction becomes slightly increased (ca. 3-13.6%) when pretreatment is conducted. This observation is consistent with the increased number of palladium active sites by pretreatment described in section 5.2.1.3. It was reported that when the surface is contacted with adsorbing gas, the thermodynamic equilibrium evolves toward a surface enrichment with the metal having the stronger interaction with the adsorbate

[112,138]. Increasing Pd surface compositions after pretreatment are thus attributed to the stronger interaction between palladium and pretreatment gases, which subsequently leads to a less pronounced surface enrichment with silver. It is speculated that the higher palladium surface concentration is the reason for activity enhancement by pretreatment.

Table 5.6 XPS binding energies of Ag 3d and Pd 3d species of Pd-Ag/Al_2O_3 catalysts before and after reaction test.

sample	Pd $3d_{5/2}$	Ag $3d_{5/2}$		Pd:Ag Atomic concentration (%)
	Peak position (eV)	Peak position (eV)	FWHM (eV)	
untreated	334.7	367.4	1.9	0.66
	334.9	*367.4*	*1.8*	*0.88*
O_2-treated	335.0	367.6	2.1	0.68
	334.5	*367.4*	*1.8*	*0.91*
CO_2-treated	334.8	367.4	2.1	0.71
	334.8	*367.4*	*1.8*	*1.23*
CO-treated	334.9	367.5	1.9	0.75
	335.0	*367.6*	*1.8*	*1.00*
NO-treated	335.2	367.8	1.8	0.73
	335.0	*367.7*	*1.7*	*0.93*
N_2O-treated	335.2	367.9	1.5	0.68
	335.2	*367.8*	*1.8*	*0.97*

Italic numbers represent the values after reaction was performed.

There is no change in O 1s, Al 2p or C 1s spectra obtained on the pretreated Pd-Ag catalysts before reaction with respect to the untreated catalyst. O 1s binding energy is ca. 532.0-532.1 eV for all samples where as the Al 2p is ca. 76.4 eV. The values of O 1s and Al 2p binding energies show the characteristic of Al_2O_3 without any additional peaks or shoulders assigned to other species. The binding energy of C 1s observed from all samples is ca. 285.0 eV. Therefore, such species will not be shown here.

The surface of the catalysts after acetylene hydrogenation at 50^{o}C for 8 hours was investigated. Details of catalyst evaluation were given in section 5.2 (Figures 5.3 **(A)** and **(B)**). Figure 5.13 displays the XPS spectra of Pd 3d and Ag 4d obtained from the Pd-Ag/Al_2O_3 catalysts after reaction. The values of Pd $3d_{5/2}$ and Ag $3d_{5/2}$ as well as the surface ratio between Pd and Ag are given in italic letters in Table 5.6. There is no significant change in the peak positions of the Pd 3d and Ag 3d spectra compared to those observed prior to reaction. The fact that there is no change of electronic state of the pretreated Pd-Ag bimetallic catalysts before and after reaction suggests that modification of the Pd-Ag surface occurs during pretreatment and the effect of pretreatment is retained even after the catalysts have been on stream for 8 h. It is seen that the surface concentration of palladium after being reacted, is increased compared to that obtained before reaction, since hydrocarbon adsorption and reaction take place on the palladium active sites. Adsorbed species such as ethylidyne (≡C-CH_3) and others formed in the course of hydrogenation steps, were also checked by examination of the C 1s signal. The C 1s signal species still lies between 285.0-285.1 eV, and there was no evidence of ethylidyne (BE = 283.3 eV [63]) or other carbonaceous species, so either the position or the surface concentrations of the C 1s is not presented here. Similarly as with C 1s signal, there is no change of the O 1s and Al 2p signals

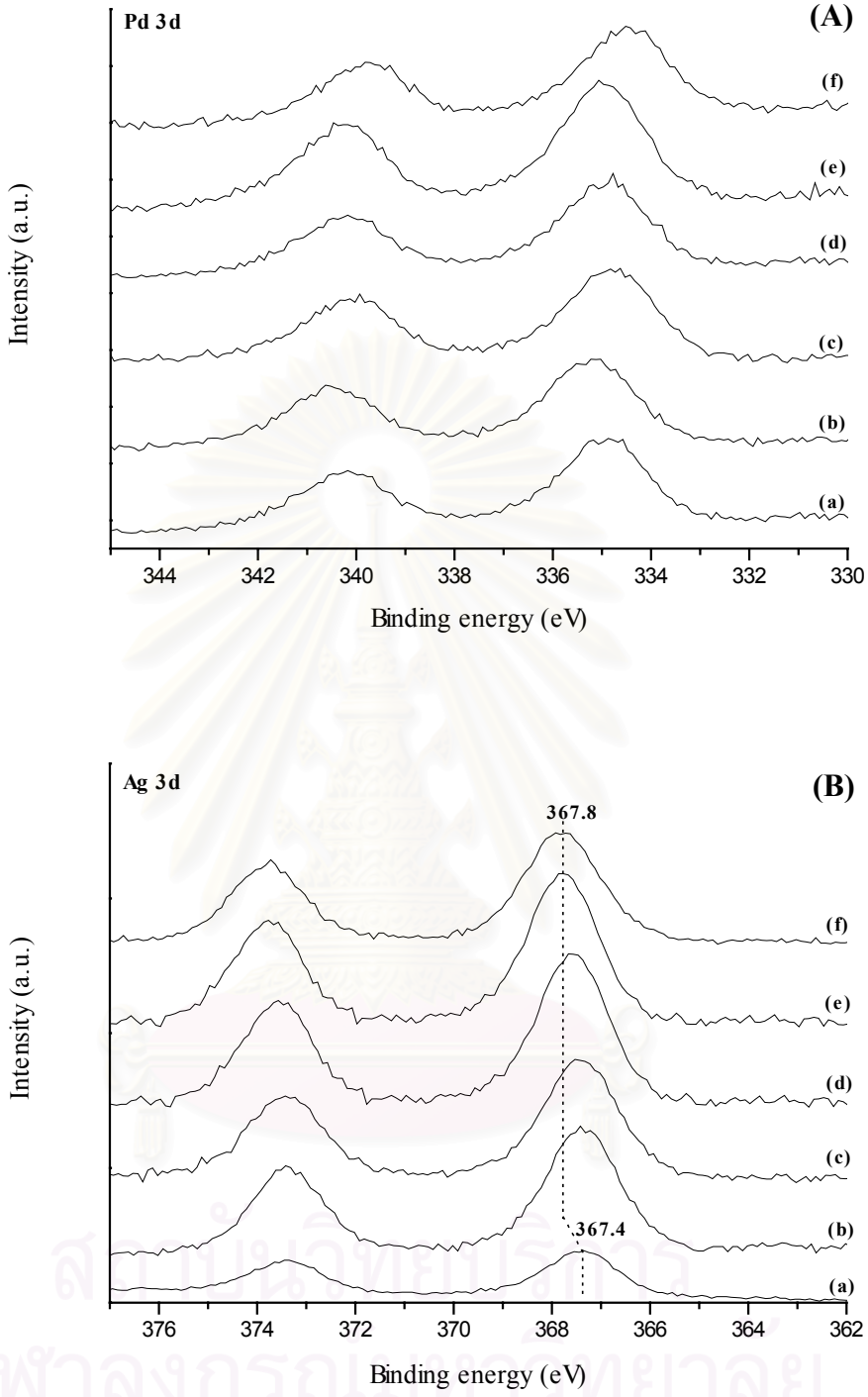

Figure 5.13 XPS Pd 3d **(A)** and Ag 3d **(B)** spectra for Pd-Ag/Al_2O_3 catalysts after reaction: (a) untreated, (b) O_2-treated, (c) CO_2-treated, (d) CO-treated, (e) NO-treated and (f) N_2O-treated.

Based on surface analysis by the XPS results, it can be concluded that the surface of Pd-Ag/Al_2O_3 catalyst after reduction contains solid solution between Pd and Ag with Ag enrichment. Pretreatment with oxygen or oxygen-containing compounds results in increased amount of palladium on the surface. A significant positive shift of the Ag $3d_{5/2}$ due to pretreatment with NO and N_2O suggests surface modification by such compounds. The surface after reaction shows no state change of either Pd or Ag compared to those measured prior to reaction, suggesting that surface modification occurs after pretreatment and is retained even after 8 h on stream. Additionally, there is no evidence of carbonaceous deposits formed after reaction for 8 h.

5.2.4 Surface Species Formation

Knowledge of the surface species formation is the key to developing a fundamental understanding of the reaction mechanism on the catalyst surface. The most widely used technique for determining the surface species on supported metal catalysts is *in situ* infrared (IR) spectroscopy. Study of species formation is performed for three aspects. The first aspect is to observe whether or not pretreatment with oxygen and oxygen-containing compounds leads to surface species at the pretreatment conditions. To investigate the origin of the shift of the Ag $3d_{5/2}$ binding energy after NO_x-pretreatment is the second aspect. Finally, reactive species involving in the acetylene hydrogenation reaction are studied.

5.2.4.1 Surface Species Formation upon Pretreatment

The catalyst surface after pretreatment was investigated by examining a transmission cell in a Nicolet Impact 400 FT-IR. Pretreatment was performed in the IR cell to avoid sample contamination. Figure 5.14 exhibits the IR spectra obtained from the Pd-Ag/Al_2O_3 catalyst after pretreatment (spectra (b) to (f)) compared with the surface prior to pretreatment (spectrum (a)). All treated samples exhibit the same behaviour in lacking of the spectra attributed to ionic palladium which have been reported in the range 2160-2110 cm^{-1} [139], confirming the XPS result that no oxide surface of Pd exists by pretreatment. Only pretreatment with NO and N_2O causes a significant change in the spectra. Pretreatment with NO causes

features at ca. 1650, 1530, 1457 and 1262 cm^{-1}. Observation of the bands observed on alumina and Ag/alumina material during DRIFTS has suggested a coupling band at 1530 and 1250 cm^{-1} corresponding to bidentate nitrate NO_3^- and a minor feature at 1465 cm^{-1} attributed to linear nitrite species. [140,141]. Therefore, it appears likely that the features at 1530 and 1262 cm^{-1} found on the NO-treated sample correspond to formation of nitrate species and the band located at 1457 cm^{-1} could be attributed to nitrite species adsorbed on either silver or Al_2O_3. It has been reported that adsorption of NO on Pd/Al_2O_3 at room temperature to 200°C results in linear surface complexes of Pd-NO with Pd in the range of 1830-1650 cm^{-1} [142,143]: therefore the feature at 1650 cm^{-1} could be ascribed to a linear complex Pd-NO. It can be concluded that, NO pretreatment at 80°C on $Pd\text{-}Ag/Al_2O_3$ catalyst leads to a linear complex Pd-NO and formation of nitrite and nitrate species on either Ag or alumina. A linear complex Pd-NO (band at ca. 1650 cm^{-1}) and a linear nitrite (band at ca. 1457 cm^{-1}) are also apparent on the N_2O-pretreated catalyst, however, such features are not as intense as those of the NO-treated catalyst. The similarity between NO and N_2O is found on formation of surface nitrite and linear complex Pd-NO.

The results observed from vibrational study are in good agreement with those from addition experiments. There, the catalyst was packed in the reactor, which was connected to the thermal conductivity detector (TCD). After the TCD signal was stable, known amount of pretreatment gas was injected into the catalyst bed via the carrier stream (He) at pretreatment temperature (80-110°C). Pretreatment species were removed from the stream according to the number of unoccupied active adsorption sites on the catalyst surface, thereby diminishing the quantity reaching the saturation approaches. The surface was considered saturated when two or more successive peaks exhibit the same area. For NO and N_2O pretreatments, the gas chromatograph column was used instead of a TCD in order to see whether or not N_2 was formed during pretreatment. It was observed that very small amount of adsorption occurred by pretreatment with O_2, NO and N_2O, while there was no adsorption detected by pretreatment with CO and CO_2 (results are not presented here). Additionally, pretreatment with NO and N_2O on the Pd-Ag surface yielded no N_2 species, indicating that neither N_2O nor NO decomposition proceeded on the surface at such pretreatment temperatures (90°C for N_2O and 80°C for NO).

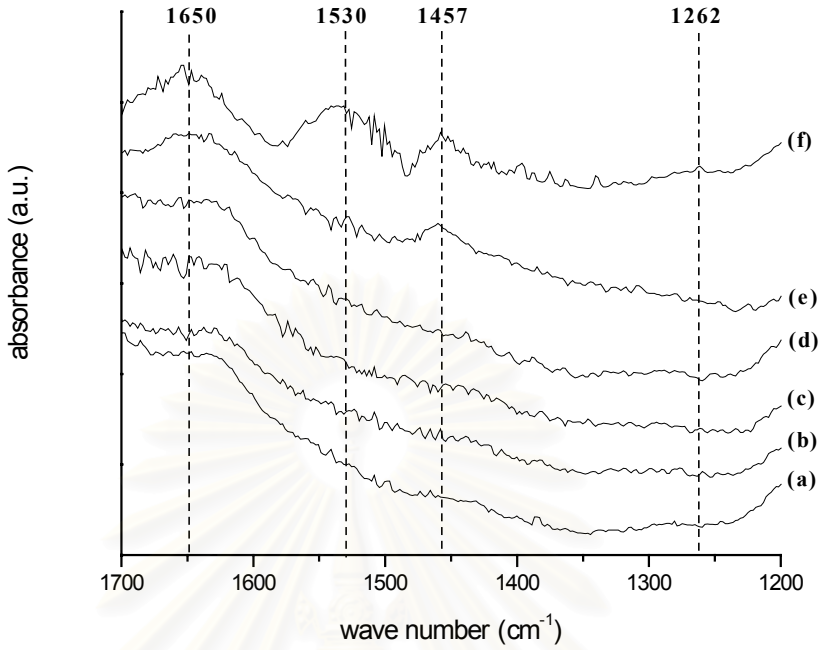

Figure 5.14 FT-IR spectra of Pd-Ag/Al_2O_3 surface: (a) untreated, (b) CO-treated, (c) CO_2-treated, (d) O_2-treated, (e) N_2O-treated and (f) NO-treated.

According to the infrared spectra and additional adsorption experiments observed on the catalyst surface after pretreatment, it can be seen that Pd-NO complex is formed together with nitrate and nitrite species on Ag-Al_2O_3 during pretreatment with NO and N_2O. The shift in the XPS Ag 3d spectra observed over the NO_x-treated catalysts is probably explained by strong surface adsorption or perhaps the formation of surface nitrate and nitrite on Ag, not the change in electronic state.

5.2.4.2 Surface Species Formation by Reactant Adsorption

Regarding the different effect on reactivity behaviours between the NO_x-treated and CO_x-treated catalysts, i.e., higher and lower ethylene gain, respectively, compared to the untreated catalyst, it is speculated that pretreatment with NO and N_2O may affect the adsorption behaviour of the catalyst exposed to the reactant. Presumably, NO and N_2O species may occupy some sites on the palladium

surface responsible for undesired reaction, thereby increasing the ethylene gain. However, in order to rationalise such effect on the Pd-Ag particles, it is necessary to study the influence of pretreatment on the surface species formed upon adsorption of molecules participating in the reactions. Consequently, *in situ* FT-IR was employed for studying individual adsorption of acetylene and ethylene on the Pd-Ag/SiO_2 catalyst. Since it was very difficult to make a self-supporting sample disk from Al_2O_3 sample, the SiO_2 support was used instead. However, it can be seen from the reactivity test and TPO results that there were no carbonaceous deposits formed over the surface after reaction for 8 h, indicating that the site on the support, where ethylene hydrogenation proceeds according to the model in Figure 3.3, can be neglected. Therefore, the change of support from Al_2O_3 to SiO_2 should be giving the same surface species on the metal sites. Three catalysts have been chosen for this experiment, i.e., untreated (as the reference), CO_2- and N_2O-treated Pd-Ag/SiO_2 catalysts.

C_2H_2 and C_2H_4 were individually exposed to the catalyst surface (after reduction and pretreatment) until saturation coverage. Then H_2 was exposed to the system for an hour in order to observe the species formed. It is to be noted that the C_2H_2 and C_2H_4 adsorption experiments were performed separately from the surface species formation by pretreatment described in section 5.2.4.1. The IR spectra of H_2 exposure to the Pd-Ag surface covered with C_2H_2 are displayed in Figure 5.15. Untreated catalyst displays a feature at 1370 cm^{-1} which is believed to be the CH_3 bending mode from adsorbed ethylidyne species (CH_3–C≡ (ads)). It has recently been reported that coadsorbing hydrogen and acetylene on Pd(111) leads to the formation of ethylidyne species at 1329-1333 cm^{-1} [43,45]. It is also seen symmetric bending vibration ($\delta_s CH_3$) occurs near 1375 cm^{-1} [144]. Therefore, the feature observed here at 1370 cm^{-1} is tentatively ascribed to adsorbed C_2H_2 as ethylidyne. However, the shift of the peak to the higher frequency observed in the Pd-Ag surface could be a result of weaker bond strength between ethylidyne and palladium surface due to the presence of Ag. A similar intense feature at 1370 cm^{-1} is also apparent on the CO_2-treated surface. On the contrary, such feature is not evidenced on the N_2O-treated catalyst. An additional feature is registered at ca. 1445 cm^{-1}, attributed to ethylene adsorbed on silica [145].

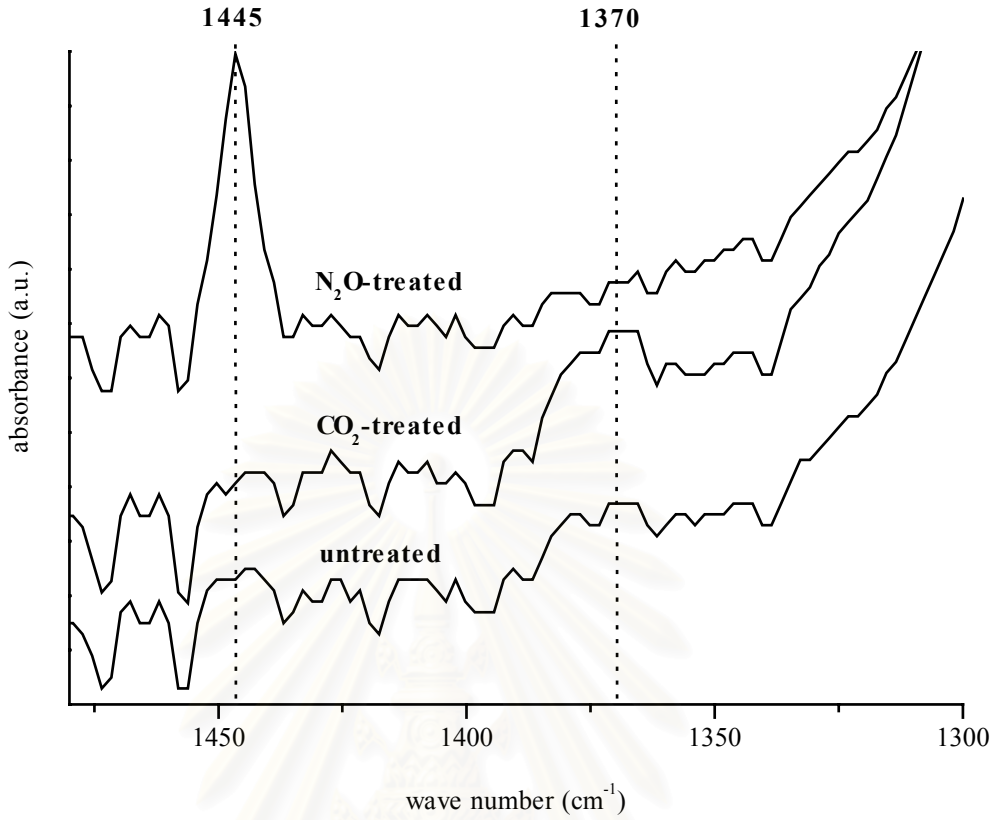

Figure 5.15 IR spectra of the H_2 exposure on C_2H_2 covered Pd-Ag/SiO_2 surface with and without pretreatment.

It is speculated that higher ethylene gain obtained from N_2O pretreatment may originate from the blockage of palladium sites responsible for ethane formation from ethylidyne species.

According to studies in UHV experiment, acetylene adsorbs more strongly than ethylene [41]. However, competitively adsorption between acetylene and ethylene has been proposed on supported palladium catalyst [76,108]. Ethylene hydrogenation was suggested to proceed on palladium sites not on alumina support via hydrogen spillover. However, such a proposed mechanism was considered for carbonaceous deposits while in this research, no carbonaceous deposits was found by TPO experiments (after reaction at 50°C for 8 h). It seems plausible that

hydrogenation of ethylene proceeds on palladium sites simultaneously with acetylene hydrogenation and the route of the former should not be via carbonaceous deposits. Exposure of C_2H_4 to the freshly reduced Pd-Ag surface or the surface after pretreatment was investigated here as a consequence. Figure 5.16 exhibits the infrared spectra of adsorbed C_2H_4 on the Pd-Ag surface. There is a strong feature at 1415 cm^{-1} which has been assigned to di-σ-adsorbed ethylene [144-146] from ethylene adsorption at 40°C on Pd-Ag catalysts with and without pretreatment. Despite the intermediate di-σ-adsorbed ethylene, other features located at 1445 and 1464 cm^{-1} appear, which have been assigned to ethylene adsorbed on silica and bending vibrations of C-H bonds in the scissoring bond ($\delta_s CH_2$) methylene group, respectively [144]. No evidence of π-adsorbed ethylene or ethylidyne species was found which would lead to absorption bands at ca. 1520-1550 cm^{-1} [145,146] and 1375 cm^{-1} [150] (as suggested as ethylidyne species from C_2H_2 exposure previously discussed). The nature of the species formed depends on the pretreatment temperature. For example, π-adsorbed ethylene was not observed after evacution the reduced Pt/Al_2O_3 at 290°C or lower [148]. Similarly, outgassing temperature of 200°C during pretreatment showed no evidence of π-adsorbed ethylene species on Pd/Al_2O_3 [43]. However, it has also been reported that exposure of C_2H_4 on Pd/SiO_2 produced mainly ethylidyne together with π-bonded and di-σ-bonded surface species. Absence of ethylidyne species together with substantial increase in π-bonded ethylene was observed with Ag addition [146]. It is feasible that Ag inhibits surface ethylidyne and π-adsorbed ethylene species on Pd-Ag/Al_2O_3 catalyst at 40°C. Pretreatment with either N_2O or CO_2 has insignificant effect on the absorption band at 1415 cm^{-1}.

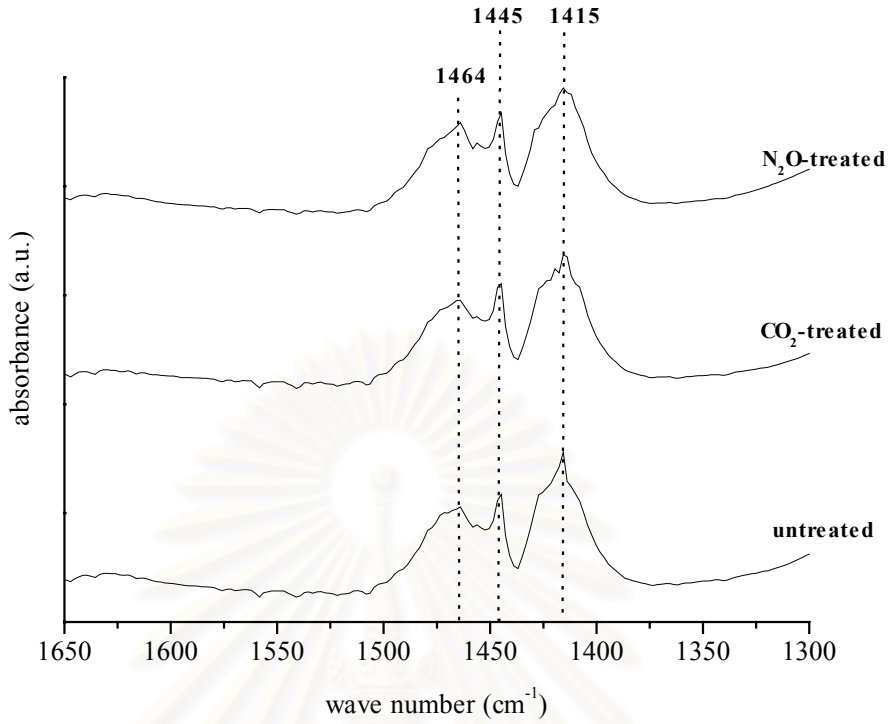

Figure 5.16 IR spectra of C_2H_4 adsorption on Pd-Ag/SiO_2 catalyst surface with and without pretreatement.

It can be summarised from the *in situ* infrared spectroscopy measurement that surface complex Pd-NO, as well as nitrite and nitrate species on Ag-Al_2O_3 particles, remained on the Pd-Ag surface after pretreatment with NO and N_2O. This is presumed to be the origin of the significant shift of the Ag 3d binding energies observed on the NO_x-treated catalysts. H_2 exposure to the surface saturated with acetylene at the reaction temperature (40^oC) leads to intermediate ethylidyne species which appeared at higher frequency (ca. 1370 cm^{-1}) compared to those reported on the monometallic Pd surface (ca. 1320-1330 cm^{-1}), suggesting that the adsorption strength of such species on the palladium surface is lessened in the presence of Ag. Interaction between C_2H_4 and the Pd-Ag surface at 40^oC results in formation of di-σ-bonded ethylene with no evidence of ethylidyne or π-bonded ethylene. Significant decrease in ethylidyne produced from exposure to C_2H_2 is observed with N_2O pretreated surface. However, insignificant change on the

absorption intensity of di-σ-bonded ethylene by pretreatment is seen. Since ethylidyne, which has been proved to be an intermediate for ethane formation, is diminished by pretreatment with N_2O, direct ethane formation on the palladium surface is lessened as well, thereby higher ethylene gain.

5.3 Study of Reaction Mechanism for the Selective Hydrogenation of Acetylene over Pd-Ag Catalysts

Through the characterisation described in section 5.2, explanation for the reactivity behaviour of untreated and pretreated Pd-Ag/α-Al_2O_3 catalysts for the selective hydrogenation of acetylene can be attempted. The main objective in the mechanistic study is to clarify the promoting effect of pretreatment with oxygen-containing compounds described in section 5.1.

It is noted that, in studying a selective hydrogenation, it is extremely important that all information of the intermediate and product, as well as the rate of surface reactions, etc., should be obtained at constant catalyst activity. Therefore, it is attempted to describe the mechanism based on the reactivity upon ageing presented in section 5.1.2 (Figures 5.3). The constancy over the course of an 8 h is measured in the experiments reported as the reaction proceeds, indicating that the reaction is not being poisoned.

Acetylene conversion and ethylene gain attain a steady state after the same period of time, i.e., 8 h. Ethylene hydrogenation that has been proposed to take place on alumina support by means of hydrogen spillover from the carbonaceous deposit bridges is hence unlikely in this study. It means, therefore, adsorption of acetylene and ethylene takes place on palladium sites and undergoes simultaneous hydrogenation. Selectivity should then be attributed to the presence of specific types of sites on palladium. According to the IR result observed from H_2 exposure to the C_2H_2 adsorbed surface at 40^{o}C, ethylidyne species are detected. Therefore an existence of sites on palladium surface where only acetylene and hydrogen can adsorb for direct ethane formation is confirmed. It is believed that ethylidyne is converted from vinylidene species when the surface was pre-adsorbed with acetylene. It has

been reported that in the absence of hydrogen, acetylene converts exclusively into vinylidene [45,150]. Pressurising a vinylidene-covered surface with hydrogen resulted in the formation of intermediate ethylidyne species, which are also removed by reaction with hydrogen [150]. This is feasible since vinylidene has been reported as an intermediate species for acetylene hydrogenation to ethylene [45,147] and, at the same time, when it reacts with hydrogen it can be converted into ethylidyne species [150]. The presence of adsorbed ethylene species on silica support (IR band at 1445 cm^{-1}) after hydrogen reacted with pre-adsorbed acetylene surface is the indirect proof that the desired reaction (hydrogenation of acetylene to ethylene) proceeds in the studied system. For C_2H_4 adsorption on a clean reduced Pd-Ag surface, di-σ-adsorbed ethylene is detected. Study of adsorption and reaction of C_2H_4 and hydrogen on $Pd/Al_2O_3/NiAl(110)$ [148] has shown that di-σ-ethylene can either desorb or dehydrogenate producing surface species such as ethylidyne and atomic hydrogen.

Reaction paths leading to possible products and the corresponding surface intermediates that observed from this study may be postulated as illustrated schematically in Figure 5.17. It is speculated that acetylene adsorption leads to vinylidene species which can react with hydrogen to form either ethylene product or ethylidyne intermediate species for ethane formation. The route for direct ethane formation is presumably via adsorbed acetylene as vinylidene, which reacts with hydrogen to form ethylidyne (Site 1). The observation of adsorbed ethylene on silica support by reaction of hydrogen with pre-adsorbed acetylene surface confirms the desired route for acetylene hydrogenation to ethylene (Site 2) which may occur via vinyl species formed by addition of hydrogen atom to vinylidene produced by acetylene adsorption. It can also dissociate to dissociatively adsorbed acetylene, which will be converted further to oligomers. It is believed that Site 3, which is responsible for oligomer formation, does exist in the alumina-supported system although intermediate species for this pathway were not detected from the IR observation where silica support was used. Site 4 for ethylene adsorption is also located on the palladium surface. On this site, di-σ-ethylene is produced and dehydrogenates to ethylidyne and atomic hydrogen, which will further hydrogenate to ethane.

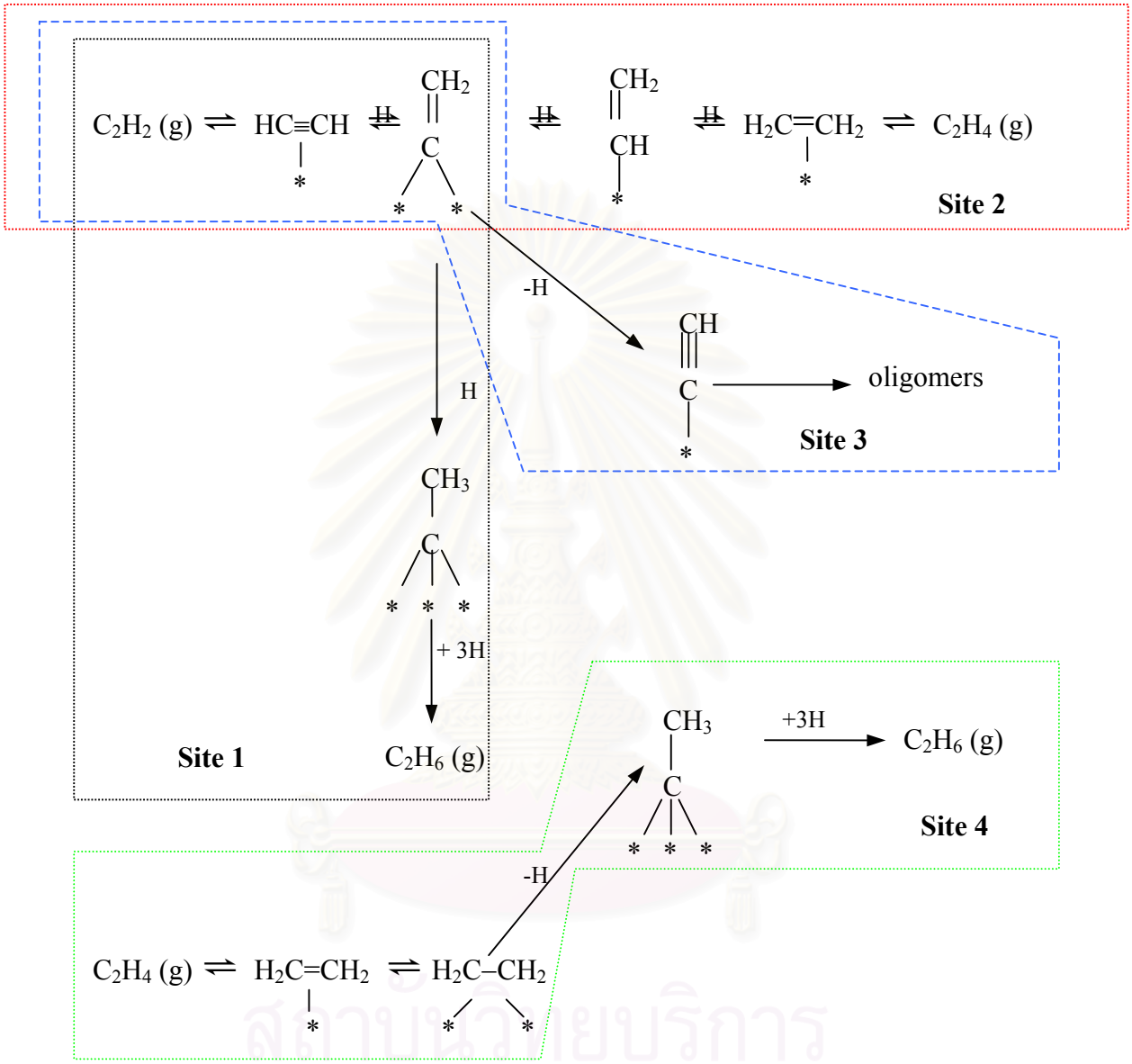

Figure 5.17 Proposed reaction mechanism proceeding on the palladium active sites.

Study of the catalyst reactivity affected by pretreatment with oxygen and other oxygen-containing compounds is attempted next. All treated catalysts improve the C_2H_2 conversion compared to untreated catalyst. However, the magnitude of improvement differs considerably. Thus, N_2O pretreatment increases conversion after 8 h on stream from 73% to 88% whereas NO pretreatment has a very small shift to

76%. Pretreatment with O_2 and CO_2 has a similar effect on C_2H_2 conversion to that of NO, whereas CO pretreatment is similar to the N_2O pretretment. Differences in ethylene gain for the different pretreatment are dramatic. With N_2O, the gain after 8 h increases from about 76% to 88%. The improvement is slightly less for NO pretreatment going from 76% to 82%. Gain decreases significantly to 70% for CO_2 pretreatment and to 63% for O_2 pretreatment.

Based on surface analysis by the XPS results, it can be concluded that the surface of Pd-Ag/Al_2O_3 catalyst after reduction contains solid solution between Pd and Ag with Ag enrichment. Pretreatment with oxygen or oxygen-containing compounds results in increased amount of palladium on the surface. This observation is consistent with the higher amount of active palladium sites measured by CO-adsorption and is proposed to be a reason for activity enhancement by pretreatment.

A significant positive shift of the Ag $3d_{5/2}$ due to pretreatment with NO and N_2O suggests surface modification by such compounds. The surface after reaction shows no state change of either Pd or Ag compared to that measured prior to reaction, suggesting that surface modification occurs after pretreatment and is retained even after 8 h on stream. The observed shift in the XPS results is believed to be a result of strong chemisorption or perhaps nitrate/nitrite formation on exposed Ag in the Pd-Ag alloy. IR experiment on C_2H_2 adsorption and reaction with hydrogen revealed less intensity of the feature corresponding to ethylidyne species together with a feature attributed to ethylene on silica from N_2O-pretreated surface. Ethylene adsorption, on the other hand, is insignificantly influenced by pretreatment. It is therefore concluded that promoting effect of N_2O and NO-pretreatment on ethylene gain originate from the strong adsorption of such species on the palladium sites which are responsible for direct ethane formation from acetylene via ethylidyne (Site 2). Presumably, the blockage of acetylene adsorption to produce ethylidyne intermediate species occurs by pretreatment with NO and N_2O.

CHAPTER VI

CONCLUSIONS AND RECOMMENDATIONS

This chapter is focused upon the conclusions of the experimental details of the selective hydrogenation of acetylene over Pd-Ag catalysts, in which effects of pretreatment with oxygen and oxygen-containing compounds were studied. Recommendations for further study are given, afterwards.

The effects of pretreatment with oxygen and oxygen-containing compounds (CO, CO_2, NO and N_2O) can be summarised as follows:

1. The Pd-Ag catalyst for the selective hydrogenation of acetylene can be activated by pretreatment with oxygen and oxygen-containing compounds. An activity increase of 8-20% for the pretreated catalysts is seen compared to that of the untreated catalyst.

2. Only pretreatment with NO and N_2O yields increased ethylene gain by ca. 4-10%.

3. Pretreatment has an insignificant effect on the catalyst morphology and bulk structure. However, modification of the surface composition by increasing the number of palladium active sites is suggested to be the origin of activity enhancement.

4. Surface analysis by XPS indicates the presence of a solid solution between palladium and silver with silver enrichment on the surface after reduction. Pretreatment has insignificant effect on the electronic state of Pd. However, an intrinsic shift of the Ag $3d_{5/2}$ by pretreatment with NO and N_2O suggests that surface modification by such species may exist.

5. Evidence of a linear complex Pd-NO as well as nitrate and nitrite species on Ag-alumina is found on the catalyst surface after pretreatment with NO and N_2O. This indicates the strong adsorption of such pretreatment species on the surface, which is suggested to be involved in the shift of the Ag core level energy.

6. The blockage of palladium sites responsible for direct ethane formation via ethylidyne species is postulated for the increased ethylene gain by pretreatment with NO and N_2O.

Recommendations for further study:

1. Effect of pretreatment on the acetylene polymerisation should be studied.

2. Reaction with longer time on stream where carbonaceous deposits are formed on the catalyst particles should be performed in order to get more information about the reaction mechanism when carbonaceous deposits are involved.

3. More powerful surface characterisation techniques such as soft X-ray absorption spectroscopy should be applied to the study in order to gain a precise knowledge of intermediate species. A better understanding not only of the activity/selectivity of the catalyst but also of its ageing should be generated as a consequence.

4. Investigation of effects of pretreatment with oxygen and oxygen-containing compounds on other bimetallic systems should be performed.

REFERENCES

1. Johnson, M.M., Walker, D.W., and Nowack, G.P. Selective hydrogenation. *US patent 4,484,015* (to Phillips Petroleum Company), 1984.
2. Bond, G.C.,and Wells, P.B. The hydrogenation of acetylene II. The Reaction of acetylene with hydrogen catalyzed by alumina-supported palladium. *J. Catal*. 5 (1965): 65-73.
3. Bond, G.C., Dowden, D.A., and Mackenzie, N. The selective hydrogenation of acetylene. *Trans. Faraday Soc.* 54 (1958): 1537-1546.
4. Larsson, M., Jansson, J. and Asplund, S. Incorporation of deuterium in coke formed on an acetylene hydrogenation catalysts. *J. Catal.* 162 (1996): 365-367.
5. Huang, Y.-J., Shun, C.F. Daniel, L.G., Mohundro, E.L., and Hartgerink, J.E. Regeneration of acetylene converter catalysts by hydrogen stripping. *US Patent 5,332,705* (to Exxon Chimical Patents Inc.),1994.
6. Flick, K., Herion, C., and Allman, H.-M. Supported palladium catalyst for selective catalytic hydrogenation of acetylene in hydrocarbons streams. *US Patent 5,856,262*, 1999.
7. Cosyns, J., and Boitiaux, J.-P. Process for selectively hydrogenating acetylene in a mixture of acetylene and ethylene. *US Patent 4,571,442* (Institut Francais du Petrole), 1984.
8. Boitiaux, J.-P., Cosyns, J., Derrien, M., and Leger, G. Newest hydrogenation catalysts. *Hydrocarbon Processing* March (1985): 51-59.
9. LeViness, S., Nair, V., and Weiss, A. Acetylene hydrogenation selectivity control on $PdCu/Al_2O_3$ catalyst. *J. Mol. Catal.* 25 (1984): 131-140.
10. Park, Y.H., and Price, G.L. Deuterium tracer study on the effect of CO on the selective hydrogenation of acetylene over Pd/Al_2O_3. *Ind. Eng. Chem. Res.* 30 (1991): 1693-1699.
11. Brophy, J.H., and Nock, A. Selective hydrogenation of acetylene. *US Patent 4,705,906*, 1987.

12. Weiss, A., LeViness, S., and Nair, V. The effect of Pd dispersion in acetylene selective hydrogenation. *Proceedings of the 8th International Congress on Catalysis.* Vol. 5, Berlin, 1984. Verlag Chemie, Weinheim, Dechema, Frankfurt am Nain, (1984): 591-600.
13. Cider, L., and Schöön, N.-H. Hydrogenation of acetylene at transient conditions in the presence of olefins and carbon monoxide over palladium/alumina. *Ind. Eng. Chem. Res.* 30 (1991): 1437-1443.
14. Park, Y.H., and Price, G.L. Temperature-programmed-reaction study on the effect of carbon monoxide on the acetylene reaction over Pd/Al_2O_3. *Ind. Eng. Chem. Res.* 30 (1991): 1700-1707.
15. Phillips, J., Auroux, A., Bergeret, G., Massardier, J, and Renoupez, A. Phase behaviour of palladium-silver particles supported on silica. *J. Phys. Chem*. 97 (1993): 3565-3570.
16. Huang, D.C., Chang, K.H., Pong, W.F., Tseng, P.K., Hung, K.J., and Huang, W.F. Effect of Ag-promotion on Pd catalysts by XANES. *Catal. Letters.* 53 (1998): 155-159.
17. Zhang, Q., Li, J., Liu, X., and Zhu, Q. Synergetic Effect of Pd and Ag Dispersed on Al_2O_3 in the Selective Hydrogenation of Acetylene. *Appl. Catal. A.* 197 (2000): 221-228.
18. Jin, Y., Datye, A.K., Rightor, E., Gulotty, R., Waterman, W., Smith, M., Holbrook, M., Maj, J. and Blackson, J. The influence of catalyst restructuring on the selective hydrogenation of acetylene to ethylene. *J. Catal.* 203 (2001): 292-306.
19. Visser, C., Zuidwijk, G.P., and Ponec, V. Reactions of hydrocarbons on palladium-gold alloys. *J. Catal.* 35 (1974): 407-416.
20. Sárkány Á., Horváth, A., and Beck, A. Hydrogenation of acetylene over low loaded Pd and $Pd-Au/SiO_2$ catalysts. *Appl. Catal. A.* 229 (2002): 117-125.
21. Shin, E.W., Choi, C.H., Chang, K.S., Na, Y.H., and Moon, S.H. Properties of Si-modified Pd catalyst for selective hydrogenation of acetylene. *Catal. Today* 44 (1998): 137-143.
22. Park, Y.H., Price, G.L. Promotion effects of potassium on palladium/alumina selective hydrogenation catalysts. *Ind. Eng. Chem. Res*. 31 (1992): 469-474.

23. Sárkány Á., Zsoldos, Z., Gy Stefler, J., Hightower, W., and Guczi, L. Promoter Effect of Pd in Hydrogenation of 1,3 Butadiene over Co-Pd Catalysts. *J. Catal*. 157 (1995): 179-189.

24. Praserthdam, P. Catalyst comprising of element from group 1B and VIIIB activated by oxygen or oxygen containing compound. *U.S. Patent*, 5,849,662 (1998).

25. Praserthdam, P., Phatanasri, S., and Meksikarin, J. Activation of acetylene selective hydrogenation catalysts using oxygen containing compounds. *Catal. Today* 63 (2000): 209-213.

26. Praserthdam, P., Phatanasri, S., and Meksikarin J. Activation of Pd-Ag catalyst for selective hydrogenation of acetylene via nitrous oxide addition. *React. Kinet. Catal. Lett.* 70 (2000): 125-131.

27. Al-Ammar, A.S., and Webb, G. Hydrogenation of acetylene over supported metal catalysts Part 1.-Adsorption of [^{14}C] acetylene and [^{14}C] ethylene on silica supported rhodium, iridium and palladium and alumina supported palladium. *J. Chem. Soc. Faraday*. 1 74 (1978): 195-205.

28. Al-Ammar, A.S., and Webb, G. Hydrogenation of acetylene over supported metal catalyst Part 2.-[^{14}C] tracer study of deactivation phenomena. *J. Chem. Soc. Faraday*. 1 75 (1978): 657-664.

29. Al-Ammar, A.S., and Webb, G. Hydrogenation of acetylene over supported metal catalyst Part 3.-[^{14}C] tracer studies of the effects of added ethylene and carbon monoxide on the reaction catalysed by silica-supported palladium, rhodium and iridium. *J. Chem. Soc. Faraday*. 1 75 (1978): 1900-1911.

30. McGown, W.T., Kemball, C., Whan, D.A., and Scurrell, M.S. Hydrogenation of acetylene in excess ethylene on an alumina supported palladium catalyst in a static system. *J. Chem. Soc. Faraday Trans.* 73 (1977): 632-647.

31. McGown, W.T., Kemball, C., and Whan, D.A. Hydrogenation of acetylene in excess ethylene on an alumina-supported palladium catalyst at atmospheric pressure in a spinning basket reactor. *J. Catal.* 51 (1978): 173-184.

32. Margitfalvi, J., Guczi, L., and Weiss, A.H. Reactions of acetylene during hydrogenation on Pd black catalyst. *J. Catal.* 72 (1981): 185-198.

33. Bortók, M., Czombos, J., Felföldi, K., Gera, L., Gőndős, Gy., Molnár, Á., Notheisz, F., Pálinkó, Wittman, Gy., and Zsigmond, Á. Stereochemistry of Heterogeneous Metal Catalysis, Wiley, Chichester, 1985 (Chapter 3 and 4).

34. Bos, A.N.R., and Westerterp, K.R. Mechanism and kinetics of the selective hydrogenation of ethyne and ethene. *Chem. Eng. Process*. 32 (1993): 1-7.

35. Molnár, Á., Sárkány, A., and Varga, M. Hydrogenation of carbon-carbon multiple bonds: chemo-, regio- and stereo-selectivity. *J. Mol. Catal.* 173 (2001): 185-221.

36. Taylor, G.F., Thomson, S.J., and Webb, G. The adsorption and retention of hydrocarbons by alumina-supported palladium catalysts. *J. Catal.* 12 (1968): 150-156.

37. Doring, T.A., Burlace, C.J., and Moss, R.L. Hydrogen adsorption on platinum/silica catalysts. *J. Catal.* 12 (1968): 207-220.

38. Guo, X.C., and Madix, R.J. Selective hydrogenation and H-D exchange of unsaturated hydrocarbons on Pd(100)-P(1x1)-H(D). *J. Catal.* 155 (1995): 336-344.

39. Guczi, L., Lapiette, R.B., Weiss, A.H., and Biron, E. Acetylene deuteration in the presence of [^{14}C] ethylene. *J. Catal*. 60 (1979): 83-92.

40. Molero, H., Bartlett, B.F., and Tysoe, W.T. The hydrogenation of acetylene catalyzed by palladium: hydrogen pressure dependence. *J. Catal.* 181 (1999): 49-56.

41. Tysoe, W.T., Nyberg, G.L., and Lambert, R.M. Photoelectron spectroscopy and heterogeneous catalysis: Benzene and ethylene from acetylene on palladium (111). *Surf. Sci.* 135 (1983): 128-146.

42. Kesmodel, L.L., Waddii, G.D., and Gates, J.A. Vibrational spectroscopy of acetylene decomposition on palladium (111) and (100) surfaces. *Surf. Sci.* 138 (1984): 464-474.

43. Beebe, T.P., Jr., and Yates, J.T., Jr. An *in situ* infrared spectroscopic investigation of the role of ethylidyne in the ethylene hydrogenation reaction on Pd/Al_2O_3. *J. Am. Chem. Soc.* 108 (1986): 663-671.

44. Hoffman, H., Zaera, F., Ormerod, R.M., Lambert, R.M., Yao, J.M., Saldin, D.K., Wang, L.P., Bennett, D.W., and Tysoe, W.T. A near-edge x-ray absorption fine structure and photoelectron spectroscopic study of the structure of acetylene on Pd(111) at low temperature. *Surf. Sci*. 268 (1992): 1-10.

45. Sandell, A., Beutler, A., Jaworowski, A., Wiklund, M., Heister, K., Nyholm, R., and Andersen, J.N. Adsorption of acetylene and hydrogen on Pd (111): formation of a well-ordered ethylidyne overlayer. *Surf. Sci.* 415 (1998): 411-422.

46. Rucker, T.G., Logan, M.A., Gentle, T.M., Muetterties, E.L., and Somorjai, G.A. Conversion of acetylene to benzene over palladium single-crystal surfaces. 1. The low-pressure stoichiometric and the high-pressure catalytic reactions. *J. Phys. Chem.* 90 (1986): 2703-2708.

47. Omerod, R.M., and Lambert, R.M. Heterogeneously catalysed cyclotrimerisation of ethyne to benzene over supported palladium catalysts. *J. Chem. Soc. Chem. Commun.* (1990): 1421-1425.

48. Omerod, R.M., and Lambert, R.M. Partial oxidation of unsaturated hydrocarbons over Pd(111): Oxygen scavenging of reactive intermediates and the formation of furan from C_2H_2 and C_2H_4. *Catal. Lett.* 6 (1990): 121-130.

49. Goetz, J., Volpe, M.A., Sica, A.M., Gigola, C.E., and Touroude, R. Low-loaded palladium on α-alumina catalysts: characterization by chemisorption, electro-microscopy, and photoelectron spectroscopy. *J. Catal.* 153 (1995) 86-93.

50. Borodzinski, A., Dus, R., Frak, R., Janko, A., and Palczewska, W. A study of the role of the palladium hydride phase in the activity and selectivity of palladium catalysts in acetylene hydrogenation. Proc. 6 th Int. Congr. on Catal. (London) 1976.

51. Den Hartog, A.J., Jongerius, F., and Ponec, V. Hydrogenation of acetylene over various group VIII metals: Effect of particle size and carbonaceous deposits. *J. Mol. Catal.* 50 (1990): 99-108.

52. Maetz, Ph., and Touroude, R. Modification of surface reactivity by adsorbed species on supported palladium and platinum catalysts during the selective hydrogenation of but-1-yne. *Appl. Catal. A*. 149 (1997): 189-206.

53. Duca, D., Frusteri, F., Parmaliana, A., and Deganello, G. Selective hydrogenation of acetylene in ethylene feedstocks on Pd catalysts. *Appl. Catal. A.* 146 (1996): 269-284.

54. Borodzinski, A. Hydrogenation of acetylene-ethylene mixtures on a commercial palladium catalyst. *Catal. Lett.* 63 (1999): 35-42.

55. Asplund, S. Coke formation and its effect on internal mass transfer and selectivity in Pd-catalysed acetylene hydrogenation. *J. Catal.* 158 (1996): 267-278.

56. Larsson, M., Jansson, K. and Asplund, S. The role of coke in acetylene hydrogenation on Pd/α-Al_2O_3. *J. Catal.* 178 (1998): 49-57.

57. Duca, D., Arena, F., Parmaliana, A., and Deganello, G. Hydrogenation of acetylene in ethylene rich feestocks: Comparison between palladium catalysts supported on pumice and alumina. *Appl. Catal. A*. 172 (1998): 207-216.

58. Asplund, S., Fornell, C., Holmgren, A., and Irandoust, S. Catalyst deactivation in liquid- and gas-phase hydrogenation of acetylene using a monolithic catalyst reactor. *Catal. Today* 24 (1995): 181-187.

59. Hub, S., Hilaire, L., Touroude, R. Hydrogenation of But-1-yne and But-1-ene on Palladium Catalysts: Particle Size Effect. *Appl. Catal.* 36 (1988): 307-322.

60. Boitiaux, J.P., Cosyns, J., and Vasudevan, S. Hydrogenation of highly unsaturated hydrocarbons over highly dispersed palladium catalyst: Part I: behaviour of small metal particles. *Appl. Catal.* 6 (1983): 41-51.

61. Gigola, C.E., Aduriz, H.R., and Bodnariuk, P. Particle size effect in the hydrogenation of acetylene under industrial conditions. *Appl. Catal.* 27 (1986): 133-144.

62. Ryndin, Y.A., Nosova, L.V., Boronin, A.I., Chuvilin, A.L. Effect of dispersion of supported palladium on its electronic and catalytic properties in the hydrogenation of vinylacetylene. *Appl. Catal.* 42 (1988): 131-141.

63. Shaiknutdinov, Sh.K., Frank, M., Bäumer, M., Jackson, S.D., Oldman, R.J., Hemminger, J.C., and Freund, H.-J. Effect of carbon deposits on reactivity of supported Pd model catalysts. *Catal. Letters*. 80 (2002): 115-122.

64. Vincent, M.J., and Gonzalez, R.D. A Langmuir-Hinshelwood model for a hydrogen transfer mechanism in the selective hydrogenation of acetylene over a Pd/γ-Al_2O_3 catalyst prepared by the sol-gel method. *Appl. Catal. A.* 217 (2001): 143-156.

65. Sárkány, Á., Weiss, A.H., and Guczi, L. Structure sensitivity of acetylene-ethylene hydrogenation over Pd catalysts. *J. Catal*. 98 (1986): 550-553.

66. Albers, P., Seibold, K., Prescher, G., and Muller, H. XPS and SIMS studies of carbon deposits on Pt/Al_2O_3 and Pd/SiO_2 catalysts applied in the synthesis of hydrogen cyanide and selective hydrogenation of acetylene. *Appl. Catal. A.* 176 (1999): 135-146.
67. Kang, J.H., Shin, E.W., Kim, W.J., Park, J.D., and Moon, S.H. Selective hydrogenation of acetylene on Pd/SiO_2 catalysts promoted with Ti, Nb and Ce oxides. *Catal. Today* 63 (2000): 183-188.
68. Choudary, B.M., Kantam, M.L., Reddy, N.M., Rao, K.K., Haritha, Y., Bhaskar, V., Figueras, F., and Tuel, A. Hydrogenation of acetylenics by Pd-exchanged mesoporous materials. *Appl. Catal. A.* 181 (1999): 139-144.
69. Ponec, F., and Bond, G.C. *Stud. Surf. Sci. Catal.* 95 (1995): Chap. 11.
70. Webb, G. The formation of role of carbonaceous residues in metal catalysed reactions of hydrocarbons. *Catal. Today* 7 (1990): 139-155.
71. Thomson, S.J., and Webb, G. Catalytic hydrogenation of olefins on metals: a new interpretation. *J. Chem. Soc. Chem. Commun.* (1976): 526-527.
72. Houzvicka, J., Pestman, R., and Ponec, V. The role of carbonaceous deposits and support impurities in the selective hydrogenation of ethyne. *Catal. Lett.* 30 (1995): 289-296.
73. Ponec, V. Catalysis by alloys in hydrocarbon reactions. *Adv. Catal*. 32 (1983): 149-211.
74. Borodzinski, A. Surface heterogeneity of supported palladium catalyst for the hydrogenation of acetylene-ethylene mixtures. *Langmuir* 13 (1997): 883-887.
75. Lee, H.H. Local effective diffusivity in a pellet deactivated by multilayer coking. *AIChE J.* 40 (1994): 2022-2027.
76. Yayun, L., Ying, Z., and Xuern, M. *Proceedings of the Joint Meeting Chem. Eng. Chem. Ind. Eng. Soc. China and Am. Inst. Chem. Eng.* Beijing, 1982.
77. Gandman, Z.E., Aerov, M.E., Men'shchikov, V.A. and Getmantsev, V.S. Formation of polymers in hydrotreating an ethane-ethylene fraction of pyrolysis gas to remove acetylene. *Int. Chem. Eng*. 15 (1975): 183-185.
78. Battiston, .G.C., Dalloro, L., and Tauszik, G.R. Performance and aging of catalysts for the selective hydrogenation of acetylene: a micropilot-plant study. *Appl. Catal.* 2 (1982): 1-17.

79. Bond, G.C., and Sheridan, J. Studies in heterogeneous catalysis Part 1.-The hydrogenation of methylacetylene. *J. Trans. Faraday Soc.* 48 (1952): 651-658.

80. Sheridan, J. The metal catalyzed reaction between acetylene and hydrogen part V, Reaction over palladium, iron, and some other catalysts. *J. Chem. Soc.* (1945): 470-476.

81. King, F., Jackson, S.D., and Hancock, F.E., in: Malz, R.E., Jr. *Catalysis of organic reactions*, Marcel Dekker, New York, 1996: 53-.

82. Bailey, S., Hancock, F.E., and Booth, J.S., *8th Ethylene Procedures Conference*, New Orleans (1996): 65 e.

83. Derrien, M.L. Selective hydrogenation applied to the refining of petrochemical raw materials produced by steam cracking. *Stud. Surf. Sci. Catal.* 27 (1986): 613-666.

84. Huang, W. Optimize acetylene removal. *Hydrocarbon Process*. Int. Ed. 58 (10) (1979): 131-132.

85. Pope, D., Walker, D.S., and Moss, R.L. The structure and activity of supported metal catalysts VII. CO poisoning and metal location in palladium-charcoal catalysts. *J. Catal.* 28 (1973): 46-53.

86. Palczewska, W., Rataczykowa, Szymerska, I., and Krawczyk, M. Proceedings of the 8th International Congress on Catalysis, Vol. 4, Berlin, 1984, Verlag Chemie, Weinheim, Dechema, Frankfurt am Main, (1984): 173-.

87. Ratajczykowa, I., and Szymerska, I. The influence of preadsorbed hydrogen and CO on adsorption of ethylene on the Pd(111) surface. *Chem. Phys. Lett.* 96 (1983): 243-246.

88. Angel, G.D., and Benitez, J.L. *J. Mol. Catal. A.* 94 (1994): 409-.

89. Lindlar, H., and Dubuis, R. *Org. Synth. Coll.* 5 (1973): 880-.

90. Barbier, J., Lamy-Pitara, E., Boitiaux, J.P., Marecot, P., Cosyns, J., and Verna, F. Role of sulfur in catalytic hydrogenation reactions. *Adv. Catal.* 37 (1990): 279-319.

91. Anderson, J.R. *Structure of Metal Catalysts,* Academic Press, New York, 1975.

92. Guczi, L., and Sárkány, Á., in: Spivey, J.J., Agarwal, S.K. (Senior Reporters), Catalysis, Vol. 11, The Royal Society of Chemistry, Thomas Graham House, Cambridge (1994): 318-.

93. Sassen, N.R.M., Hartog, A.J.D., Jongerius, F., Aarts, J.F.M, and Ponec, V. Adsorption and reactions of ethyne. *Faraday Discuss. Chem. Soc.* 87 (1989): 311-320.

94. Guczi, L., Schay, Z., Stefler, G., Liotta, L.F. Liotta, Deganello, G., Venezia, and A.M. Pumice-supported Cu-Pd catalysts: Influence of copper on the activity and selectivity of palladium in the hydrogenation of phenylacetylene and but-1-ene. *J. Catal.* 182 (1999): 456-462.

95. Grantom, R.L., and Royer, D.J., in: W. Gerhartz (Ed.), Ullman's Encyclopedia of Industrial Chemistry, 5th Edition, Verlag chemie, Weinheim, 1987, Vol. 10A, p. 45.

96. McCue, R.H., and Hicks, E.B. Mixed phase front end C.sub.2 acetylene hydrogenation. *US Patent* 5,414,170 (To Stone & Webster Engineering Corporation) 1995.

97. Bruce, M.C. Selective hydrogenation of highly unsaturated hydrocarbons in the presence of less unsaturated hydrocarbons. *US Patent* 4,216,645 (To Imperial Chemical Industries Limited) 1978.

98. Cheung, T.-T.P., Johnson, M.M. Selective acetylene hydrogenation. *US Patent* 5,510,550 (To Phillips Petroleum Company) 1996.

99. Hermen F. Mark, Donald F. Othmer, Charles G. Iverberger, Glenn T. Seaborg, Encyclopedia of Chemical Techonology, Vols. 1,9,15,18, 3 rd. edition, John Wiley & Sons, Inc., New York, 1978.

100. McFarland, Cecil G., Acetylene removal process. *US Patent* 4,658,080, 1987.

101. Ullmann's Encyclopedia of Industrial Chemistry, Vols. A1, A5 and A10, 5 th. Edition, VCH, Weinheim, Germany, 1987.

102. Moses, J.M., Weiss, A.H., Matusek, K., Guczi, L. The effect of catalyst treatment on the selective hydrogenation of acetylene over palladium/alumina. *J. Catal.* 86 (1984): 417-426.

103. Magitfalvi, J., Guczi, L., Weiss, A. Reaction routes for hydrogenation of acetylene-ethylene mixtures using a double labelling method. *React. Kinet. Catal. Lett.* 15 (1980): 475-479.

104. Borodzinski, A., and Cybulski, A. The kinetic model of hydrogenation of acetylene-ethylene mixtures over palladium surface covered by carbonaceous deposits. *Appl. Catal. A.* 198 (2000): 51-66.

105. Meksikarin, J. Effect of group 1B on the selective hydrogenation of acetylene over the palladium catalyst. Master's Thesis, Department of Chemical Engineering , Graduate School, Chulalongkorn University, 1995.

106. Anderson,J.R., and Pratt, K.C., Introduction to characterisation and testing of catalysts, Australia: Academic Press Australia, 1985.

107. Burch, R., Millington, P.J., and Walker, A.P. Mechanism of the selective reduction of nitrogen monoxide on platinum-based catalysts in the presence of excess oxygen. *Appl. Catal. B*. 4 (1994): 65-94.

108. Venezia, A.M., Rossi, A., Duca, D., Martorana, A., and Deganello, G. Particle size and metal-support interaction effects in pumice supported palladium catalysts. *Appl. Catal. A.* 125 (1995): 113-128.

109. Sárkány, Á., Horváth, A., and Beck, A. Hydrogenation of acetylene over low loaded Pd and Pd-Au/SiO_2. *App. Catal. A.* 229 (2002): 117-125.

110. Sandoval, V.H., Gigola, C.E. Charaterization of Pd and Pd-Pb/α-Al_2O_3 catalysts. A TPR-TPD study. *Appl. Catal. A*. 148 (1996): 81-96.

111. Chou, C.-W., Chu, S.-J., Chiang, H.-J., Huang, C.-Y., Lee, C., Sheen, S.-R., Perng, T.P., and Yeh, C. Temperature-programmed reduction study on calcination of nano-palladium. *J. Phys. Chem. B.* 105 (2001): 9113-9117.

112. Ponec, V., and Bond, G.C. Catalysis by metals and alloys. Elsevier, Amsterdam, 1995.

113. Soma-Noto, Y. and Sachtler,W.M.H. Infrared spectra of carbon monoxide adsorbed on supported palladium and palladium-silver alloys. *J. Catal.* 32 (1974): 315-324.

114. Sachtler, W.M.H. Chemisorption complexes on alloy surfaces. *Catal. Rev. Sci. Eng.* 14 (1976): 193-210.

115. Scholten, J.J. Cummunication at the workshop micromeritics, Veldhoven, 5-6 April, 1993.

116. Cormack, D., Pritchard, J., and Moss, R.L. CO chemisorption on silica-supported palladium-silver alloys. *J. Catal.* 37 (1975): 548-552.

117. Foger, K. in: Anderson, J.R., and Bourdart, (M. Eds), Catalysis: Science and Technology, Vol. 6, 1984, p 227.

118. Heinrichs, B., Delhez, P., Schoebrecht, J.-P., and Pirard, J.-P. Palladium-silver sol-gel catalysts for selective hydrodechlorination of 1,2-dichloroethane into ethylene. *J. Catal.* 172 (1997): 322-335.

119. Rieck, J. and Bell, A. The influence of dispersion on the interactions of H_2 and CO with Pd/SiO_2. *J. Catal.* 103 (1987): 46-54.

120. Leary, K., Michaels, J., and Stacy, A. Penetration of hydrogen into subsurface sites of silica-supported palladium during temperature-programmed desorption. *Langmuir* 4 (1988): 1251-1257.

121. Kim, K.S., Gossman, A.F., and Winogard, N. X-ray photoelectron spectroscopic studies of palladium oxides and the palladium-oxygen electrode. *Anal. Chem*. 46 (1974): 197-200.

122. Fuentes, S., Bogdanchikova, N., Avalos-Borja, M., Boronin, A., Faras, M.H., Diaz, G., Cortes, A.G., and Barrera, A. Structural and catalytic properties of Pd/Al_2O_3-La_2O_3 catalysts. *Catal. Today* 55 (2000): 301-309.

123. Legare, P., Finck, F., Roche, R. and Maire, G. XPS investigation of the oxidation of the Al/Pd surface: The Al_2O_3/Pd interface. *Surf. Sci.* 217 (1989): 167-178.

124. Brun, M., Berthet, A., and Bertolini, J.C. XPS, AES and Auger parameter of Pd and PdO. *J. Elec. Spec. Rel. Phe.* 104 (1999): 55-60.

125. Bhan, M.H., Nag, P.K., Miller, G.P., and Gergory, J.C. Chemical and morphological changes on silver surfaces produced by microwave generated atomic oxygen. *J. Vac. Sci. Technol.* 12 (1994): 699-706.

126. Schön, G. ESCA studies of Ag, Ag_2O and AgO. *Acta Che. Scand.* 27 (1973): 2623-2633.

127. Weaver, J.F. and Hoflund, G.B. Surface characterization study of the thermal decomposition of AgO. *J. Phys. Chem.* 98 (1994): 8519-8524.

128. Hoflund, G.B. and Hazos, Z.F. Surface characterization study of Ag, AgO and Ag_2O using x-ray photoelectron spectroscopy and electron energy-loss spectroscopy. *Phys. Rev. B.* 62 (2000):11126-11133.

129. Chae, K.H., Lee, Y.S., Jung, S.M., Jeon, Y., Croft, M., and Whang, C.N. *Nucl. Instr. And Meth. In Phys. Res. B.* 106 (1995): 60-64.

130. Chae, K.H., Jung, S.M., Lee, Y.S., Whang, C.N., Jeon, Y., Croft, M., Sills, D., Ansari, P.H., and Mack, K. Local density of unoccupied states in ion-beam-mixed Pd-Ag alloys. *Phys. Rev. B*. 53 (1996): 10328-10335.

131. Pauling, L. The Nature of the Chemical Bond. Cornell University Press, New York, 1960: p. 93.

132. David, L. R. (Ed.) Handbook of Chemistry and physics, 80th ed., p.1999.

133. Sales, E.A., Benhamida, B., Caizergues, V., Lagier, J.-P., Fievet, F., and Bozon-Verduraz, F. Alumina-supported Pd, Ag and Pd-Ag catalysts: Preparation through the polyol process, characterization and reactivity in hexa-1,5-diene hydrogenation. *Appl. Catal. A*. 172 (1998): 273-283.

134. Liotta, L.F., Venezia, A.M., Deganello, Longo, G. A., Martorana, A., Schay, Z., and Guczi, L. *Catal. Today* 66 (2001): 271-276.

135. Kinsinger, V., Sander, I., Steiner, P., Zimmermann, R. and Hufner, S. Screening and exchange splitting core level XPS. *Solid State Commun*. 73 (1990): 527-530.

136. Steiner, P. and Hufner, S. Thermochemical analysis of Pd_xAg_{1-x} alloys from XPS core-level binding energy *shifts. Solid State Commun.* 37 (1981): 79-81.

137. Boyer, H.E. in Gell, T.L. (Eds.). Metals Handbook Desk Edition, ASM, 1985, pp. 2-19.

138. Bouwman, R., Lippits, G.J.M., and Sachtler, W.M.H. Photoelectric Investigation of the surface composition of equilibrated Ag-Pd alloys in ultrahigh vacuum and in the presence of CO. *J. Catal.* 25 (1972): 350-361.

139. Tessier, D., Rakai, A. and Bozon-Verduraz, F. Spectroscopic study of the interaction of carbon monoxide with cationic and metallic palladium in palladium-alumina catlaysts. *J. Chem. Soc. Faraday Trans*. 88 (1992): 741-749.

140. Kijlstra, W.S., Brands, D.S., Poels, E.K., and Bliek, A. Mechanism of the selective catalytic reduction of NO by NH_3 over MnO_x/Al_2O_3. *J. Catal*. 171 (1997): 208-218.

141. Meunier, F.C., Breen, J.P., Zuzaniuk, V., Olsson, M., and Ross, J.R.H. Mechanistic aspects of the selective reduction of NO by propene over alumina and silver-alumina catalysts. *J. Catal.* 187 (1999): 493-505.

142. Valden, M., Keiski, R.L., Xiang, N., Pere, J., Aaltonen, J., Pessa, M., Maunula, T., Savimäki, A., Lahti, A., and Härkönen, M. Reactivity of Pd/Al_2O_3, Pd/La_2O_3 and $Pd/LaAlO_3$ catalysts for the reduction of NI by CO: CO and NO adsorption, *J. Catal.* 161 (1996): 614-625.

143. Almusaiteer K., and Chuang, S.S.C. Isolation of active adsorbates for the NO-CO resaction on Pd/Al_2O_3 by selective enhancement and selective posioning. *J. Catal.* 180 (1998): 161-170.

144. Silvestein, R.M., Bassler, C.G., Morrill, T.C. Spectrometric identification of organic compounds, John Wiley&Son, New York, 1974.

145. Hill, J.M., Shen, J., Watwe, R.M., and Dumesic, J.A. Microcalorimetric, infrared spectroscopic and DFT studies of ethylene adsorption on Pd and Pd/Sn catalysts. *Langmuir* 16 (2000): 2213-2219.

146. Li, M., and Shen, J. Microcalorimetric and infrared spectroscopic studies of CO and C_2H_4 adsorption on Pd/SiO_2 and $Pd-Ag/SiO_2$ catalysts. *Mater. Chem. Phys.* 68 (2001): 204-209.

147. Stacchiola, D., Kaltchev, M., and Tysoe, W.T. The adsorption and structure of carbon monoxide on ethylidyne-covered Pd(111). *Surf. Sci.* 420 (2000): L32-L38.

148. Moshin, S.B., Trenary, M., and Robota, H.J. Identification of ethylene-derived species on Al_2O_3-supprted Rh, Ir, Pd and Pt catalysts by infrared spectroscopy. *J. Phys. Chem.* 95 (1991): 6657-6661.

149. Stacchiola, D., and Tysoe, W.T. The adsorption of ethylene on ethylidyne-covered Pd(111). *Surface science.* 513 (2002): L431-L435.

150. Azad, S., Kaltchev, M., Stacchiola, D., and Tysoe, W.T. On the reaction pathway for the hydrogenation of acetylene and vinylidene on Pd(111). *J. Phys. Chem. B.* 104 (2000): 3107-3115.

APPENDICES

APPENDIX A

CALCULATION FOR CATALYST PREPARATION

The calculation shown below is for 0.03%Pd-0.235%Ag/Al_2O_3. The alumina support weight used for all preparation is 2 g.

Based on 100 g of catalyst used, the composition of the catalyst will be as follows:

Palladium = 0.03 g

Silver = 0.235 g

Alumina = 100–(0.03+0.235) = 99.735 g

For 2 g of alumina

Palladium required = $2 \times 0.035/99.735$ g = 7.02×10^{-4} g

Palladium nitrate 0.1 g dissolved in de-ionised water with 0.4 ml of hydrochloric acid (concentration of HCl is 37% v/v)

Then Pd content in stock solution = $\frac{\text{weight of Pd } (NO_3)_2 \times \text{MW of Pd}}{\text{MW of Pd } (NO_3)_2}$

= $0.1 \times 106.4/230.4$ = 0.046 g

Pd $(NO_3)_2$ taken from stock solution = $7.02 \times 10^{-4} \times 10/0.046$ = 0.153 g

Since the pore volume of the alumina support is 0.25 ml/g and the total volume of impregnation solution which must be used is 0.5 ml by the requirement of dry impregnation method, the de-ionised water is added until the total volume of impregnation solution is 0.5 ml.

APPENDIX B

CALCULATION CURVES

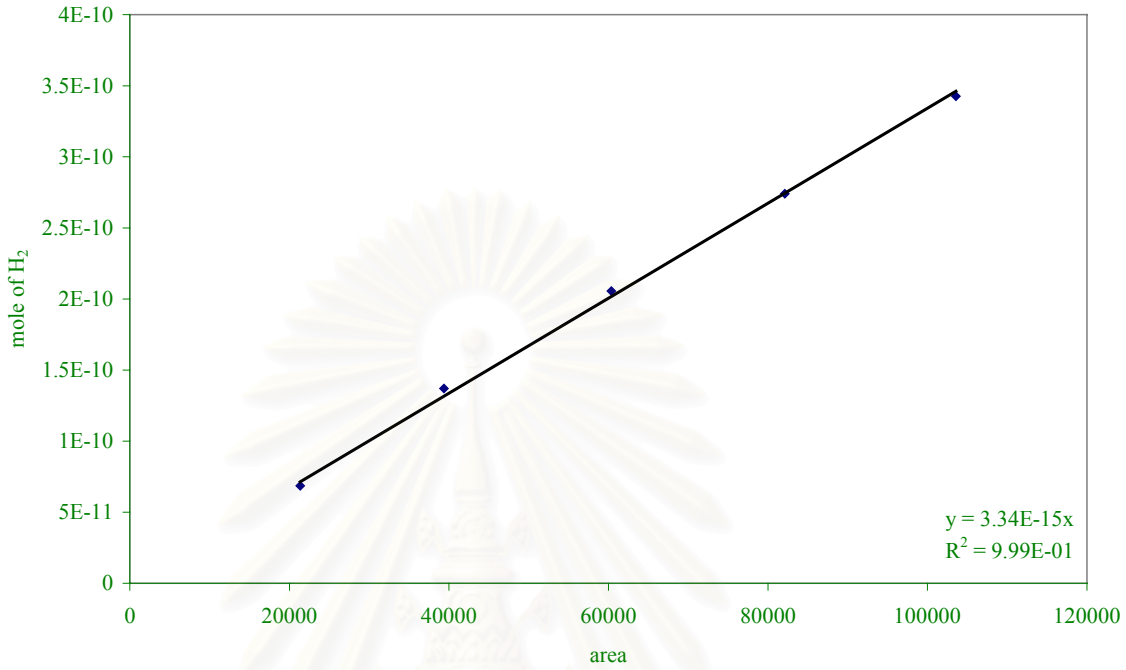

Figure B.1 The calibration curve of hydrogen from TCD of GC-8A.

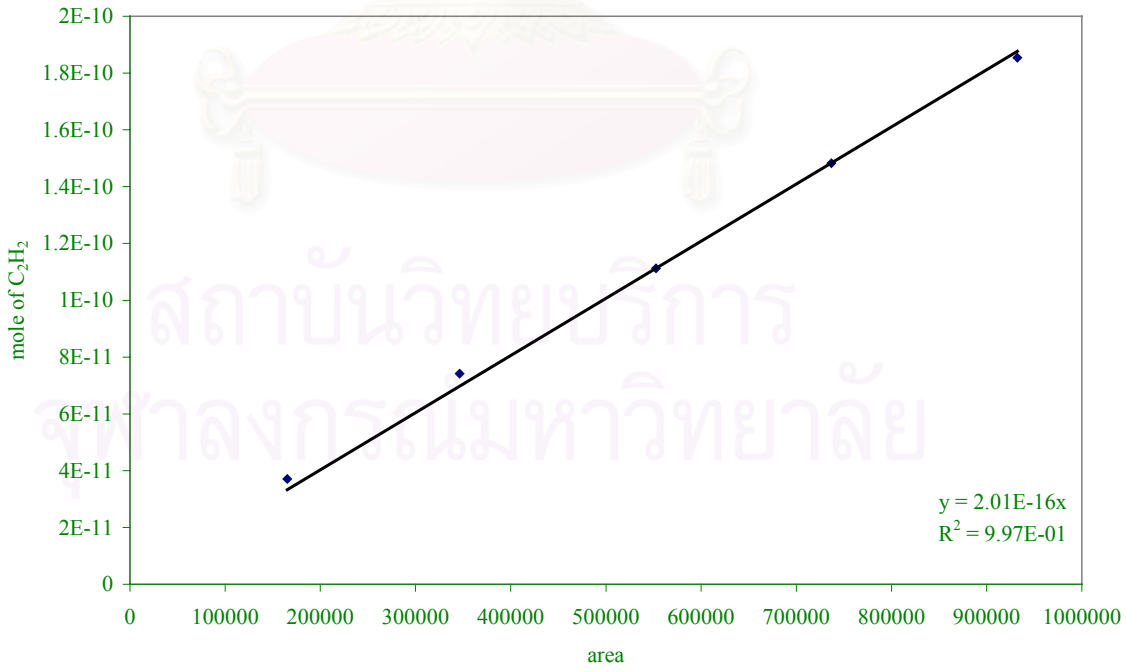

Figure B.2 The calibration curve of acetylene from FID of GC-9A.

APPENDIX C

EFFECTIVE PRETREATMENT CONDITIONS

Prior to the reaction test, the Pd-Ag/Al_2O_3 catalyst was activated with oxygen and oxygen-containing compounds (CO, CO_2, NO and N_2O). And effective amount of pretreatment compounds addition (between 0.02 to 0.20 ml) was determined where the pretreatment temperature was kept constant at 90oC. Variation of the acetylene conversion with the addition amount is illustrated in Figure C.1.

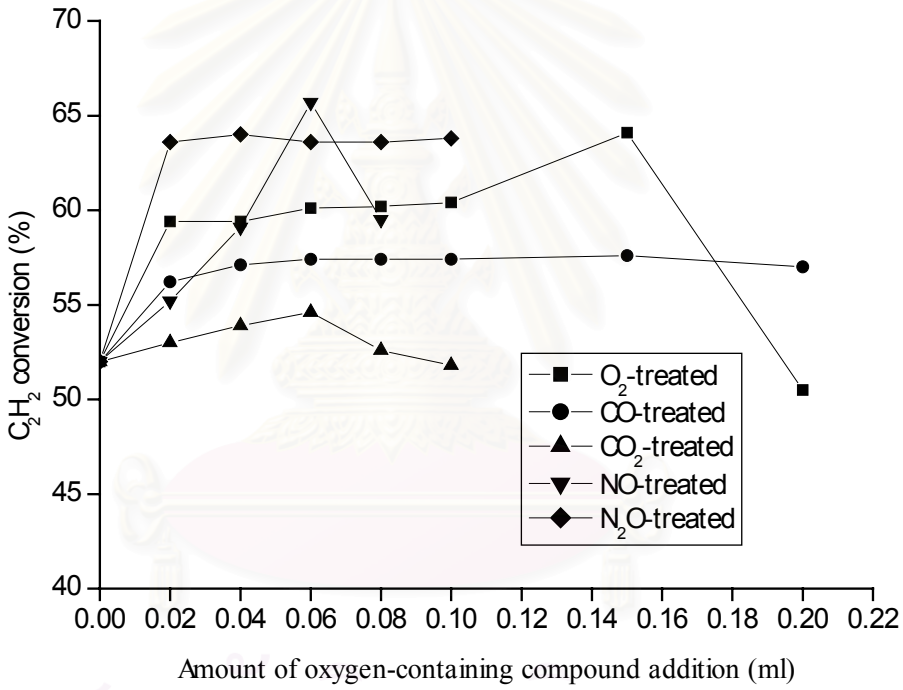

Figure C.1 Variation of C_2H_2 conversion with the added amount of oxygen and oxygen-containing compounds. Pretreatment temperature, 90^oC; reaction temperature 50^oC; GHSV, 2000 h^{-1}.

The different addition amounts in the range 0.02-0.20 ml resulted in no significant difference in the acetylene conversion except in the case of NO pretreatment. The addition amount which gives the highest C_2H_2 conversion for each pretreatment was selected for further study.

Another crucial parameter for pretreatment was the temperature at which an oxygen or oxygen-containing compounds was introduced to the catalyst after reduction. Figure C.2 depicted the effect of pretreatment temperature on the C_2H_2 conversion over Pd-Ag/Al_2O_3 catalysts. The effective amount previously studied (Figure C.1) was kept constant.

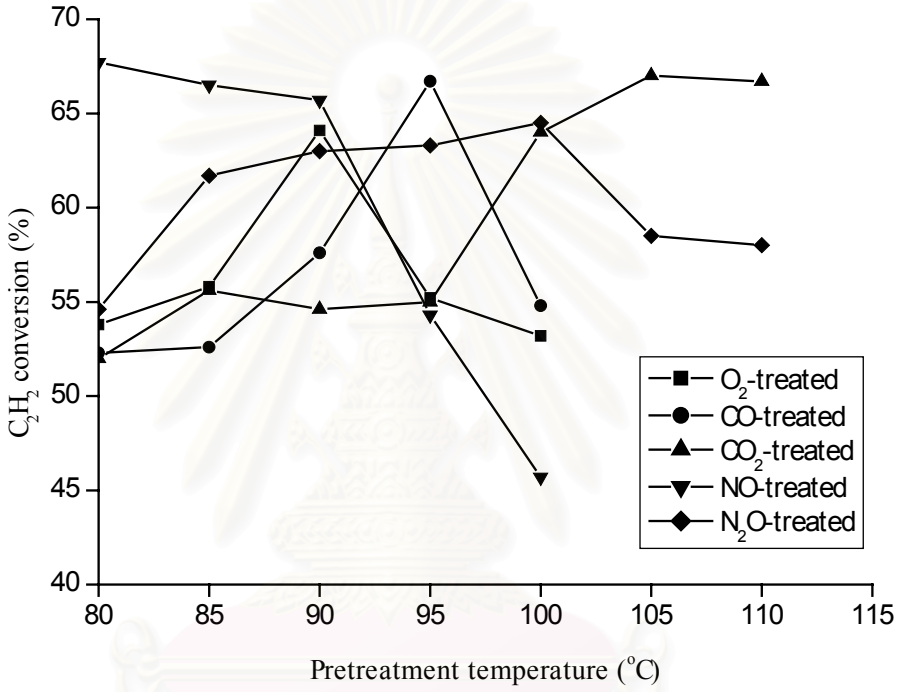

Figure C.1 Effect of pretreatment temperature on C_2H_2 conversion of treated Pd-Ag/Al_2O_3 catalysts; Reaction temperature, 50°C; GHSV, 2000 h^{-1}.

The pretreatment temperature of each pretreatment compound at which highest acetylene conversion was observed was selected for pretreatment the catalysts for further study.

APPENDIX D

CALCULATION OF C_2H_2 CONVERSION AND C_2H_4 GAIN

The catalyst performance for the selective hydrogenation of acetylene was evaluated in terms of activity for acetylene conversion and ethylene gain based on the following equations:

$$C_2H_2 + H_2 \longrightarrow C_2H_4 \qquad (D.1)$$

$$C_2H_4 + H_2 \longrightarrow C_2H_6 \qquad (D.2)$$

Activity of the catalyst for acetylene conversion is defined as moles of acetylene converted with respect to acetylene in the feed:

$$C_2H_2 \text{ conversion (\%)} = \frac{100\times[\text{ mole of } C_2H_2 \text{in feed} - \text{mole of } C_2H_2 \text{ in product}]}{\text{mole of } C_2H_2 \text{in feed}} \qquad (i)$$

where mole of C_2H_2 can be measured employing the calibration curve of C_2H_2 in Figure B.1, Appendix B., i.e.,

mole of C_2H_2 = (area of C_2H_2 peak from integrator plot on GC-9A) $\times 2.01\times10^{-16}$ (ii).

Ethylene gain was calculated from moles of hydrogen and acetylene as explained in section 5.1.1:

$$C_2H_4 \text{ gain (\%)} = \frac{100\times[dC_2H_2 - (dH_2 - dC_2H_2)]}{dC_2H_2} \qquad (iii)$$

where dC_2H_2 = mole of acetylene in feed – mole of acetylene in product (iv)

dH_2 = mole of hydrogen in feed – mole of hydrogen in product (v)

mole of C_2H_2 is calculated by using (ii) whereas mole of H_2 can be measured employing the calibration curve of H_2 in Figure B.2, Appendix B., i.e.,

mole of H_2 = (area of H_2 peak from integrator plot on GC-8A) $\times 3.34\times10^{-15}$ (vi).

APPENDIX E

CALCULATION FOR METAL ACTIVE SITES

Calculation of the metal active sites and metal dispersion of the catalyst measured by CO adsorption is as follows:

Let the weight of catalyst used	= W	g
Integral area of CO peak after adsorption	= A	unit
Integral area of 40 μl of standard CO peak	= B	unit
Amounts of CO adsorbed on catalyst	= B-A	unit
Volume of CO adsorbed on catalyst	= $40\times[(B-A)/B]$	μl
Volume of 1 mole of CO at 30°C	= 24.86×10^{6}	μl

Mole of CO adsorbed on catalyst = $[(B-A)/B]\times[40/24.86\times10^{6}]$ mole

Molecule of CO adsorbed on catalyst = $[1.61\times10^{-6}]\times[6.02\times10^{23}]\times[(B-A)/B]$ molecules

Metal active sites = $9.68\times10^{17}\times[(B-A)/B]\times[1/W]$ molecules of CO/g of catalyst

APPENDIX F

LIST OF PUBLICATIONS

1. Piyasan Praserthdam, Bongkot Ngamsom, Nina Bogdanchikova, Suphot Phatanasri, and Mongkonchanok Pramotthana, "Effect of the pretreatment with oxygen and/or oxygen-containing compounds on the catalytic performance of Pd-Ag/Al_2O_3 for acetylene hydrogenation", Applied Catalysis A: General, 230 (2002): 41-51.

ELSEVIER

Applied Catalysis A: General 230 (2002) 41–51

APPLIED CATALYSIS A: GENERAL

www.elsevier.com/locate/apcata

Effect of the pretreatment with oxygen and/or oxygen-containing compounds on the catalytic performance of Pd-Ag/Al_2O_3 for acetylene hydrogenation

Piyasan Praserthdam [a,*], Bongkot Ngamsom [a], Nina Bogdanchikova [b], Suphot Phatanasri [a], Mongkonchanok Pramotthana [a]

[a] *Research Center on Catalysis and Catalytic Reaction Engineering, Department of Chemical Engineering, Chulalongkorn University, Bangkok 10330, Thailand*

[b] *Centro de Ciencias de La Materia Condensada UNAM, A.P. 2681, Ensenada, BC 22800, Mexico*

Received 25 June 2001; received in revised form 26 September 2001; accepted 15 November 2001

Abstract

Catalytic performance of Pd-Ag/α-Al_2O_3 was studied for the selective hydrogenation of acetylene in the presence of excess ethylene. The catalyst activation was undertaken prior to the reaction test by the pretreatment with oxygen and/or oxygen-containing compounds, i.e. O_2, NO, N_2O, CO and CO_2. The enhancement of catalytic performances by the pretreatment was a consequence of an increase in accessible Pd sites responsible for acetylene hydrogenation to ethylene. Furthermore, the sites involving direct ethane formation from acetylene could be suppressed by NO_x treatment.

Keywords: Acetylene hydrogenation; Pd-Ag/Al_2O_3; Oxygen-containing compounds; Pretreatment

1. Introduction

The selective hydrogenation of acetylene to ethylene is an important process used to purify ethylene streams containing trace amounts of acetylene for the production of polyethylene. When acetylene is catalytically hydrogenated, it is desirable that ethylene should remain intact during hydrogenation. Typically, supported palladium catalyst is employed for this process due to its good activity and selectivity. Nevertheless, Pd catalyst has poor selectivity at high acetylene conversion and there is also oligomer formation during acetylene hydrogenation on this catalyst, which lessens the catalyst lifetime [1–5]. Attempts to improve the performance of palladium-based catalysts in terms of selectivity and recycle time have been studied by the addition of a second metal such as Ag, Cr and Cu [6–10]. Ag has received considerable attention in the literature as a selectivity promoter [11–15]. Recently, it has been discovered that a catalyst comprising IB and VIIIB groups could be activated with oxygen and/or oxygen-containing compounds prior to use [16].

The present study was undertaken in an attempt to determine the effect of the pretreatment with oxygen, and other oxygen-containing compounds, on the catalytic performance of the silver-promoted

* Corresponding author. Fax: +66-2-218-6769.
E-mail address: piyasan.p@chula.ac.th (P. Praserthdam).

0926-860X/02/$ – see front matter
PII: S0926-860X(01)00993-0

palladium catalyst for selective hydrogenation of acetylene.

2. Experimental

2.1. Catalyst

2.1.1. Catalyst preparation

Pd-Ag/α-Al_2O_3 (0.03%Pd-0.235%Ag and 3%Pd-4%Ag) catalysts were prepared by the impregnation technique. Alumina support type CS-303 was obtained from United Catalyst Incorporation (UCI), USA Palladium was loaded first using $Pd(NO_3)_2$ in 37% HCl (aq) as the Pd source. Then the alumina, impregnated with Pd, was dried at 110 °C for 12 h and calcined in air at 550 °C for 2 h. A second impregnation was performed using $AgNO_3$ (aq) as the source of Ag. The impregnated catalyst was then dried at 110 °C for 12 h and calcined in air at 370 °C for 1 h. The catalyst composition is illustrated in Table 1.

2.1.2. Pretreatment

The prepared catalyst was pretreated with oxygen and other oxygen-containing compounds, i.e. N_2O, NO, CO_2 and CO, prior to the reaction test. The catalyst was reduced in H_2 flow at 150 °C for 2 h with a heating rate of 10 °C/min, and then cooled down to the pretreatment temperature, which was varied between 80 and 120 °C, with Ar flow. A small proportion of pretreatment gas in the range 0.02–0.20 ml was injected into the system afterwards. Effective conditions were studied for each pretreatment gas and results were used for further study of catalytic performance upon pretreatment. The prereduction before catalytic evaluation was not performed again after pretreatment.

Table 1
Catalyst properties of 0.03%Pd-0.235%Ag/Al_2O_3

Carrier	α-Al_2O_3
Pd source	$Pd(NO_3)_2$
Ag source	$AgNO_3$
Pd content (wt.%)	0.03
Ag content (wt.%)	0.235
BET surface area (m^2/g)	30
Pore volume (cm^3/g)	0.45
Metal active site (CO molecule/g cat.)	1.16×10^{17}
Pd dispersion (%)	6.84

2.2. Catalyst characterizations

2.2.1. CO-adsorption measurement

The metal active sites of the catalysts were assessed by adopting a CO-adsorption technique using a pulse method. This technique involved pulsing a known volume of carbon monoxide over a catalyst sample at room temperature. The sample was reduced in a H_2 flow at 150 °C for 2 h; this was followed by the replacement of H_2 with He, and the sample was then cooled down to ambient temperature in a He flow. When the treated catalysts were used, the sample reduced with H_2, as mentioned above, was cooled down to the pretreatment temperature and held at that temperature for 10 min in a He flow before oxygen and/or oxygen-containing compounds, i.e. O_2, NO, N_2O, CO and CO_2, was/were introduced to the catalyst. CO-adsorption was measured after the reactor was cooled down to the ambient temperature.

2.2.2. X-ray diffraction (XRD)

The X-ray diffraction (XRD) spectrum of the catalysts with and without pretreatment were carried out ex situ employing an X-ray refractometer, SIEMENS XRD D5000, with Cu Kα radiation, accurately measured in the 10–80°, 2 theta angular region.

2.2.3. X-ray photoelectron spectroscopy (XPS)

XPS analyses were performed ex situ, using an analysis chamber equipped with a Riber-CAMECA MAC-3 system. X-ray photoelectron spectroscopy (XPS) data were collected after excitation of Mg Kα radiation ($h\nu = 1253.6$ eV).

2.3. Catalytic activity test

Each catalytic activity test was carried out in a 9 mm (i.d.) quartz reactor packed with 40/60 mesh catalyst. Prior to the start of each experimental run, the catalyst was reduced in situ with hydrogen by heating from room temperature to 150 °C at a heating rate of 10 °C/min. Then the reactor was purged with argon and cooled down to the reaction temperature. The reaction was carried out after the pretreatment with oxygen and/or oxygen-containing compounds using a feed composition of 0.716% C_2H_2, 0.823% H_2, 33.707% C_2H_6 and balanced C_2H_4 with a GHSV of 2000 h^{-1}. The optimum conditions for the

pretreatment were investigated by examining the effective addition amount and the pretreatment temperature.

The products and feeds were analyzed by a gas chromatograph equipped with a FID detector (SHIMADZU FID GC 9A, carbosieve column S-2) for C_2H_2, C_2H_4 and C_2H_6. H_2 was analyzed by a gas chromatograph equipped with a TCD detector (SHIMADZU TCD GC 8A, molecular sieve-5A).

The temperature dependence of the catalytic performance was observed during the range of 40–100 °C in 10 °C increments.

3. Results and discussion

The catalytic performance is evaluated in terms of activity and ethylene gain (%) in accord with the following reaction schemes:

$$C_2H_2 + H_2 \rightarrow C_2H_4 \quad (1)$$

$$C_2H_4 + H_2 \rightarrow C_2H_6, \quad \text{hence} \quad (2)$$

$$C_2H_2 + 2H_2 \rightarrow C_2H_6 \quad (3)$$

Activity or acetylene conversion as used herein is defined as moles of acetylene converted with respect to acetylene in feed:

$$\text{Ethyelene gain} = \frac{(C_2H_2 \text{ hydrogenated to } C_2H_4) \times 100}{\text{totally hydrogenated } C_2H_2} \quad (4)$$

The acetylene being hydrogenated to ethylene (gained) is the difference between the totally hydrogenated acetylene and the ethylene being lost by hydrogenation to ethane.

The ethylene being hydrogenated to ethane is the difference between all the hydrogen consumed and all the acetylene which has been totally hydrogenated:

$$\text{Ethylene gain} = \frac{[dC_2H_2 - (dH_2 - dC_2H_2)] \times 100}{dC_2H_2} \quad (5)$$

or in other words, as Eqs. (1) and (2) show, 2 mol of hydrogen are consumed for the acetylene lost to ethane, but only 1 mol of hydrogen for the acetylene gained as ethylene. The overall gain can also be written as:

$$\text{Ethylene gain} = \left(2 - \frac{dH_2}{dC_2H_2}\right) \times 100 \quad (6)$$

Forms (5) and (6) are, of course the same, and the ethylene gain (%) discussed in the manuscript was then calculated based upon Eq. (6).

A Pd-Ag/Al_2O_3 (0.03 wt.% Pd and 0.235 wt.% Ag) was catalytically evaluated for the selective hydrogenation of acetylene at 50 °C and GHSV 2000 h^{-1}. The catalyst was activated with oxygen and/or oxygen-containing compounds (O_2, CO, CO_2, NO and N_2O) prior to the reaction test. An effective amount of oxygen and/or oxygen-containing compounds addition was determined where the pretreatment temperature was kept constant at 90 °C. Variation of the catalytic activity with the addition amount is illustrated in Fig. 1. An increase in the catalytic activity was observed over the treated catalysts compared to the activity of the untreated one at the same reaction conditions. The different addition amounts in the range of 0.02–0.20 ml resulted in no significant difference in the catalytic activity except in the case of NO treatment, where the maximum point was obviously seen at a certain addition amount. The improvement in catalytic activity of Pd-Ag/Al_2O_3 by various pretreatments depends on the characteristics of oxide formation among Ag and Pd and oxygen atoms in oxygen-containing compounds. The temperature at which oxygen and/or oxygen-containing compounds was/were introduced to the catalyst was expected to be another crucial parameter. As depicted

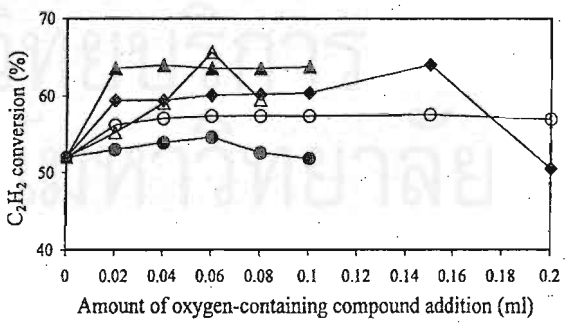

Fig. 1. Variation of C_2H_2 conversion with the added amount of oxygen and/or oxygen-containing compounds; (◆) O_2-treated, (●) CO_2-treated, (○) CO-treated, (▲) N_2O-treated and (△) NO-treated. Pretreatment temperature, 90 °C; reaction temperature, 50 °C; GHSV, 2000 h^{-1}.

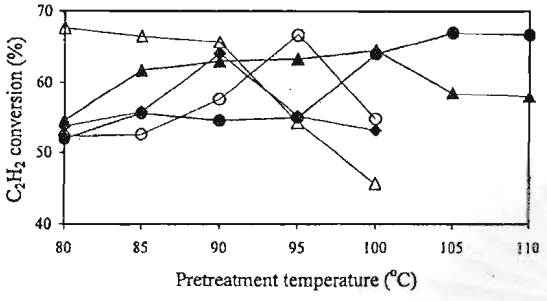

Fig. 2. Effect of the pretreatment temperature on the catalytic activity of treated Pd-Ag/Al_2O_3 catalysts; (◆) O_2-treated, (●) CO_2-treated, (○) CO-treated, (▲) N_2O-treated and (△) NO-treated. Reaction temperature, 50 °C; GHSV, 2000 h^{-1}.

in Fig. 2, the pretreatment temperature had a remarkable influence on the activity of the treated catalysts.

The surface analyses of the untreated and treated catalysts were performed using XRD and XPS techniques. Due to the low content of metal loading in the catalyst samples (0.03% Pd and 0.235% Ag), we experienced difficulty in direct observation of palladium and silver phases by XRD for these samples. The higher contents of metals, i.e. 3% Pd and 4%Ag, were therefore loaded. The effects of pretreatment on the catalytic performances of these high metal loaded catalysts were also investigated and the similarity between the 0.03%Pd-0.235%Ag/Al_2O_3 and the 3%Pd-4%Ag/Al_2O_3 catalysts was revealed. These samples were then studied as models of the catalysts used in the XRD test. The details of sample resemblance will be discussed later. Fig. 3 shows the X-ray diffractograms of Pd-Ag/α-Al_2O_3 samples after calcination (curve A), after reduction (curve B) and after pretreatment with N_2O (curve C). All diffractograms contained characteristic peaks of α-Al_2O_3. The calcined samples exhibited PdO (33.9°), Ag_2O (32.3°), Pd (2 0 0) (46.2°) and Ag (3 1 1) (77.6°) besides the peaks attributed to Al_2O_3 [17–19]. After the sample had been reduced (curve B), the peaks corresponded to PdO and Ag_2O disappeared while the Ag (3 1 1) peak remained. Between the (1 1 1) Bragg lines of pure Pd and Ag ($2\theta = 40.1$ and 38.1°, respectively) the reduced sample exhibited a broad peak, which indicates the presence of a solid solution in the form of small Pd–Ag alloy particles [17]. Except for the alloy surface, a Ag_2O characteristic peak was detected on the pretreated sample (curve C).

Results of XPS study are presented in Table 2. For all studied samples the binding energies of 2p electron of Al were found to be in the range 73.8–74.0 eV and the binding energies of O 1s electrons were 530.8–531.0 eV, which are typical values for Al_2O_3. The Ag $3d_{5/2}$ binding energy of 0.03%Pd-0.235%Ag/Al_2O_3 samples was 366.8 eV whereas for the 3%Pd-4%Ag/Al_2O_3 catalysts, it was in the range 366.8–367.0 eV, which are typical values for oxidized silver [20].

The Pd $3d_{5/2}$ binding energies were found to be 334.0–334.2 eV for the 3%Pd-4%Ag/Al_2O_3 catalysts, whereas those of the 0.03%Pd-0.235%Ag/Al_2O_3 samples could not be observed by XPS. The Pd $3d_{5/2}$ binding energies observed for Pd-Ag/Al_2O_3 catalysts were lower compared to that observed on the Pd/Al_2O_3 sample (binding energy of Pd $3d_{5/2}$ was 335.0 eV). Pd $3d_{5/2}$ binding energy recorded for Pd/Al_2O_3 catalyst is typical for metal Pd, while values of Pd $3d_{5/2}$ binding energy observed for Pd-Ag/Al_2O_3 catalysts are unusually low. The shift of Pd $3d_{5/2}$ binding energy observed for Pd-Ag/Al_2O_3 cannot be assigned to

Table 2
Elemental binding energies (eV) of studied samples

Catalyst	Al 2p	O 1s	Binding energy (eV)			
			Pd $3d_{5/2}$	Pd $3d_{3/2}$	Ag $3d_{5/2}$	Ag $3d_{3/2}$
3%Pd/Al_2O_3	73.5	530.8	335.0	340.0	–	–
3%Pd-4%Ag (untreated)	74.0	531.0	334.0	339.1	366.8	372.7
3%Pd-4%Ag (N_2O treated)	73.8	531.0	334.2	–	366.8	–
3%Pd-4%Ag (CO_2 treated)	73.8	530.8	334.0	–	366.8	–
0.03%Pd-0.235%Ag (untreated)	74.0	531.0	–	–	367.0	–
0.03%Pd-0.235%Ag (N_2O treated)	74.0	530.9	–	–	366.8	–
0.03%Pd-0.235%Ag (CO_2 treated)	74.0	530.9	–	–	366.8	–

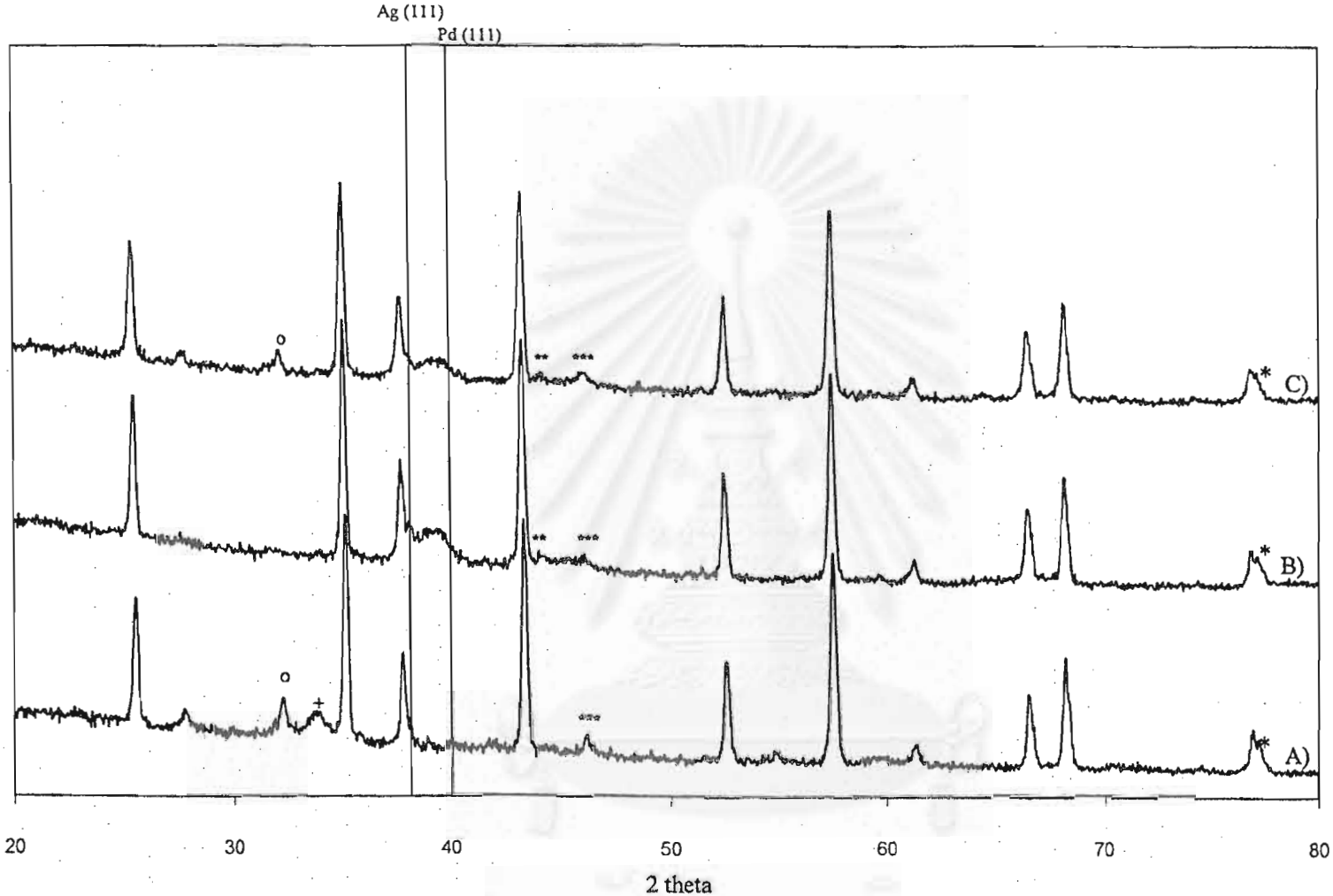

Fig. 3. X-ray diffraction patterns of Pd-Ag/Al_2O_3 catalysts; (A) calcined sample, (B) reduced (untreated) sample and (C) treated sample. o, +, * *, * * * and * represent Ag_2O, PdO, Ag (200), Pd (200) and Ag (311), respectively.

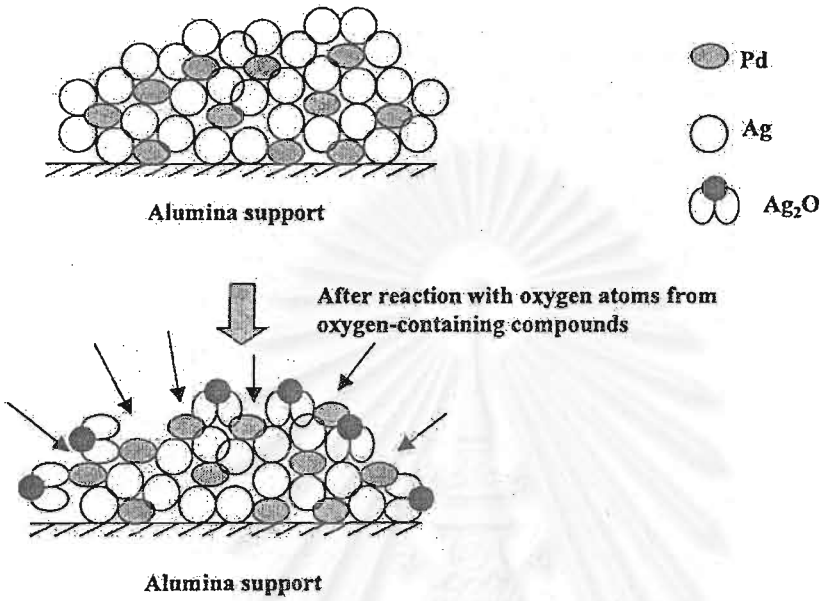

Fig. 4. Proposed model illustrating the effect of the pretreatment with oxygen and/ or oxygen-containing compounds on enhancing the accessible Pd active sites responsible for acetylene hydrogenation to ethylene.

palladium oxides because the shift for palladium oxides is observed at lower energies [21]. It was suggested that there was a change of electronic state of Pd in Pd-Ag/Al_2O_3 catalysts. Pd–Ag alloy or solid solution can be formed by electron density transfer from Ag to Pd resulting in the appearance of negative charge on Pd and positive charge on Ag.

Electronegativity (the tendency of an atom in a molecule to attract bonding electrons) of Pd (2.20) is higher than that of Ag (1.93) [22]. It is therefore, possible that in alloys bonding electrons could be attracted from Ag to Pd.

Table 2 shows that the states of Pd and Ag did not change with the pretreatments. Thus, the changes after pretreatment, which influenced the catalytic activity, occurred in the adsorbed layer of the catalyst without modification of the catalyst structure of the surface layers studied by XPS (ca. 15–25 A).

It is suggested, from the sample analysis by XRD and XPS, that Pd and Ag formed a solid solution or an alloy. Pd–Ag alloy was registered by XRD upon reduction with H_2 and after pretreatment with oxygen-containing molecules. Additionally, the formation of Ag_2O and chemisorbed oxygen on Pd surface (Pd-O) occurred when some small quantity of oxygen and/or oxygen-containing compounds was introduced to the catalyst, as modeled in Fig. 4.

The phenomenon of oxygen titration by CO over Pd surfaces was reported by Palazov et al. [23]. Their observation by in situ IR showed that the CO reacts readily with the preadsorbed oxygen layer to yield the same spectrum as that on the reduced catalyst. Additionally, Garland et al. [24] also argued that the effect of oxygen pretreatment over the Pd catalyst is insignificant up to 180 °C, presumably because the surface is immediately reduced by the excess CO. Thus, the Pd surfaces with preadsorbed species should react with H_2 in the feed stream in a virtually identical behavior to that with CO. This suggests an explanation for the increasing activity upon pretreatment, i.e. the oxygen chemisorbed over Pd surface is easily reduced by H_2 in the reaction feed. In contrast with the Pd surface, the chemical bond between Ag surface and oxygen atoms in pretreatment gases, in the form Ag_2O, is presumably strong and cannot be reduced by hydrogen at such low temperatures during the reaction (40–90 °C).

As a result, Ag_2O formed upon the pretreatment with oxygen and/or oxygen-containing compounds will expose the accessible Pd sites to react with C_2H_2 and H_2 in the feed stream. This should be responsible

Table 3
The metal dispersion of 0.03%Pd-0.235%Ag/ Al_2O_3 catalysts measured by CO-adsorption

Catalyst	Pd dispersion (%) at different pretreatment temperatures						
	80 °C	85 °C	90 °C	95 °C	100 °C	105 °C	110 °C
O_2-treated Pd-Ag/ Al_2O_3	15.32	19.09	22.51	16.03	7.48	–	–
NO-treated Pd-Ag/ Al_2O_3	31.88	24.22	22.98	17.09	6.48	–	–
N_2O-treated Pd-Ag/ Al_2O_3	9.55	20.45	20.86	29.23	29.52	26.75	16.09
CO-treated Pd-Ag/ Al_2O_3	9.25	14.44	15.44	16.50	15.62	–	–
CO_2-treated Pd-Ag/ Al_2O_3	9.43	9.37	15.14	18.15	20.68	21.45	–

Note: percentage of Pd dispersion of untreated Pd-Ag/Al_2O_3 catalyst = 6.84%.

for the improved catalyst activity upon pretreatment with oxygen and/or oxygen-containing compounds.

The assessment of metal active sites of the catalysts by CO-adsorption was used to verify the proposed model and to confirm that the pretreatment with oxygen and/or oxygen-containing compounds affects the surface of Pd-Ag bimetallic particles in the catalysts. It has been reported in some references [25–31] that the CO chemisorption does not occur either on the support or on the Ag particles in Pd-Ag bimetallic catalysts. Thus, the measured metal active sites are attributed to the interaction between CO and Pd particles. The metal active sites, reported as percentage of Pd metal dispersion, of the treated catalysts with an effective amount of oxygen and/or oxygen-containing compounds at various pretreatment temperatures are shown in Table 3. It was found that the catalyst activities increased with increasing Pd dispersion.

Turnover number (the number of C_2H_2 molecules reacted per active site, TON) of the N_2O-treated catalysts, which were used at different periods of time-on-stream (20–600 min) at the reaction temperature of 50 °C, was also examined, as shown in Table 4. It was found that TON of the N_2O-treated catalysts remained constant during 600 min on-stream. Thus, the significant effect of pretreatment on the catalytic activity is confirmed.

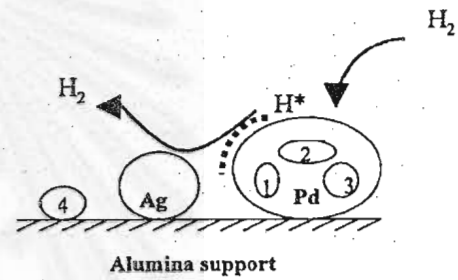

1: Site for oligomer formation
2: Site for direct ethane formation from acetylene
3: Site for ethylene production from acetylene
4: Site for ethane production from ethylene
.....carbonaceous deposit bridge

Fig. 5. Conceptual model demonstrating four main types of surface sites on alumina-supported palladium catalyst and the role of Ag promoter as desorption site for transferred H_2.

The existence of three types of active sites created on the palladium surface and one site on the support has been reported for the acetylene hydrogenation over supported palladium based catalyst, as modeled in Fig. 5 [32–39]. Three types of active sites locating on the palladium surface, are responsible for selective hydrogenation of acetylene to ethylene, direct ethane formation from acetylene, and oligomer formation.

Table 4
N_2O-treated 3%Pd-4%Ag/Al_2O_3 catalysts for various time-on-stream.

Time-on-stream (min)	C_2H_2 conversion (%)	Active site of spent catalyst (molecule/g catalyst)	TON (s^{-1})
20	85.3	5.94×10^{17}	9.8×10^{-2}
120	83.1	5.63×10^{17}	10.1×10^{-2}
240	83.4	5.64×10^{17}	10.1×10^{-2}
360	82.3	5.65×10^{17}	9.9×10^{-2}
480	82.5	5.60×10^{17}	10.0×10^{-2}
600	83.0	5.78×10^{17}	9.8×10^{-2}

Table 5
Product distribution in C wt.% over untreated and treated 0.03%Pd-0.235%Ag/Al_2O_3 catalysts

Reaction temperature (°C)	Product	Untreated[a]	O_2-treated[b]	NO-treated[c]	N_2O-treated[d]	CO-treated[e]	CO_2-treated[f]
50	CH_4	0.037	0.037	0.037	0.037	0.037	0.037
	C_2H_2	0.344	0.273	0.246	0.254	0.238	0.236
	C_2H_4	65.268	65.336	65.568	65.641	65.337	65.338
	C_2H_6	34.352	34.391	34.150	34.068	34.389	34.389
	C_2H_2 conv. (%)	52	64.1	67.7	64.5	66.7	67
	C_2H_4 gain (%)	127.2	123.5	129.2	129.6	125.2	118.7
60	CH_4	0.037	0.037	0.037	0.037	0.037	0.037
	C_2H_2	0.135	0.092	0.105	0.086	0.105	0.084
	C_2H_4	65.405	65.436	65.559	65.673	65.425	65.438
	C_2H_6	34.424	34.435	34.299	34.205	34.434	34.441
	C_2H_2 conv. (%)	81.2	87.1	85.4	88	85.4	88.3
	C_2H_4 gain (%)	121.2	118.2	128.8	125.2	119.2	119.5

[a] Untreated Pd-Ag/Al_2O_3.
[b] Treated Pd-Ag/Al_2O_3 (0.15 ml O_2, 90 °C).
[c] Treated Pd-Ag/Al_2O_3 (0.06 ml NO, 80 °C).
[d] Treated Pd-Ag/Al_2O_3 (0.04 ml N_2O, 100 °C).
[e] Treated Pd-Ag/Al_2O_3 (0.15 ml CO, 95 °C).
[f] Treated Pd-Ag/Al_2O_3 (0.06 ml of CO_2, 105 °C).

Ethylene hydrogenation is believed to take place on the support by means of a hydrogen transfer mechanism, facilitated by the presence of retained carbonaceous deposits acting as H_2 bridges [32]. The role of the pretreatment with oxygen and/or oxygen-containing compounds was elucidated by considering the product distribution in wt.% carbon observed at the early period (20 min on-stream) during which only a negligible amount of carbonaceous deposit was formed. However, the coke accumulated

Table 6
Product distribution in C wt.% over untreated and treated 3%Pd-4%Ag/Al_2O_3 catalysts

Reaction temperature (°C)	Product	Untreated[a]	O_2-treated[b]	NO-treated[c]	N_2O-treated[d]	CO-treated[e]	CO_2-treated[f]
50	CH_4	0.024	0.024	0.024	0.024	0.024	0.024
	C_2H_2	0.160	0.089	0.096	0.099	0.123	0.067
	C_2H_4	62.432	62.476	62.522	62.609	62.462	62.490
	C_2H_6	37.384	37.411	37.358	37.268	37.391	37.419
	C_2H_2 conv. (%)	73.6	85.3	84.1	83.7	79.7	89.0
	C_2H_4 gain (%)	110.0	106.5	111.4	114.0	108.2	98.8
60	CH_4	0.024	0.024	0.024	0.024	0.024	0.024
	C_2H_2	0.042	0.029	0.032	0.033	0.032	0.020
	C_2H_4	62.506	62.514	62.562	62.581	62.509	62.519
	C_2H_6	37.428	37.433	37.382	37.362	37.435	37.437
	C_2H_2 conv. (%)	93.0	95.2	94.7	94.5	94.7	96.7
	C_2H_4 gain (%)	100.2	96.5	102.5	104.9	97.0	97.0

Feed (C wt.%) contained 0.024% CH_4, 0.607% C_2H_2, 62.512% C_2H_4, and 37.217% C_2H_6.
[a] Untreated Pd-Ag/Al_2O_3.
[b] Treated Pd-Ag/Al_2O_3 (0.15 ml O_2, 90 °C).
[c] Treated Pd-Ag/Al_2O_3 (0.06 ml NO, 80 °C).
[d] Treated Pd-Ag/Al_2O_3 (0.04 ml N_2O, 100 °C).
[e] Treated Pd-Ag/Al_2O_3 (0.15 ml CO, 95 °C).
[f] Treated Pd-Ag/Al_2O_3 (0.06 ml of CO_2, 105 °C).

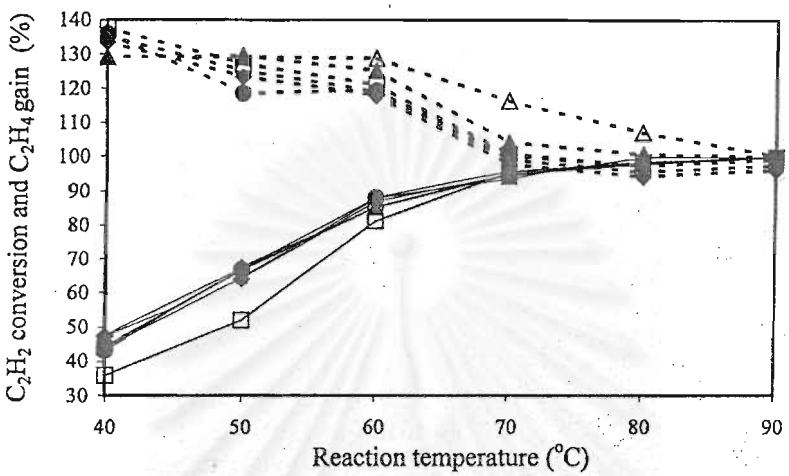

Fig. 6. Temperature dependence of the catalytic performance of 0.03%Pd-0.235%Ag/Al_2O_3 catalysts; (□) untreated, (◆) O_2-treated, (●) CO_2-treated, (○) CO-treated, (▲) N_2O-treated and (△) NO-treated. Solid line and dashed line represent % C_2H_2 conversion and % C_2H_4 gain, respectively.

on the 20 min on-stream catalysts was experimentally determined to confirm the speculation using temperature programmed oxidation (TPO). It is possible to see the effect of these different treatments on the catalytic performance concerning the product distribution summarized in Tables 5 and 6. All treated catalysts exhibited the same results in improving the C_2H_2 conversion compared to untreated ones, but interestingly, larger ethylene gains were observed only over NO_x-treated catalysts. Moreover, an inversely

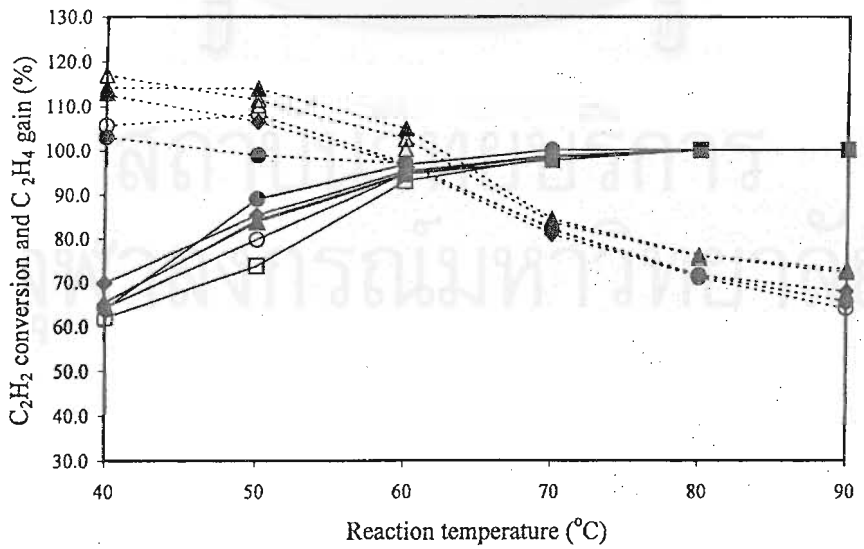

Fig. 7. Temperature dependence of the catalytic performance of 3%Pd-4%Ag/Al_2O_3 catalysts; (□) untreated, (◆) O_2-treated, (●) CO_2-treated, (○) CO-treated, (▲) N_2O-treated and (△) NO-treated. Solid line and dashed line represent % C_2H_2 conversion and % C_2H_4 gain, respectively.

proportional relationship can be seen between ethane formation and ethylene gain. One possible explanation is that O_2 and CO_x treatments resulted in an enhancement of the accessible sites corresponding to direct ethane formation, so that C_2H_2 was predominantly converted to ethane and the lower ethylene gains were exhibited as a consequence. The higher ethylene gains obtained on NO_x-treated catalysts should be ascribed to the enhancement of the accessible Pd active sites responsible for acetylene hydrogenation to ethylene.

The temperature dependence on the catalytic performance was additionally studied and the results are shown in Figs. 6–7. The effects of the pretreatment with oxygen and/or oxygen-containing compounds on the catalytic activities of both 0.03%Pd-0.235%Ag/Al_2O_3 and 3%Pd-4%Ag/Al_2O_3 catalysts were obviously revealed at a relatively low reaction temperatures (40–50 °C) and became less pronounced in the higher region (60–90 °C) where C_2H_2 conversion over all catalysts was nearly 100%. It is worth noting that the higher ethylene gains were achieved in most reaction temperatures by NO_x treatment; therefore, the temperature at the start of a run could be decreased with NO_x-treated catalysts.

4. Conclusions

The pretreatment with oxygen and/or oxygen-containing compounds resulted in the formation of Ag_2O, which will expose the accessible Pd sites to react with C_2H_2 and H_2 in the feed stream, thereby enhancing the catalytic activity of Pd-Ag/Al_2O_3 catalysts. In addition, the different behaviors of the pretreatment with O_2, NO_x and CO_x were examined. NO_x-treated catalysts gave higher ethylene gains because the number of sites for direct ethane formation was lessened, whereas the opposite behaviors were revealed for O_2-treated or CO_x-treated catalysts.

Acknowledgements

The financial supports of The Thailand Research Fund and TJTTP-JBIC and Mexican CONACYT Grants 31366-U AND IN 115800 are gratefully acknowledged. The authors would also like to thank Dr. M. Farias and Dr. J.A. Diaz for their assistance with the XPS measurements used in this work.

References

[1] Q. Zhang, X. Liu, Q. Zhu, Petrochem. Technol. 27 (1998) 53.
[2] G.C. Bond, P.B. Wells, J. Catal. 5 (1965) 65.
[3] A.N.R. Bos, L. Van de Beld, H.J. Martens, K.R. Westerterp, Chem. Eng. Commun. 21 (1993) 27.
[4] A.N.R. Bos, L. Van de Beld, H.J. Martens, K.R. Westerterp, Chem. Eng. Commun. 121 (1993) 55.
[5] C. Gaudiness, A.L. Cabanes, G. Villora, Can. J. Chem. Eng. 74 (1996) 84.
[6] J. Phillips, A. Auroux, G. Bergeret, J. Massardier, A. Renoupez, J. Phys. Chem. 97 (1993) 3565.
[7] A. Borgna, B. Moraweck, J. Massardier, A. Renoupez, J. Catal. 128 (1991) 99.
[8] S. Leviness, V. Nair, A.H. Weiss, Z. Schay, L. Guczi, J. Mol. Catal. 25 (1984) 131.
[9] A. Sarkany, Z. Zsoldos, Gy. Stefler, J.W. Hightower, L. Guczi, J. Catal. 157 (1995) 179.
[10] Y.H. Park, G.L. Price, Ind. Eng. Chem. Res. 31 (1992) 469.
[11] B. Cordts, D. Pease, L. Azaroff, Phys. Rev. B 24 (1981) 538.
[12] G. Meitzer, J.H. Sinfelt, Catal. Lett. 30 (1995) 1.
[13] K.H. Chae, Phys. Rev. B 53 (1996) 10328.
[14] I. Coulthard, T.K. Sham, Phys. Rev. Lett. 77 (1996) 4824.
[15] Q. Zhang, J. Li, X. Liu, Q. Zhu, Appl. Catal. A 197 (2000) 221.
[16] P. Praserthdam, US Patent 5,849,662 (1998), to Chulalongkorn University.
[17] B. Heinrichs, P. Delhez, J.-P. Schoebrechts, J.-P. Pirard, J. Catal. 192 (2000) 108.
[18] E.A. Sales, B. Benhamida, V. Caizergues, J.-P. Lagier, F. Fievet, F. Bozon-Verduraz, Appl. Catal. A 172 (1998) 273.
[19] M. Misono, G. Koyano, S. Yokoyama, Appl. Catal. A 4737 (1999) 1.
[20] Z. Li, M. Flytzani-Stephanopoulos, Appl. Catal. B 22 (1999) 35.
[21] J.F. Moulder, W.F. Stickle, P.E. Sobol, K.D. Bomben, Handbook of X-ray Photoelectron Spectroscopy, A Reference Book of Standard Spectra for Identification and Interpretation of XPS Data, Perkin-Elmer Corporation, Physical Electronics Division, Eden Prairie, 1992, p. 261.
[22] L.R. David (Ed.), Handbook of Chemistry and Physics, 80th Edition, p. 1999.
[23] A. Palazov, C.C. Chang, R.J. Kokes, J. Catal. 36 (1975) 338.
[24] C.W. Garland, R.C. Lord, P.F. Triano, J. Phys. Chem. 69 (1965) 1188.
[25] V. Ponec, G.C. Bond, Catalysis by Metals and Alloys, Elsevier, Amsterdam, 1995.
[26] Y. Soma-Noto, W.M.H. Sachtler, J. Catal. 32 (1974) 315.
[27] W.M.H. Sachtler, Catal. Rev. Sci. Eng. 14 (1976) 193.
[28] J.J. Scholten, Communication at the Workshop Micromeritics, Veldhoven, 5–6 April, 1993.
[29] E. Iglesia, M. Boudart, J. Catal. 37 (1975) 548.

[30] K. Foger, in: J.R. Anderson, M. Boudart (Eds.), Catalysis: Science and Technology, Vol. 6, 1984, p. 227.
[31] B. Heinrichs, P. Delhez, J.-P. Schoebrecht, J.-P. Pirard, J. Catal. 172 (1997) 322.
[32] S. Asplund, J. Catal. 158 (1996) 267.
[33] A.S. Al-Ammar, G. Webb, J. Chem. Soc., Faraday Trans. 174 (1978) 195.
[34] A.S. Al-Ammar, G. Webb, J. Chem. Soc., Faraday Trans. 174 (1978) 657.
[35] A.S. Al-Ammar, G. Webb, J. Chem. Soc., Faraday Trans. 175 (1978) 1900.
[36] J. Margitfalve, L. Guczi, A.H. Weiss, J. Catal. 75 (1984) 417.
[37] J. Margitfalve, L. Guczi, React. Kinet. Catal. 72 (1980) 475.
[38] J.M. Moses, A.H. Weiss, K. Matsusek, L. Guczi, J. Catal. 56 (1984) 417.
[39] A.H. Weiss, S. Leviness, V. Nau, L. Sakany, Z. Schay, in: Proceedings of the 8th International Congress on Catalysis, Vol. 5, 1984, p. 591.

VITAE

Miss Bongkot Ngamsom was born on 20th December, 1974, in Rayong province, Thailand. She received her Bachelor degree of Engineering with a major in Chemical Engineering from Srinakarinwirot University in March 1996. She achieved her Master's degree in Chemical Engineering (Biochemical Engineering) from Chulalongkorn University in April 1999. Since June 1, 1999, she has been studying for her Doctoral degree of Engineering from the department of Chemical Engineering, Chulalongkorn University.